January 2020

On the Convergence of Transportation and Power Systems in Smart and Connected Communities

Kevin A. Melendez
University of South Florida

On the Convergence of Transportation and Power Systems in Smart and Connected Communities

by

Kevin A. Melendez Valencia

A dissertation submitted in partial fulfillment
of the requirements for the degree of
Doctor of Philosophy
Department of Industrial and Management Systems Engineering
College of Engineering
University of South Florida

Co-Major Professor: Tapas K. Das, Ph.D.
Co-Major Professor: Changhyun Kwon, Ph.D.
Lingling Fan, Ph.D.
Andrei Barbos, Ph.D.
Hadi Charkhgard, Ph.D.

Date of Approval:
March 10, 2020

Keywords: Electric Vehicles, Shared Autonomous Electric Vehicles,
End-Use Consumers of Electricity, Option Contract, Demand Response

Dedication

This dissertation is dedicated to my parents, Hector Muñoz and Lily Valencia.

Acknowledgments

This dissertation would not have been possible without the extensive guidance of my co-advisors Dr. Tapas K. Das and Dr. Changhyun Kwon. Thank you both for all the advises, patience, and for your unconditional support throughout this journey. You have taught everything I know about how to be a researcher.

I would like to thank all my professors at the Department of Industrial and Management Systems Engineering. When I started my PhD, I knew very little about operations research or data science - you taught me all the tools and methods I used in this dissertation and in my papers. Your constant support and guidance help me greatly during this process.

I would like to thank the members of my committee: Dr. Lingling Fan, Dr. Andrei Barbos, and Dr. Hadi Charkhgard. All your comments, challenges, and support significantly improved the quality of this dissertation.

This journey started with the timely advice of Dr. Marco Sanjuan. You gave the push I needed to pursue my PhD and trusted that I was going to do well. All of this would not have been possible without your guidance.

Table of Contents

Abstract

Even though the total number of light-duty vehicles in the U.S. is expected to increase by 2030, total fuel consumption is expected to significantly decrease in the same timeframe. This contradictory behavior is in part explained by the increasing utilization of electricity as the primary source of energy in the transportation sector. Due to its potential to decrease dependency on fossil fuels, electric transportation has become a promising approach to alleviate the increasing environmental crisis. Passenger car markets are expected to experience a flood of new Electric vehicles (EVs) in the next few years. EVs are considered effective resources to support both transportation and power systems in urban areas. Such effectiveness arises from their ability to store energy for later use and their potential to reduce greenhouse gas emissions.

The overarching goal of this dissertation is to examine the integration of EVs in smart and connected communities and to understand how these vehicles can link smart power markets and transportation systems. Using a combination of optimization and data science tools, this dissertation intends to develop the methodologies and frameworks with which a large fleet of EVs can optimally be coordinated to support the operations of power system operators, end-use consumers of electricity, ride-sharing providers, and generate economic benefit to the EV-owners. If not properly coordinated, these new EVs can potentially be highly disruptive to both power and transportation networks, reducing reliability in both systems.

Chapter 1: Introduction

With the increasing deployment of advanced metering infrastructure and the ability to remotely manage loads using Internet-enabled tools, it is now feasible for end-use consumers of electricity to aggregate together and actively participate in the market as demand side players. Such participation is further motivated by the increasing adoption of dynamic pricing in power networks as well as consumers' ability to store energy and share it among peers. End-use consumers of electricity are envisioned to not only become key demand-side participants but been the center piece of the so called smart and connected communities (SCC).

Ability to store energy can potentially increase economic benefits of energy trading among end-use consumers. Although energy storage using stand-alone batteries is still quite expensive, impending growth of electric vehicles (EVs) may soon offer a solution. It is estimated that the number of EVs in the U.S. will grow to 7.3 million by 2023 [1]. Considering an average battery capacity of 70 kWh, these vehicles have the potential to optimally store and share up to 500,000 MWh per day. An aggregation of EVs can schedule charge and discharge of the batteries based on dynamically varying prices, owner preferences, and contracts with third parties. This will also facilitate load balancing and reduce stress on the network.

Research has already started to examine the potential benefits of a coordinated fleet of EVs. For example, in [2], a stochastic programming methodology is developed to maximize an aggregation's profit by optimally charging EVs under varying market prices. However, mechanisms to schedule load and trade electricity among peers using EVs are still in their early

stages of development. The first objective of this dissertation is designing such mechanism. We intend to further encourage local energy trading among aggregations of empowered end-use consumers while integrating large fleet of EVs in SCC. For such purpose, we have developed operational models for load scheduling and trading among aggregations of end-used consumer using EVs as the main technology to store and trade electricity. We have also developed and efficient mechanism to design optimal option contracts among the consumers and the EV owners. The results obtained from this first component of the dissertation are introduced in more detail in Chapters 2 and 3.

Various alliances of technology and manufacturing companies are earnestly developing and testing autonomous vehicles (AVs) capable of navigating busy streets in major cities. Since vehicle electrification and automation are arising simultaneously, most AVs are likely to be EVs; Tesla's latest models (2018-2019) are archetypes of this phenomenon. Vehicle automation have the potential to improve operations of traditional EVs. For example, although it is generally infeasible to dictate routes of traditional EVs, we can design AVs' travel plans to fulfill system-wide objectives [3].

The impending growth of AVs will also address many of the current carsharing barriers, including the issue of users having to travel to access the available vehicles. Hence, a fraction of the privately-owned transportation is expected to shift to on-demand services [4]. Car-sharing penetration, vehicle automation, and vehicle electrification are expected to bring a major transformation to the way we conceive local transportation in urban areas. Shared autonomous electric vehicles (SAEVs) will replace a significant part of the human driven automobiles on city roads. Companies providing ride sharing service in cities and surrounding suburbs are expected

to adopt a new business model partially switching from cars owned and driven by individuals to SAEVs leased from large feet owning companies.

SAEVs have the potential to solve most of the practical limitations of conventional EVs including traveler range anxiety, access to charging infrastructure, and charging time management [5]. However, switching to SAEVs for ride sharing will only be feasible if proper cyber-physical infrastructure is in place to support the operations of these vehicles, i.e., efficient charging/discharging of batteries and coordination of the transportation services. The second main objective of this dissertation is to design the operational methodologies of this cyber-physical infrastructure and thus facilitate the realization of the vision where thousands of SAEVs would optimally ply the streets of smart cities to maximize service to consumers at a minimal cost.

1.2 Research Contributions

The detailed description of research contributions is presented in the subsequent chapters. In what follows, an overview of the research contributions and the broader impacts are presented.

1.2.1 Empowering End-Use Consumers of Electricity

Among the recent papers dealing with peer-to-peer (P2P) cooperation, only a few consider dynamically varying hourly prices, network constraints, as well as DA and RT market settlements. To our knowledge, the presence of price spikes in the RT market has not been properly considered in any of the existing models. Another major issue in this context that has not been adequately explored is the fairness among the peers, without which the P2P cooperation may not be stable. Our paper offers a comprehensive methodology to support P2P cooperation by incorporating all of the above-mentioned features. Additionally, sharing of electricity is accomplished via temporal arbitrage using the electric vehicle parking lots in the aggregation. Promoting demand side participation among end-use consumers, feasibility of which is demonstrated by our methodology,

will bring added benefits of load balance and increased reliability in power networks. The fairness considerations that are embedded in the methodology will incentivize consumers participation

1.2.2 Bilateral Trading of Electricity

Peer-to-peer trading in a power network is a well examined topic, where peers are commonly assumed to be prosumers (households with generation and storage capabilities). However, growth of IoT and advanced metering infrastructure has led to the rise of a set of newly empowered peers, namely smart homes and businesses and EVs. In our previous work [6], we have shown how these peers are now able to form coalitions and reduce their operational cost by engaging in demand response, in markets with hourly price variations and price spikes. In this paper, we demonstrate that, in markets with price variations and spikes, aggregations formed by these peers can also effectively engage in energy trading and derive financial benefits that are fair to all. This is demonstrated by developing a generalized Nash bargaining solution (GNBS) model for obtaining trading contract between two aggregations and implementing it on a sample problem. The operational optimization models for the aggregations that we have formulated as input for the GNBS model are also novel in how they schedule load consumption and plan for energy sharing. Our contributions also include a computational strategy where instead of solving the GNBS model as one single nonlinear mixed integer program, we separately solve the operational models and use their results to solve GNBS model and obtain the contract parameters.

1.2.3 System of Smart Hubs for Shared Autonomous Electric Vehicles

The main goal of this research is the creation of knowledge needed to design and operate a new cyber-physical infrastructure by integrating research from well-established areas, namely transportation, facility design and location, and electric power systems. Inter-dependency among the above three disparate areas is a new phenomenon that has risen in the context of the impending

new era of passenger transportation using SAEVs. Consequently, this phenomenon has not yet been examined and thus a significant knowledge discovery was obtained from this research.

Chapter 2: Empowering End-Use Consumers of Electricity to Aggregate for Demand-Side Participation

The complete article titled "E*mpowering end-use consumers of electricity to aggregate for demand-side participation"* [6] (published in Applied Energy) can be found in Appendix C. This article presents a multi-objective optimization-based methodology to trade fairness and efficiency in the context of the daily operations of an aggregation of end use consumers. The proposed methodology considers a number of practical features of the power markets, including actual price and demand data from existing power grids, network constraints, day ahead commitment and price, real time price spikes, optimal load scheduling, energy sharing strategies using EVs, and fairness of cost. It is demonstrated through a sample network that neither strategies arising from total cost minimization and fairness maximization may be ideal for the participants. Hence, a hybrid approach for operation scheduling and cost-sharing is proposed, which is shown to yield significant benefits to participants without sacrificing much fairness. Promoting demand-side participation among end-use consumers, feasibility of which is demonstrated by the proposed methodology, will bring added benefits of load balance and increased reliability in power networks. The fairness considerations embedded in the methodology will also incentivize consumers participation.

2.1 Abstract

End-use consumers (peers) are being empowered to aggregate for direct demand-side participation through load scheduling and energy sharing. This is the result of the growth of

Internet of Things (IoT) enabled loads, availability of advanced metering infrastructure, and the move towards real-time (RT) pricing of electricity. Peer-to-peer (P2P) cooperation has received significant interest in recent years, though the focus of this growing body of research is on modeling prosumer behavior in microgrids. Hence, there is a need for new methodologies to examine empowerment of all end-use consumers (not limited to prosumers) to form aggregations and develop fair rules of cooperation to reduce cost. This paper offers an optimization-based methodology to address the above need for power systems. It minimizes the total cost and considers fairness using a Nash bargaining approach. Since cost and fairness are often in conflict, trade-off strategies are also presented. The model to asses fairness is nonlinear. Hence, it is transformed into a second order cone program (SOCP) and solved using GUROBI software version 7.5.2. The methodology is implemented on a sample 5-bus network, built using price and demand data from one of the load zones of Pennsylvania, New Jersey, and Maryland (PJM) power network in the United States. It is shown that two aggregations of peers participating in the sample network can reduce their total cost by 14.17% and 22.7%, while maintaining fairness. Concluding remarks highlight some of the limitations of the methodology

Chapter 3: A Nash-bargaining Model for Trading of Electricity Between Aggregations of Peers

The complete article titled "Bilateral Trading of Electricity Between Aggregations of End-Use Consumers" (submitted to IEEE Transactions on Smart Grids) can be found in Appendix D. This paper is a direct continuation of the work presented in Chapter 2. Energy trading among end-use consumers in local power networks has become an important research topic in recent years. Although cooperation in power markets is gradually expanding at the peer-to-peer level, this concept has not been fully explored yet. Also, mechanisms to schedule load and trade electricity among peers are still in their early stages of development. In this paper, our intention has been to further encourage local energy trading among aggregations of empowered end-use consumers. We have developed a bilateral option contract framework between two types of aggregations of end-use consumers, namely, aggregation of load consuming entities only (ALCE) and aggregation electric vehicles (EVA). The framework uses a generalized Nash bargaining solution approach to find the optimal contract parameters. Using a sample numerical problem, we have examined the properties of two different kinds of option contracts (plain and swing) and assessed their benefits to the participating aggregations. It is demonstrated via numerical results that temporal arbitrage can significantly increase the financial benefits to the end-use consumers.

3.1 Abstract

In the last several years, the growth in household solar generation and the lack of success of the feed-in-tariff programs have led to the rise of peer-to-peer (P2P) energy trading schemes

among prosumers. However, a change that has started more recently is the growth of smart homes and businesses, of which loads are IoT controlled and are supported by advanced metering infrastructure (AMI). This has created a new opportunity for smart homes and businesses to form aggregations (coalitions) and participate in cooperative load management and energy trading. Unlike energy trading among individual prosumers in most P2P networks, a new trading opportunity that is emerging is between aggregations of peers of smart homes and businesses and electric vehicles (EVs). In this paper, we consider one such trading scenario between two aggregations, of which one has smart homes and businesses with load consuming entities (not prosumers), and the other has EVs only. The aggregation with smart homes and businesses derive cost reduction through optimal load scheduling based on load preferences, market-based pricing of electricity, and opportunity to trade (buy) energy from the aggregation with EVs. Whereas the aggregation of EVs optimally schedules charging to meet EV needs and uses stored energy to trade (sell). A generalized Nash bargaining model is developed for obtaining optimal trading strategies in the form of plain or swing option contracts. A sample numerical problem scenario is used to show that suitable contracts can be derived that allow aggregations of peers to mutually benefit from energy trading. Interactions among contract parameters (such as strike price, option value, and option quantity) and the relative market power of the aggregations are also examined.

Chapter 4: System of Smart Hubs for Shared Autonomous Electric Vehicles: Operation, Location, and Solution Approaches

The complete article titled "System of Smart Hubs for Shared Autonomous Electric Vehicles: Operation, Location, and Solution Approaches" (to be submitted to Applied Energy) can be found in Appendix E. In this work, we intend to create the knowledge needed to design a system of smart hubs, and thus facilitate the realization of the vision where thousands of shared autonomous electric vehicles (SAEVs) would optimally ply the streets of smart cities to maximize service to consumers at a minimal cost. Key focus of our research is on developing optimal operational strategies to assess ride sharing demand for a fleet of SAEVs while maximizing profit from optimally charging/discharging of the batteries, pick-up/drop-off of passengers, and rent of the available charging stations to third parties. We use this operational strategy to asses smart hubs capacities and locations across the road and electric power networks (covering the ride sharing service area).

4.1 Abstract

Shared autonomous electric vehicles (SAEVs) are expected to replace a significant fraction of human driven ride sharing vehicles in cities and surrounding urban areas. This change will only be possible if proper cyber-physical system (CPS) infrastructure is made available to support their operations. We address this need by developing a methodology for planning as well as real-time decision making for operating a system of SAEVs and charging hubs located across the serving area. The charging hubs are considered to host limited capacity battery banks and photo voltaic

(PV) generators. Our methodology considers a number of practical features of power and transportation systems, including consideration of day-ahead load commitment by solving an alternating current power flow model, real time price spikes of electricity, energy arbitrage, randomness in passenger demand, balking of passengers while waiting for a ride, and allowing charging for privately owned electric vehicles in the hubs. We demonstrated the utility of our methodology by implementing it on a sample CPS. It is shown through numerical results that the methodology is able to make planning decisions for day ahead commitment of power, as well as make real time operating decisions for the SAEVs and the hubs (including for its battery banks and PV generators). We also examine some of the system design issues such as hub capacity needed to support a fleet of given size, and impact of hub capacity and fleet size on system performance. We discuss the computational challenges of our methodology and propose a simplified myopic solution approach that is capable of dealing with much larger fleet sizes and a variety of hub capacities. Reduction in computation time and the optimality gap for the myopic approach are examined.

Chapter 5: Conclusions

The impending growth of electric and autonomous vehicles will soon bring a major transformation to the way we conceive local transportation in urban areas. The key intellectual merit of this research is in the creation of knowledge needed to design and operate a new EV-based cyber-physical infrastructure by integrating research from three distinct areas, namely transportation, facility design and location, and electric power systems. Inter-dependency among the above disparate areas is a new phenomenon that has risen in the context of the impending new era of passenger transportation using SAEVs in cities and their suburbs.

The results from this research will also translate into a number of critical benefits for the electric power systems. As vehicle electrification soars, the percentage of electricity consumed for transportation will rise dramatically. A sizable part of this increase will be due to proliferation of SAEV-supported passenger transportation. Hence, a cyber-connected infrastructure for planned charging/discharging of large fleets of SAEVs will create an opportunity for network load balancing. Moreover, the temporal arbitrage potential of these fleets of vehicles would help power systems operators to reduce reserve generation requirement for maintaining system reliability. This will help to reduce operational cost of the power networks and consequently reduce cost to the consumers.

References

[1] Block, D., J. Harrison, F. S. E. Center, M. D. Dunn. 2014. Electric vehicle sales and future projections. Electric Vehicle Transportation Center, Tech. Rep 1.

[2] Alipour, M., B. Mohammadi-Ivatloo, M. Moradi-Dalvand, K. Zare. 2017. Stochastic scheduling of aggregators of plug-in electric vehicles for participation in energy and ancillary service markets. Energy 118 1168–1179.

[3] Lam, A. Y., James, J., Hou, Y. & Li, V. O. (2018), `Coordinated autonomous vehicle parking for vehicle-to-grid services: Formulation and distributed algorithm', IEEE Transactions on Smart Grid 9(5), 4356{4366

[4] Fagnant, D. J. & Kockelman, K. M. (2018), `Dynamic ride-sharing and fleet sizing for a system of shared autonomous vehicles in austin, texas', Transportation 45(1), 143{158.

[5] Chen, T. D., Kockelman, K. M. & Hanna, J. P. (2016), `Operations of a shared, autonomous, electric vehicle fleet: Implications of vehicle & charging infrastructure decisions', Transportation Research Part A: Policy and Practice 94, 243{254.

[6] Melendez, K.A., Subramanian, V., Das, T.K. and Kwon, C., (2019). Empowering end-use consumers of electricity to aggregate for demand-side participation. Applied Energy, 248, pp.372-382.

Appendix A: General Information About the Appendices

Appendices include the complete published material in the journal of Applied Energy and the corresponding copyright authorization. Other unpublished documents are also included.

Appendix B: Copyrights for Published Materials in Applied Energy Journal

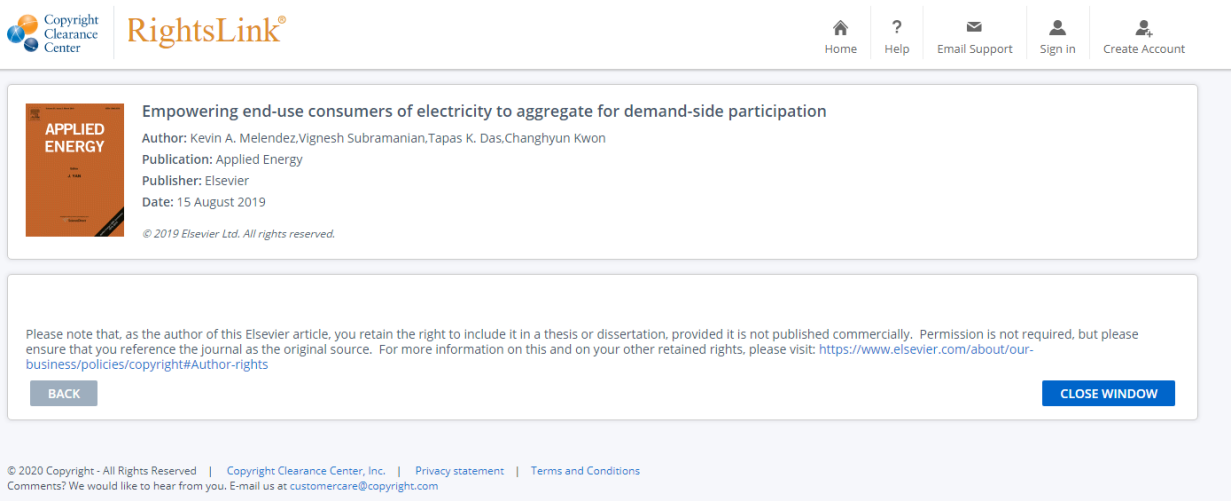

Appendix C: Published Materials in Applied Energy Journal

Applied Energy 248 (2019) 372–382

Contents lists available at ScienceDirect

Applied Energy

journal homepage: www.elsevier.com/locate/apenergy

Empowering end-use consumers of electricity to aggregate for demand-side participation

Kevin A. Melendez*, Vignesh Subramanian, Tapas K. Das, Changhyun Kwon

Department of Industrial and Management Systems Engineering, University of South Florida, United States

HIGHLIGHTS

- Aggregation and cooperation among peers will expand beyond prosumers in microgrids.
- Growth in IoT and metering infrastructure is empowering end-use consumers.
- Methodology allows aggregated consumers to schedule load and share energy.
- Application demonstrates a significant cost reduction while assuring fairness.
- Offers a novel cost-sharing strategy guided by cost minimization and Nash bargaining.

ARTICLE INFO

Keywords:
Demand-side participation
Aggregation of end-use consumers
Fairness
Peer-to-peer trading
Energy sharing using EVs
Optimization of power systems

ABSTRACT

End-use consumers (peers) are being empowered to aggregate for direct demand-side participation through load scheduling and energy sharing. This is the result of the growth of Internet of Things (IoT) enabled loads, availability of advanced metering infrastructure, and the move towards real-time (RT) pricing of electricity. Peer-to-peer (P2P) cooperation has received significant interest in recent years, though the focus of this growing body of research is on modeling prosumer behavior in microgrids. Hence, there is a need for new methodologies to examine empowerment of all end-use consumers (not limited to prosumers) to form aggregations and develop fair rules of cooperation to reduce cost. This paper offers an optimization based methodology to address the above need for power systems. It minimizes the total cost and considers fairness using a Nash bargaining approach. Since cost and fairness are often in conflict, trade-off strategies are also presented. The model to asses fairness is nonlinear. Hence, it is transformed into a second order cone program (SOCP) and solved using GUROBI software version 7.5.2. The methodology is implemented on a sample 5-bus network, built using price and demand data from one of the load zones of Pennsylvania, New Jersey, and Maryland (PJM) power network in the United States. It is shown that two aggregations of peers participating in the sample network can reduce their total cost by 14.17% and 22.7%, while maintaining fairness. Concluding remarks highlight some of the limitations of the methodology.

1. Introduction

With the increasing deployment of advanced metering infrastructure and the ability to remotely manage loads using Internet-enabled tools, it is now feasible for end-use consumers of electricity to aggregate together and actively participate in the market as demand-side players. Such participation is further motivated by the increasing adoption of dynamic pricing in power networks as well as consumers' ability to store energy and share it among peers. Large aggregations of load consuming entities (ALCEs) can optimally schedule their operations considering participant and network constraints, dynamically varying prices of electricity, and RT price spikes. These operations include load scheduling and energy sharing among the peers, which can be guided by the objectives of total cost minimization and fairness of cost shared by the participants. A schedule that minimizes the total cost of the aggregation may not satisfy the fairness criterion. Also, due to network, market, and operational constraints, a 100% fair schedule may not be feasible. However, fairness consideration is critical to maintain participation in an aggregation. Therefore, our goal is to develop a methodology that assists aggregations of end-use consumers to reduce their operational cost while maintaining an acceptable level of fairness.

* Corresponding author.
E-mail address: kmelendez7@mail.usf.edu (K.A. Melendez).

https://doi.org/10.1016/j.apenergy.2019.04.092
Received 14 February 2019; Received in revised form 7 April 2019; Accepted 16 April 2019
Available online 24 April 2019
0306-2619/

We consider that ALCEs are comprised of households, businesses, and electric vehicle (EV) parking lots with the ability to store and share energy. The households and businesses are characterized by their load portfolio and operational constraints. EV parking lots' operations are guided by the charge and discharge rates, arrival and departure patterns, upper and lower bounds on the state of charge, battery capacities, and state of charge of the EVs. The ALCEs strive to reduce the cost of energy consumption for all its entities, generate profit from temporal arbitrage of the stored energy in the EVs, and guarantee fairness among its participants. Our methodology allows the aggregations to optimally schedule their expected power needs from the day-ahead (DA) market and procure any imbalance from the RT market, which may be subjected to random price spikes. The methodology increases the DA commitment for the hours when high RT price spikes are expected and vice versa. Any unused hourly DA commitment is assumed to be sold by the ALCEs in the RT market at the prevailing prices.

1.1. Relevant literature

Motivated by evolving technologies and market infrastructures, demand-side cooperation in power markets continue to elicit the attention of researchers in recent years [1]. It has been shown that coordinated demand-side peers can significantly reduce the overall cost of electricity in power networks [2]. A cooperative market provides efficient means to address network uncertainties, reduce bidding risk, and reduce overall cost of electricity. However, fair distribution of the monetary benefits from the cooperation is an important and open research issue [3]. Also, although the topic of cooperation among relatively large demand-side players, e.g., aggregators [3] and microgrids operators [4], has received significant attention, acceptable mechanisms to schedule load and share electricity among the peers are still in early stages of development [5].

End-use consumers are envisioned to be key participants in future electricity markets. Although the cooperation in power markets is gradually converging to the level of peer-to-peer (P2P) sharing, this concept has not been fully explored [6]. A widely referenced paper on the topic of demand-side management and cooperation can be found in Mohsenian-Rad et al. [7], in which the authors develop (1) a pricing scheme for cooperative customers and (2) an incentive-based consumption scheduling algorithm to minimize the cost of energy. Feasibility of integrating a community energy storage (CES) with consumer-owned photovoltaic systems for demand-side management of a residential neighborhood is presented in Mediwaththe et al. [8]. An optimization model and blockchain-based architecture to manage the operation of crowdsourced energy systems with P2P trading can be found in Wang et al. [9]. The model allows P2P trading among individual prosumers and the system operator (SO). Two market designs centered on the role of electricity storage are proposed in Lüth et al. [5]. The authors examine the value of prosumer batteries in P2P trading and necessary market features for the battery systems to operate. It is shown that storage systems can produce savings of up to 31% for the end-users, of which more than half derives from cooperation and trading in the community. A framework to integrate prosumer communities into the existing DA and intraday markets is proposed in Zepter et al. [6]. The study examines how residential battery storage contributes to local demand-side flexibility in an integrated market setting. A four-layer P2P architecture is proposed in Zhang et al. [10] to determine the key elements and technological needs of P2P energy trading. It is shown through a case study that P2P will facilitate penetration of renewable energy resources in power grids. Long et al. [11] proposed a two-stage model to facilitate P2P trading in microgrids. A coordinator minimizes the total energy costs of the community in the first stage, and the model parameters are updated based on new information in the second stage. The paper assumes flat electricity prices for both buying and selling, does not incorporate power flow analysis, and does not address unfairness of economic gains. In Barabadi and Yaghmaee [12] an incentive-based demand response program is proposed, where consumers' loads are shifted to minimize cost. A billing mechanism linked with the overall load of the system is also proposed. The model does not consider power market constraints, storage systems, and two-time settlements of the market. Abushnaf and Rassau [13] offers a model for residential load scheduling integrated with a demand response program. The model manages renewable generators, storage systems, and smart appliances. However, it does not consider uncertainties in the electricity prices (e.g., price spikes), network constraints, and the option to transact with the SO. Furthermore, the model is solved to minimize the total electricity cost, which does not always guarantee fairness among the participants. Zhu et al. [14] proposes an optimization model to schedule the operations of aggregations of smart houses with an objective to reduce demand peaks. Fairness in scheduling, dynamic pricing, and network/market constraints were not considered. A demand response methodology to schedule large numbers of residential appliances for smoothing power variations resulting from renewable integration was presented in Elghitani and El-Saadany [15]. The methodology was evaluated based on long-term average performance and short-term sample-path performance. Economic benefits to the participating entities was not considered. Hence, no incentive was provided for the homes to yield control of their loads. Gonçalves et al. [16] presents a multiobjective model to minimize the total cost and dissatisfaction of smart residential homes. Two types of contract with the SO were examined, namely, (1) contracted power with known fixed costs and (2) limits on the power purchased with variable prices. The model considers shiftable appliances, temperatures of thermostatically controlled loads, and EVs. Selling stored energy in the EVs to third parties and fairness among the participants were not considered. In Elsayed et al. [17] a multiobjective optimization approach was adopted to coordinate residential loads in Egypt while ensuring satisfaction of end-use consumers and the utility. The main focus of this model is network reliability. Hence, though it minimizes consumers cost, features such as two-time market settlement, temporal arbitrage, and price variations were not considered.

1.2. Contributions of this paper

Among the recent papers dealing with P2P cooperation, none consider all of the following features: dynamic pricing of electricity, network constraints, two time (DA and RT) market settlements, and price spikes in the RT market. Another major issue that has not been adequately explored is fairness among peers, without which the P2P cooperation may not be stable. Our paper offers a comprehensive methodology to support P2P cooperation by incorporating all of the above mentioned features. Implementation of this methodology on a sample network, formulated with real-life data from an existing power network in the United States, establishes the benefits of empowerment of end-use consumers. Results form our multiobjective model expose the cost of fairness among the participants. We do not model households and businesses as prosumers with self-generation capacities, and sharing of electricity is accomplished via temporal arbitrage by the EV parking lots.

2. Preliminaries

In this section, we introduce some definitions and formulations needed to facilitate the presentation of the methodology. Consider the general form of a multiobjective optimization problem:

$$\min_{(x,y)\in\mathscr{F}} \left\{ z_1\left(x, y\right), \ldots, z_p\left(x, y\right) \right\}, \tag{1}$$

where $\mathscr{F} \coloneqq \{(x, y) \in \mathbf{Z}_+^{n_1} \times \mathbf{R}_+^{n_2} : Ax + \overline{A}y \leqslant b\}$ is the feasible set of the problem, and $z_k(x, y)$ is the linear objective function of entity k. Let us define $\mathscr{O} = z(\mathscr{F})$ as the image of $\mathscr{F}$ in the objective or *criterion* space,

where $z(\cdot) = \{z_1(\cdot), ..., z_p(\cdot)\}$. Then we have the following.

Definition 1. A feasible solution $(x', y') \in \mathscr{F}$ is called efficient or Pareto optimal, if there is no other $(x, y) \in \mathscr{F}$ such that $z_k(x, y) \leqslant z_k(x', y')$ for $k = 1, ..., p$ and $z_k(x, y) \neq z_k(x', y')$ for at least one k. If (x', y') is efficient, then $z(x', y')$ is called a nondominated point. The set of all efficient solutions $(x', y') \in \mathscr{F}$ is denoted by $\mathscr{F}_E$. The set of all nondominated points $z(x', y') \in \mathscr{O}$ for some $(x', y') \in \mathscr{F}_E$ is denoted by $\mathscr{O}_N$ and referred to as the nondominated frontier or the efficient frontier.

The bargaining problem examines how several players share a payoff or cost that they jointly generate. An approach to address the problem was proposed in Nash [18], which yields a unique and Pareto optimal solution. Let u_k, for $k = 1, ..., p$, be the utility function of the player k and d_k be the *disagreement point* (payoff received without cooperation) of player k. Then the Nash bargaining solution (NBS) is the point $(x, y) \in \mathscr{F}$ obtained from the following optimization problem

$$\max_{(x,y)\in\mathscr{F}} \prod_{k=1}^{p} (u_k(x, y) - d_k). \tag{2}$$

It has been shown that, NBS has the following properties: invariant, Pareto optimal, independent of irrelevant alternatives and symmetrical [18]. If the aim of the cooperation is to minimize the costs of player k ($c_k(x, y)$), then (2) may be written as

$$\max_{(x,y)\in\mathscr{F}} \prod_{k=1}^{p} (d_k - c_k(x, y)), \tag{3}$$

For a given $z \in \mathscr{F}_E$, let z_{conv} be a convex combination of some nondominated points excluding z. Then, we define other important nondominated points as follows.

Definition 2. A point $z \in \mathscr{F}_E$ is an extreme supported nondominated point (ESNDP) if and only if there exists no z_{conv} such that $z_{\text{conv}} \leqslant z$.

Definition 3. A point z is a nonextreme supported nondominated point if and only if there exists no z_{conv} such that $z_{\text{conv}} < z$ but there exists a z_{conv} such that $z_{\text{conv}} = z$.

3. Methodology

We consider that the ALCEs have two type of loads, fixed and deferrable, of which only the schedules of the latter are optimized. Deferrable loads are considered to have two subcategories: shiftable and adjustable loads. Shiftable loads are scheduled at any time within predefined time windows. Whereas, for adjustable loads, both schedule and power consumption are controlled, while satisfying the total energy requirements of the loads within the operational time window.

Let $\mathscr{C}$ be the set of all households and businesses in the aggregation (except the EV parking lots). Each load consuming entity (LCE) $i \in \mathscr{C}$ has a set of shiftable loads denoted by $\mathscr{S}_i$. This set comprises individual loads j with consumption level s_{ij} per unit time. The length of operation of a shiftable load is denoted by τ_{ij}. The operational time window of shiftable load j is bounded by $\underline{T_j}, \overline{T_j} \in \mathscr{T}$, where $\underline{T_j}$ denotes the initial time period, $\overline{T_j}$ denotes the final time period, $\mathscr{T}$ denotes the set of all time periods over which the load can potentially be scheduled, and $\underline{T_j} < \overline{T_j}$. Let x_{ijt} denote a binary variable indicating the on/off status of shiftable load j of LCE i during time period $t \in \mathscr{T}$. Then, we can write that

$$\sum_{t=\underline{T_j}}^{\overline{T_j}} x_{ijt} = \tau_{ij}, \qquad \forall\, i \in \mathscr{C},\ \forall\, j \in \mathscr{S}_i. \tag{4}$$

The set of adjustable loads within an LCE $i \in \mathscr{C}$ is denoted by $\mathscr{A}_i$. The maximum and minimum consumption levels per unit time of an individual load $j \in \mathscr{A}_i$ is denoted by $\overline{R_{ij}}$ and $\underline{R_{ij}}$, respectively. Similar to shiftable loads, each individual adjustable load j can be scheduled within a time window defined by $\underline{R_j}, \overline{R_j} \in \mathscr{T}$. Let y_{ijt} be a binary variable indicating the on/off status of the adjustable load j of LCE i, r_{ijt} denote its energy consumption level at time period $t \in \mathscr{T}$, and σ_{ij} denote the total required energy consumption. Then, operation of an adjustable load is guided by

$$\underline{R_{ij}} y_{ijt} \leqslant r_{ijt} \leqslant \overline{R_{ij}} y_{ijt}, \quad \forall\, i \in \mathscr{C},\ \forall\, j \in \mathscr{A}_i,\ \forall\, t \in \mathscr{T}, \tag{5}$$

$$\sum_{t=\underline{R_j}}^{\overline{R_j}} r_{ijt} = \sigma_{ij}, \qquad \forall\, i \in \mathscr{C},\ \forall\, j \in \mathscr{A}_i. \tag{6}$$

Note that, unlike shiftable loads that are either off or operating at full capacity, if an adjustable load is on (per binary variable y_{ijt}), we can regulate its power consumption between $\underline{R_{ij}}$ and $\overline{R_{ij}}$. Let $\mathscr{F}_i$ be the set of fixed loads and $f_{ijt} \in \mathscr{F}_i$ be the j-th fixed load of LCE $i \in \mathscr{C}$ at time period t. Then, the total energy that LCE i consumes at a given time period t is:

$$d_{it} = \sum_{j\in\mathscr{F}_i} f_{ijt} + \sum_{j\in\mathscr{S}_i} s_{ij} x_{ijt} + \sum_{j\in\mathscr{A}_i} r_{ijt}, \ \forall\, t \in \mathscr{T},\ i \in \mathscr{C}. \tag{7}$$

Let $\mathscr{B}$ denote the set of EV batteries in the aggregation. For a given time period $t \in \mathscr{T}$, energy balance of the battery $b \in \mathscr{B}$ can be written as:

$$\phi_b s_{bt} = \phi_b s_{b,t-1} + p_{bt}^{+} - p_{bt}^{-}, \qquad \forall\, t \in \mathscr{T},\ \forall\, b \in \mathscr{B}, \tag{8}$$

where ϕ_b is battery's b capacity, $s_{bt} \in (0, 1)$ is the state of charge of battery b at the end of time period t, p_{bt}^{+} is the amount of energy that is injected in battery b at time period t, and p_{bt}^{-} is the amount of energy that is extracted from battery b at time period t. We assume that the state of charge of the batteries is not allowed to be 0 nor 1. We define $\underline{S_{bt}}$ and $\overline{S_{bt}}$ as the minimum and maximum allowable state of charge of battery b at time period t, respectively. Then we write that

$$\underline{S_{bt}} \leqslant s_{bt} \leqslant \overline{S_{bt}}, \forall\, t \in \mathscr{T},\ \forall\, b \in \mathscr{B},\ 0 < \underline{S_{bt}} \leqslant \overline{S_{bt}} < 1. \tag{9}$$

Note that, at the time of departure, the bounds $\underline{S_{bt}}$ and $\overline{S_{bt}}$ are set to the desired level specified by the EV-owner. For simplicity, we assume that both charging and discharging rates of a battery are constant and given by P^{+} and P^{-}, respectively. Hence, we can write that

$$0 \leqslant p_{bt}^{+} \leqslant P^{+} w_{bt}^{+} \qquad \forall\, t \in \mathscr{T},\ \forall\, b \in \mathscr{B}, \tag{10}$$

$$0 \leqslant p_{bt}^{-} \leqslant P^{-} w_{bt}^{-}, \qquad \forall\, t \in \mathscr{T},\ \forall\, b \in \mathscr{B}, \tag{11}$$

where w_{bt}^{+} and w_{bt}^{-} are equal to 1 if battery b is charging or discharging, respectively, at time period t, and 0 otherwise. The next constraint guarantees that battery b is not charging and discharging simultaneously during time period t.

$$w_{bt}^{+} + w_{bt}^{-} \leqslant \omega_{bt}, \qquad \forall\, t \in \mathscr{T},\ \forall\, b \in \mathscr{B}, \tag{12}$$

where ω_{bt} is a binary parameter with the value of 1 if battery b is connected, i.e., the EV is in the parking lot, and 0 otherwise. We consider that the energy drawn from the batteries is shared among the LCEs in $\mathscr{C}$. We denote the amount of battery-supplied energy used by each $i \in \mathscr{C}$ as q_{it}. Then we can write that

$$\sum_{b\in\mathscr{B}} p_{bt}^{-} = \sum_{i\in\mathscr{C}} q_{it} \quad \forall\, t \in \mathscr{T}, \quad \text{and} \quad q_{it} \leqslant d_{it} \qquad \forall\, i \in \mathscr{C}, t \in \mathscr{T}. \tag{13}$$

In order to develop an optimal load scheduling and energy sharing strategy, the ALCE estimate the DA and RT prices and use that knowledge to determine the hourly DA commitment with the SO. We assume that if the actual consumption in any hour is less than the DA commitment, any excess quantity is sold in the RT market. Similarly, if the hourly consumption exceeds the DA commitment, the excess energy is procured from the RT market. Our methodology consists of two major phases: (1) determine the DA load commitment considering expected RT prices, and (2) develop an hourly load scheduling and energy sharing strategy using DA prices, actual RT prices of the current hour, and expected RT prices for the remaining hours of the day. DA

commitment is determined as follows.

- **Step 1:** Using a large number of historical price patterns at the node, generate a set of minimal cost load schedules. Then select a representative subset by using a scenario reduction technique.
- **Step 2:** For each selected load scenario, and using the generator DA bids, solve a direct current optimal power flow (DCOPF) model to estimate hourly market clearing prices (MCP). Generate the expected hourly RT prices based on these MCP.
- **Step 3:** Use the generator DA bids and expected RT prices to determine the DA commitment of the aggregation.

Details of the above steps are presented below.

3.1. DA load commitment

Step 1 Generating load schedules: We define $\boldsymbol{\Pi}$ as the set of historical daily price vectors (24-tuples, if each hour is considered a time unit). For each price realization $\boldsymbol{\pi} \in \boldsymbol{\Pi}$, the hourly load schedule ($D_t^{\boldsymbol{\pi}}$) is calculated as

$$D_t^{\boldsymbol{\pi}} = \sum_{i \in \boldsymbol{C}} [d_{it}^{\bullet} - q_{it}^{\bullet}] + \sum_{b \in \boldsymbol{B}} p_{bt}^{+\bullet} \qquad \forall\, t \in \boldsymbol{\mathcal{T}}, \tag{14}$$

where $^{\bullet}$ indicates the optimal solution of the variables from the following optimization problem:

$$\min \sum_{t \in \boldsymbol{\mathcal{T}}} \sum_{i \in \boldsymbol{C}} \pi_t [d_{it} - q_{it}] + \sum_{t \in \boldsymbol{\mathcal{T}}} \sum_{b \in \boldsymbol{B}} \pi_t p_{bt}^{+}, \tag{15}$$

s.t. (4)–(13).

We solve (15) for each $\boldsymbol{\pi} \in \boldsymbol{\Pi}$ to construct the optimal hourly load schedules based on historical price data. We then use a scenario reduction technique —as given in Growe-Kuska et al. [19]— to select a smaller subset (denoted by $\boldsymbol{\Omega}$) of representative load schedule scenarios.

Step 2 Estimating RT prices: For each load scenario $\boldsymbol{\omega} \in \boldsymbol{\Omega}$, and given the generator DA bids, we solve a DCOPF model to estimate the market clearing prices (MCPs) at the node. We then use these MCPs to obtain the expected RT prices ($\pi_t^{\boldsymbol{\omega}}$) at time period t, as $\pi_t^{\boldsymbol{\omega}} = \text{MCP}_t^{\boldsymbol{\omega}}[1 + \boldsymbol{\epsilon}]$, where $\boldsymbol{\epsilon} = M_1\, \boldsymbol{\epsilon}_1 + M_2\, \boldsymbol{\epsilon}_2$. The values of the random variables $\boldsymbol{\epsilon}_1$ and $\boldsymbol{\epsilon}_2$ are drawn from normal and Cauchy distributions, respectively. The bivariate random variable (M_1, M_2) is equal to (0, 1) with probability p_s and (1,0) with probability $(1 - p_s)$, where p_s denotes the probability of occurrence of price spikes. The normal random variable $\boldsymbol{\epsilon}_1$ captures the usual variability in the RT prices, whereas the Cauchy random variable $\boldsymbol{\epsilon}_2$ generates the price spikes.

Step 3 Obtaining DA commitment: Using the selected scenarios and the corresponding estimated RT prices $\boldsymbol{\pi}_t^{\boldsymbol{\omega}}$, a two-stage stochastic DCOPF problem is solved. This allows the ALCEs to optimally determine the DA commitment to the SO by considering the possibility of selling or buying quantities in the RT market. We define $\boldsymbol{\mathcal{G}}$ as the set of all generators in the network; $\boldsymbol{\mathcal{N}}$ as the set of all buses in the network; $\boldsymbol{\mathcal{N}}_L$ as the load buses; $\boldsymbol{\mathcal{G}}_n$ as the subset of generators that are connected to bus $n \in \boldsymbol{\mathcal{N}}$; and $\boldsymbol{\mathcal{N}}_n$ as the subset of buses that are directly linked to bus $n \in \boldsymbol{\mathcal{N}}$. Furthermore, we define P_{gt} as the output of generator $g \in \boldsymbol{\mathcal{G}}$ at time period t in the DA market.

For each scenario $w \in \boldsymbol{\Omega}$, let $\mu_{\boldsymbol{\omega}}$ denote its probability. The additional quantities purchased in the RT market in scenario $w \in \boldsymbol{\Omega}$ are denoted by P_{gt}^{w+}. If the DA quantity exceeds the demand in scenario w, the excess amount P_{gt}^{w-} is sold in the RT market at the current price. Let $C_g(\cdot)$ be the cost function of generator g in the DA market, and $\boldsymbol{\pi}_{nt}^{w}$ be the RT price at bus n, time period t, and scenario w. The schedule of the DA quantity is obtained by solving:

$$\min \sum_{t \in \boldsymbol{\mathcal{T}}} \left[\sum_{g \in \boldsymbol{\mathcal{G}}} C_g(P_{gt}) + \sum_{w \in \boldsymbol{\Omega}} \sum_{n \in \boldsymbol{\mathcal{N}}} \sum_{g \in \boldsymbol{\mathcal{G}}} \mu_w \boldsymbol{\pi}_{nt}^{w} \left(P_{gt}^{w+} - P_{gt}^{w-} \right) \right]. \tag{16}$$

The above objective function is subject to the following constraints:

- power balance in the DA market:

$$\sum_{g \in \boldsymbol{\mathcal{G}}_n} P_{gt} + \sum_{m \in \boldsymbol{\mathcal{N}}_n} b_{nm} \Big[\boldsymbol{\delta}_{nt} - \boldsymbol{\delta}_{mt} \Big] - D_{nt}^{\text{DA}} = 0, \qquad \forall\, n \in \boldsymbol{\mathcal{N}},\, t \in \boldsymbol{\mathcal{T}}, \tag{17}$$

where D_{nt}^{DA} is a variable that denotes the DA commitment, b_{nm} denotes the susceptance of the line between the buses n and m, and $\boldsymbol{\delta}_{nt}$ ($\boldsymbol{\delta}_{mt}$) denotes the voltage angle (in radians) at bus n (m) and time period t. Note that bus one is used as reference ($\boldsymbol{\delta}_{1t} = 0$) and the voltage angles are bounded by $-\boldsymbol{\pi} \leqslant \boldsymbol{\delta}_{nt} \leqslant \boldsymbol{\pi}$, $\forall\, n \in \boldsymbol{\mathcal{N}}, t \in \boldsymbol{\mathcal{T}}$.

- line flow constraints:

$$-\overline{F}_{nm} \leqslant b_{nm}[\boldsymbol{\delta}_{nt} - \boldsymbol{\delta}_{mt}] \leqslant \overline{F}_{nm}, \qquad \forall\, m \in \boldsymbol{\mathcal{N}}_n,\, n \in \boldsymbol{\mathcal{N}},\, t \in \boldsymbol{\mathcal{T}}:\, m < n, \tag{18}$$

where F_{nm} denotes the maximum line flow in MW.

- generator constraints:

$$\underline{P}_g \leqslant P_{gt} \leqslant \overline{P}_g, \qquad \forall\, g \in \boldsymbol{\mathcal{G}},\, t \in \boldsymbol{\mathcal{T}}, \tag{19}$$

where $\underline{P}_g$ and $\overline{P}_g$ are the generator lower and upper bounds.

The same set of constraints must be included for each possible scenario in the RT market.

- power balance in the RT market:

$$\sum_{g \in \boldsymbol{\mathcal{G}}_n} \left(P_{gt}^{w+} - P_{gt}^{w-} \right) + \sum_{m \in \boldsymbol{\mathcal{N}}_n} b_{nm} \left[\left(\boldsymbol{\delta}_{nt}^{w} - \boldsymbol{\delta}_{mt}^{w} \right) - \left(\boldsymbol{\delta}_{nt} - \boldsymbol{\delta}_{mt} \right) \right] - \left(D_t^{w+} - D_t^{w-} \right) = 0, \qquad \forall\, n \in \boldsymbol{\mathcal{N}},\, w \in \boldsymbol{\Omega},\, t \in \boldsymbol{\mathcal{T}}. \tag{20}$$

- line constraints:

$$-\overline{F}_{nm} \leqslant b_{nm}[\boldsymbol{\delta}_{nt}^{w} - \boldsymbol{\delta}_{mt}^{w}] \leqslant \overline{F}_{nm}, \qquad \forall\, m \in \boldsymbol{\mathcal{N}}_n,\, n \in \boldsymbol{\mathcal{N}},\, w \in \boldsymbol{\Omega},\, t \in \boldsymbol{\mathcal{T}} : m < n. \tag{21}$$

- generator constraints:

$$\underline{P}_g \leqslant P_{gt} + P_{gt}^{w+} - P_{gt}^{w-} \leqslant \overline{P}_g, \qquad \forall\, g \in \boldsymbol{\mathcal{G}},\, w \in \boldsymbol{\Omega},\, t \in \boldsymbol{\mathcal{T}}. \tag{22}$$

Beside the above constraints, we consider that the total load must be supplied by the power committed to in the DA market plus the RT compensations of each possible scenario,

$$D_{nt}^{\text{DA}} + D_t^{w+} - D_t^{w-} = D_{nt}^{w}, \qquad \forall\, n \in \boldsymbol{\mathcal{N}}_L,\, w \in \boldsymbol{\Omega},\, t \in \boldsymbol{\mathcal{T}}. \tag{23}$$

To ensure stable load scheduling, we add the following constraints,

$$D_{nt}^{\text{DA}} \geqslant \min_{w \in \boldsymbol{\Omega}} D_{nt}^{w}, \qquad \forall\, n \in \boldsymbol{\mathcal{N}}_L,\, t \in \boldsymbol{\mathcal{T}}, \text{ and} \tag{24}$$

$$D_{nt}^{\text{DA}} \leqslant \max_{w \in \boldsymbol{\Omega}} D_{nt}^{w}, \qquad \forall\, n \in \boldsymbol{\mathcal{N}}_L,\, t \in \boldsymbol{\mathcal{T}}, \tag{25}$$

such that the energy scheduled in the DA market is within the bounds of the realized demand. A similar approach to obtain the DA commitment was used in Subramanian and Das [20].

3.2. Load scheduling and energy sharing strategy

For notational simplicity, we will ignore index n, and denote the actual DA prices given by the SO as $\boldsymbol{\pi}_t^{\text{DA}}$, and the DA commitment as D_t^{DA}. We calculate the RT prices (with spikes) as $\boldsymbol{\pi}_t^{\text{RT}} = \boldsymbol{\pi}_t^{\text{DA}}(1 + \boldsymbol{\epsilon})$. We consider that drawing energy from the EVs has a fix cost $\boldsymbol{\lambda}$ per unit of

time. The load consumed by each LCE $i \in \mathcal{C}$ at any time period is supplied by (1) the committed power in the DA market, (2) power acquired from the RT market, and (3) power drawn from the EVs, denoted as d_{it}^{DA}, d_{it}^{RT}, and q_{it} respectively. Then we can write

$$d_{it} = d_{it}^{DA} + d_{it}^{RT} + q_{it}, \qquad \forall\, t \in \mathcal{T},\ i \in \mathcal{C}. \tag{26}$$

Similarly, for the EVs, p_{bt}^{DA+} and p_{bt}^{RT+} are the DA and RT components, respectively, of the power consumed at time period t. Then we can write

$$p_{bt}^{+} = p_{bt}^{DA+} + p_{bt}^{RT+}, \qquad \forall\, t \in \mathcal{T},\ \forall\, b \in \mathcal{B}. \tag{27}$$

Note that, d_{it}^{DA}, $p_{bt}^{DA+} \geqslant 0$ but d_{it}^{RT}, p_{bt}^{RT+} are free variables. We also consider the following:

$$\sum_{i \in \mathcal{C}} d_{it}^{DA} + \sum_{b \in \mathcal{B}} p_{bt}^{DA+} = D_t^{DA}, \qquad \forall\, t \in \mathcal{T}, \text{ and} \tag{28}$$

$$d_{it}^{DA} \leqslant d_{it} \qquad \forall\, i \in \mathcal{C},\ \forall\, t \in \mathcal{T}. \tag{29}$$

Hence the cost for each LCE $i \in \mathcal{C}$ can be written as,

$$z_i = \sum_{t \in \mathcal{T}} [\pi_t^{DA} d_{it}^{DA} + \pi_t^{RT} d_{it}^{RT} + \lambda q_{it}]. \tag{30}$$

Similarly, the total cost for the parking lots (all EVs) can be written as

$$z_{EV} = \sum_{t \in \mathcal{T}} \left[\pi_t^{DA} \sum_{b \in \mathcal{B}} p_{bt}^{DA+} + \pi_t^{RT} \sum_{b \in \mathcal{B}} p_{bt}^{RT+} - \lambda \sum_{i \in \mathcal{C}} q_{it} \right]. \tag{31}$$

In what follows, we present two separate approaches to obtain the load scheduling and energy sharing strategy: (1) total cost minimization (TCM) and (2) NBS. In the TCM model, we minimize the combined cost of LCEs and EV parking lots. This model, however, does not guarantee fairness to all peers. Hence, the need for the NBS model, where the total cost is fairly distributed among the peers based on their power consumption levels and flexibility of usage. For the TCM model, we can write

$$\min \ \textstyle\sum_{i \in \mathcal{C}} z_i + z_{EV}, \tag{32}$$

s.t. , (4)–(13) and (26)–(31).

The NBS model can be given as

$$\max \ \prod_{i \in \mathcal{C}} \left(z_i^{0} - z_i \right) \left(z_{EV}^{0} - z_{EV} \right), \tag{33}$$

s.t. , (4)–(13) and (26)–(31),

where z_*^0 denotes the disagreement point. The TCM model can be solved efficiently using any available mixed integer linear program (MILP) solver. However, to efficiently solve the NBS model we transform it into a mixed integer SOCP, which can be solved using commercial solvers such GUROBI or CPLEX. Details of this transformation are given in Appendix A. In this paper, the model was solved using GUROBI software version 7.5.2.

In most problem scenarios, the consideration of fairness is likely to increase the total cost to the aggregation. Hence, the two different objectives, i.e., total cost minimization and fairness among peers, should be considered simultaneously. To address this trade-off, we present the following bi-objective model.

3.3. A bi-objective model for trade-off between cost and fairness

By definition, the total cost per NBS model will be higher than (or equal to, in the best-case scenario) the TCM cost. While minimizing the total cost, the TCM solution is not always fair to all (even to identical peers). Also, it does not have a mechanism to guarantee more benefits to participants with higher load flexibility. On the contrary, participants with higher flexibility may end up being sacrificed and thus charged more. Hence, there is a need to generate solutions that can reduce the total cost below the NBS cost while also maintaining some level of fairness that is acceptable to all participants. To address this, we develop a bi-objective model.

Let z_i^{NBS} and z_{EV}^{NBS}, obtained from (33), denote the optimal costs of LCE i and EV parking, respectively, per NBS model. Also, let e_i and e_{EV} ($0 \leqslant e_i, e_{EV} \leqslant 1$) be parameters that determine the maximum allowable deviations from z_i^{NBS} and z_{EV}^{NBS}, respectively. These deviations give the model needed flexibility to reduce the total cost and increase fairness. Then, we can write that

$$z_i \leqslant (1 + e_i) z_i^{NBS} \quad \text{and} \quad z_i \geqslant (1 - e_i) z_i^{NBS} \qquad \forall\, i \in \mathcal{C}, \tag{34}$$

$$z_{EV} \leqslant (1 + e_{EV}) z_{EV}^{NBS} \quad \text{and} \quad z_{EV} \geqslant (1 - e_{EV}) z_{EV}^{NBS}. \tag{35}$$

Note that, we have set the upper bound for the cost equal to twice the value of the NBS cost. Then, the bi-objective model is given by:

$$\begin{aligned} &\min \ \textstyle\sum_{i \in \mathcal{C}} z_i + z_{EV}, \\ &\min \ \textstyle\sum_{i \in \mathcal{C}} e_i + e_{EV}, \end{aligned} \tag{36}$$

s.t. , (4)–(13), (26)–(31), (34), and (35).

Clearly, when $\sum_{i \in \mathcal{C}} e_i + e_{EV} = 0$, the total cost is equal to the NBS cost. As the summation increases above zero, the total cost decreases. The bi-objective model can be solved using the algorithm proposed in Boland et al. [21], the triangle slitting method (TSM), which is one of the most efficient algorithms found in the literature. In what follows, we present a high-level description of the algorithm. For a detailed explanation, including enhancements and implementation issues, please refer to the work of Boland et al. [21]. The TSM explores the criterion space of the problem by maintaining a list of rectangles and right-angled triangles that need to be explored. At the beginning of the algorithm, this list is empty. The first rectangle is added to the list by computing the endpoints of the nondominated frontier. This rectangle contains all the yet to be found nondominated points, as shown Fig. 1 (iteration 0). The algorithm explores a rectangle by finding the locally ESNDP within the rectangle. Refer to Section 2 for the formal definition of an ESNDP. Boland et al. [21] showed that by finding these points, the rectangle can be split into a set of right-angled triangles containing all yet to be found nondominated points, as shown in Fig. 1 (iteration 1). The algorithm explores a triangle by checking if its hypotenuse is part of the nondominated frontier. When it is the case, then the triangle is removed from the list, otherwise it is split into at most two other rectangles, as shown in Fig. 1 (iteration 2). The algorithm repeats these procedures until finding the entire nondominated frontier.

4. Case study and computational results

We demonstrate the implementation of our methodology on a modified PJM 5-bus network (see Fig. 2). This sample network is widely used by researchers to test methodologies, e.g., Li and Bo [23] and Li et al. [24]. The network was originally published around 1999 and is still used in some PJM training materials.[1] The network has two load nodes (2 and (3), three generating nodes (1, 4, and 5), each with three generators, and six transmission lines. We consider that at each load node an ALCEs operates. Lines susceptances and capacity of line 1–4 are also shown in Fig. 2. The ALCEs is comprised of multifamily residential homes and EV parking lots. Aggregation at each node has 4,000 participating homes, which represent 10% and 40% of the total number of homes at nodes 2 and 3, respectively. All participating homes are considered to have identical load characteristics with fixed (40%), shifTable (30%) and adjusTable (30%) loads. All nonparticipating homes are considered to have 100% fixed loads. The EV parking lots at nodes 2 and 3 have 300 and 500 vehicles respectively. Without loss of

[1] https://www.pjm.com/training/training-material.aspx.

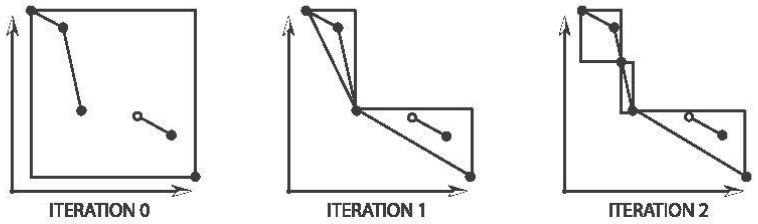

Fig. 1. Representative progression of the triangle slitting method used for solving the bi-objective model (figure adapted with permission from Dai and Charkhgard [22]).

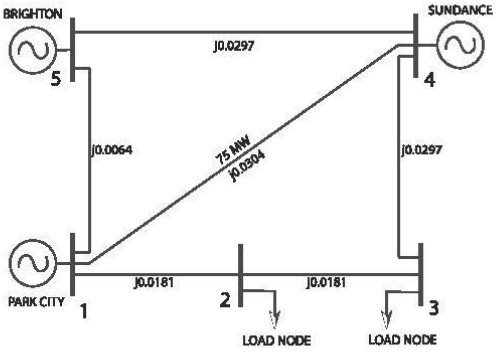

Fig. 2. Modified 5-bus PJM network.

generality, we consider a homogeneous fleet of EVs, each with a battery capacity of 70kWh. The EVs are assumed to remain in the parking lot between 9 AM and 5 PM.

We used scaled down load curves at the DAY zone of the PJM market (from July 15, 2017 to July 30, 2017 [25]) to model the hourly fixed loads in the network. The load scaling factor was chosen to match the total consumption of the multifamily homes (5 MWh per month per home) and the EVs in the 5-bus network. Generator supply functions are considered to be quadratic with parameters given in Appendix B. Capacity of each generator is considered to be 800 MW and hence the total capacity at each generating node is 2,400 MW. We also used the hourly locational marginal prices (LMPs) from the DAY zone during July 15–30, 2017 to generate the historical prices for both load nodes. We computed the mean and variance of the LMPs, and use them as parameters of a normal distribution to generate 300 price scenarios. For each of these price scenarios, we solved (15) to generate the demand patterns. Then, the scenario reduction technique was used to obtain ten representative scenarios (with respective probabilities), which are shown in red in Fig. 3. Considering the selected demand patterns and their probabilities, we solved the two-stage model (16) to obtain the hourly DA commitments, which are shown in blue in Fig. 3. The areas shaded in grey represent the fixed loads of the nonparticipant homes. In what follows, we contrast the DA commitment with the actual hourly demand, and the DA and RT prices, using the results from the load scheduling and energy sharing strategy.

Fig. 4a and b show the plots of the actual scheduled load, the corresponding DA commitment, and DA/RT prices for all 24 h of the day. It can be seen that during the times of price spikes, the DA commitments are higher and the consumption is shifted away, and vice versa. The impact of price spikes can be seen during hours 10, 14–15 and 17–18 at node 2 (see Fig. 4)a, and during hours 7–9, 10, 14–16 and 18 at node 3 (see Fig. 4b). The variations between DA commitment and actual consumption are much more pronounced at node 3, as it has a higher proportion of deferrable loads compared to node 2. Fig. 4c and d show the EV charge/discharge patterns over the hours of a day. It can be seen that, as expected, energy is drawn from the EVs at the times of price spikes. By solving the corresponding SOCP formulation, similar results are obtained for NBS model. Note that, the SOCP transformation does

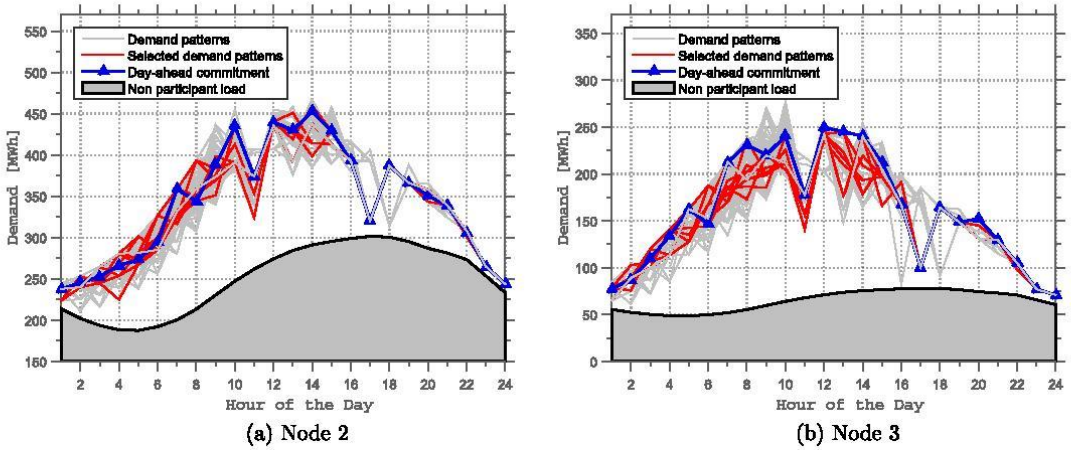

Fig. 3. Selected demand patterns and corresponding DA quantities obtained from our solution for nodes 2 and 3 of the sample network; demand patterns adopted from the DAY zone of PJM network.

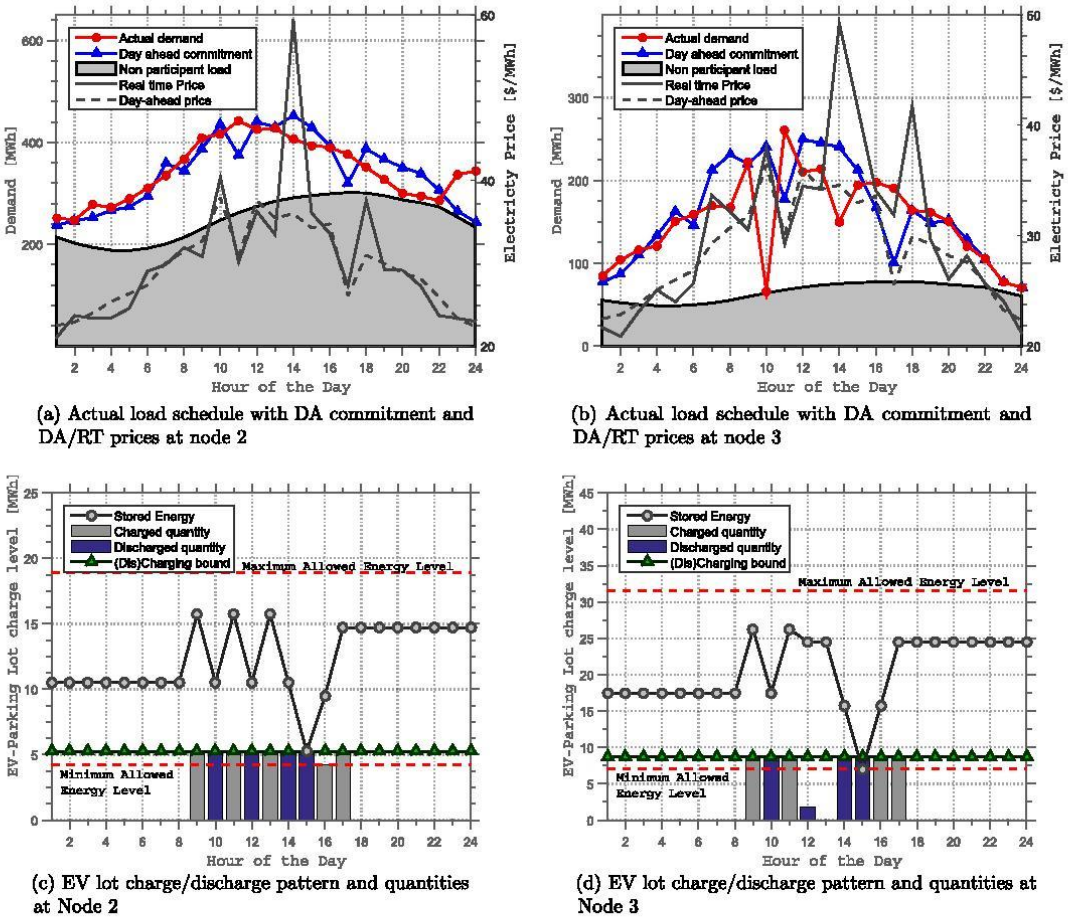

Fig. 4. Comparison of DA and RT prices and schedules, and EV charge/discharge pattern at nodes 2 and 3 of the sample network.

not modify the original variables of the problem, instead, it adds new dummy variables to the formulation. Therefore, the solution of the SOCP model, informed by GUROBI, is also solution to the original NBS model, and hence no further transformations are required.

Both the TCM and the NBS models are able to significantly reduce the total cost of meeting the loads of the participating homes at both nodes. To assess the savings, we first computed the cost at the disagreement point, as benchmark, where homes do not participate in load scheduling or energy sharing and always pay the DA price. The daily cost reductions from the disagreement point per TCM model for nodes 2 and 3 are $11,339 and $16,912, respectively. The corresponding reductions for the NBS model are $8,001 and $14,403. In percentages, these reductions are 14.28% and 21.84% for TCM model, and 10.08% and 18.6% for NBS model. Note that, the 100% fixed loads of the nonparticipating homes are always scheduled in the DA commitment. Hence, those homes are billed using the DA prices and do not share any of the cost savings generated by the participating homes and EV parking lots.

We now assess the fairness issue by examining how the total cost is shared among the participating homes according to the TCM and NBS models. Fig. 5 shows the costs per day for each participating multifamily home sorted in an ascending order. Though the participating homes are identical, their costs per TCM model vary widely. The costs to the homes obtained from the fairness driven NBS model, on the other hand, are identical. This fairness is achieved at a much higher total cost. The differences in the total cost between TCM and NBS models at node 2 (node 3) are $3,338 ($2,509) per day. It may be noted that, even for identical homes, cost allocation per NBS model may not always be the same in the presence of DA commitment restrictions and additional network and market constraints.

To demonstrate the ability of our models to accommodate heterogeneous participating homes, we considered a scenario where two thousand homes can be scheduled over all 24 h, while the remaining could only be scheduled from hours 12 to 24. Fig. 6 shows the TCM and NBS costs comparison at node 2, where the first 2000 homes represent the more flexible ones. For these homes, the TCM costs do not vary as widely, which may be attributed to their high scheduling flexibility. Also, both the TCM and NBS costs are significantly lower and close to each other. It can be seen that lower load scheduling flexibility of the remaining homes results in higher costs as well as relatively higher difference between TCM and NBS models outcomes.

Hereafter, we implemented the bi-objective model (36) to examine

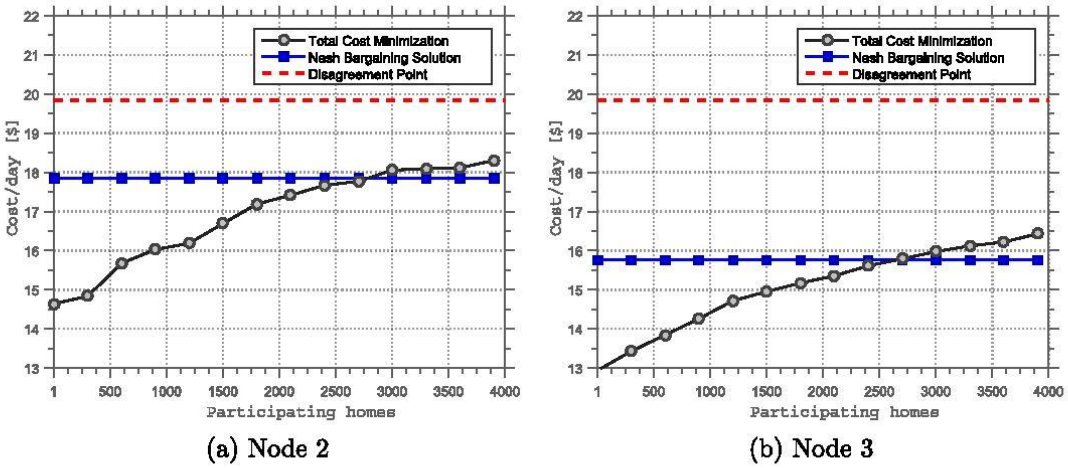

Fig. 5. Cost comparison between two solution approaches (TCM and NBS) for nodes 2 and 3.

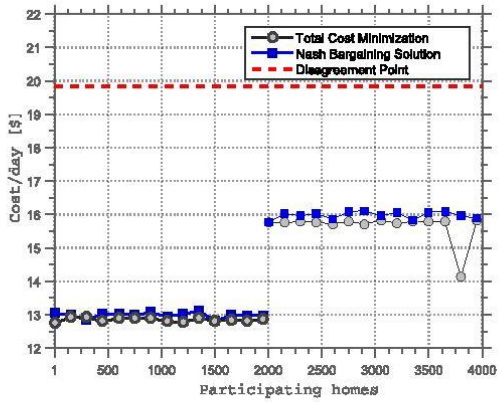

Fig. 6. Performance comparison between two solution approaches (TCM and NBS) for heterogeneous participating homes at node 2.

the cost and fairness trade-off for identical homes at node 2. Fig. 7a depicts the non-dominated frontier of the problem. It can be seen that, as the unfairness decreases, the total cost to the participating homes increases. There are only two ESNDPs: the one with zero unfairness (NBS solution) and the one with maximum unfairness (TCM solution). For a few selected points on the frontier, the corresponding daily costs to the participating homes at node 2 (sorted in ascending order) are shown in Fig. 7b. It demonstrates how the costs get higher and closer to the NBS costs as the unfairness decreases. The above bi-objective modeling approach allows us to sacrifice some level of fairness to reduce cost via a chosen value for $\sum_{i \in C} e_i + e_{EV}$. However, this approach, though perhaps elegant, is difficult to implement in practice as the term $\sum_{i \in C} e_i + e_{EV}$ has no easily interpretable meaning for the participating LCEs. Hence, we offer an alternative approach to address the trade-off. The basic idea behind the approach is to bill the LCEs using the higher (but fair) NBS cost, but schedule the loads and energy sharing using the TCM approach, which should generally yield a lower cost. Subsequently, distribute the cost savings as rebate among the LCEs appropriately. Here is how the alternative approach can be implemented. Schedule operations of the current hour of the day (per TCM model) using the following: settled DA prices, actual RT price for the current hour, and the predicted RT prices for the remaining hours. Repeat the process for all 24 h. This gives the actual cost of operation. At the end of the day, solve the NBS model to derive the billing costs to the participants using the DA prices and the actual (realized) hourly RT prices. The difference between the total costs of NBS and TCM models is then apportioned as rebates among the participants based on their fraction of the total load. We note, however, that in some circumstances it is possible that the TCM cost may be higher than the NBS cost, and thus the rebate will become negative (added cost). This may happen, as the NBS (billing) model uses the actual DA and RT prices and is therefore deterministic, whereas and the TCM (operational) model suffers from the uncertainty of the predicted RT prices. We implemented this strategy for loads at node 2 and 3. After redistribution of the rebate, the participating homes were billed at an uniform (fair) cost of $17.03/day and $14.97 for nodes 2 and 3, respectively. This represents a cost reduction of $0.809/day (4.53%) from the NBS cost and $2.81/day (14.17%) from the disagreement point (cost of nonparticipants) at node 2. The corresponding cost reduction at node 3 are $0.786/day (4.99%) from the NBS cost and $4.38/day (22.7%) from the disagreement point at node 3.

5. Concluding remarks

Our methodology considers a number of practical features of the power markets, including actual price and demand data from existing power grids, network constraints, day ahead commitment and price, real time price spikes, optimal load scheduling and energy sharing strategies, cost minimization and fairness of cost. It is demonstrated through a sample network that neither strategies arising from total cost minimization and fairness maximization may be ideal for the participants. Hence, a hybrid approach for operation scheduling and cost-sharing is recommended, which is shown to yield significant cost benefits to participants without sacrificing fairness. Promoting demand-side participation among end-use consumers, feasibility of which is demonstrated by our methodology, will bring added benefits of load balance and increased reliability in power networks. The fairness considerations embedded in the methodology will incentivize consumers participation. Our methodology, however, has a few limitations that require further work. Finding the Nash Bargaining Solution (even with a Second order cone program transformation) is computationally challenging, especially with a large number of load consuming entities

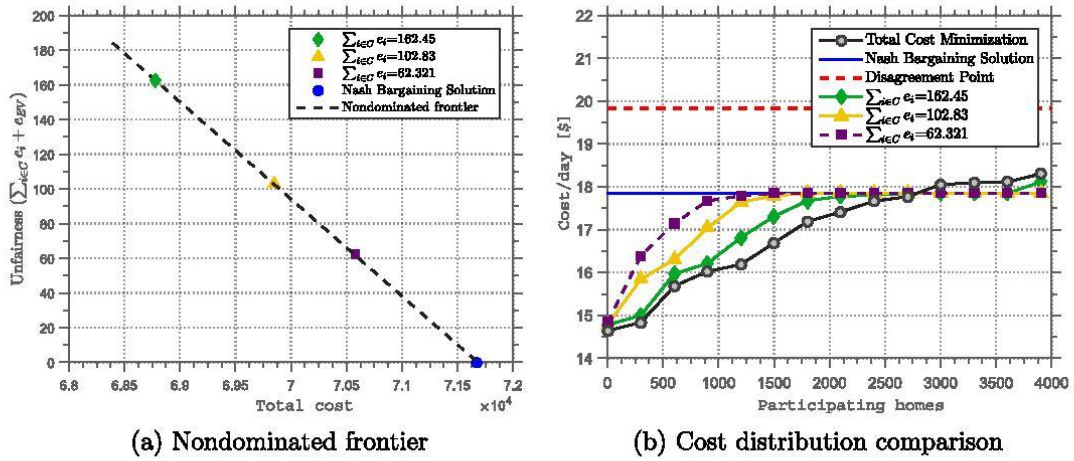

(a) Nondominated frontier (b) Cost distribution comparison

Fig. 7. Nondominated frontier, and cost comparison between selected nondominated points for node 2.

in the aggregation. Regarding operational considerations, we assumed that the availability of the electric vehicles in the parking lots are known. A way to further generalize our model is to consider the parking lots as smart hubs where these vehicles go in and out throughout the day depending on their trip plans and parking/charging/discharging needs. This will introduce additional complexity in the model as we have to incorporate a transportation model to address vehicle availability and charging needs. Also, our methodology does not consider individual electric vehicles as entities and hence fairness among them is not considered. As a result, though cost may be equally shared by all vehicles, some of their batteries may be subjected to more cycles of charge and discharge and thus higher battery degradation.

6. Competing interest disclosure

The authors of this paper certify that they have NO affiliations with or involvement in any organization or entity with any financial interest (such as honoraria; educational grants; participation in speakers bureaus; membership, employment, consultancies, stock ownership, or other equity interest; and expert testimony or patent-licensing arrangements), or non-financial interest (such as personal or professional relationships, affiliations, knowledge or beliefs) in the subject matter or materials discussed in this manuscript.

Appendix A. SOCP transformation for the NBS approach

Since the NBS formulation has a non-linear objective function, to solve it, we either need a non-linear solver or we can transform it into a second order (mixed integer) cone program (SOCP). The later option was chosen as it can be solved more efficiently using commercial solvers such as GUROBI and CPLEX.

As presented in Section 3.2, the feasible region of the optimal load scheduling problem can be modeled as a mixed integer linear problem. Hence, a general formulation of the NBS problem in this context can be written as:

$$\begin{aligned} \max\ & \prod_{k=1}^{p} (d_k - c_k(x, y)) \\ \text{s.t.}\ & Ax + Gy \leqslant b \\ & x, y \geqslant 0,\ x \in \mathbf{R}^{n_1},\ y \in \mathbf{Z}^{n_2} \end{aligned} \tag{37}$$

where, A is an $m \times n_1$ matrix, G is an $m \times n_2$ matrix, and b is an $m-$vector. Note that, an artificial variable w_k could be introduced, such that $w_k = (d_k - c_k(x, y))$. Then, formulation (37) can be rewritten as:

$$\begin{aligned} \max\ & \prod_{k=1}^{p} w_k \\ \text{s.t.}\ & w_k = (d_k - c_k(x, y)) \quad \forall\, k = 1,...,p \\ & Ax + Gy \leqslant b \\ & x, y \geqslant 0,\ x \in \mathbf{R}^{n_1},\ y \in \mathbf{Z}^{n_2} \end{aligned} \tag{38}$$

It was shown in Charkhgard et al. [26] and Ben-Tal and Nemirovski [27] that a problem with the form of (38) can be formulated as a mixed integer SOCP. First, a nonnegative variable $\boldsymbol{\gamma}$ is introduced, and the model is modified to:

$$\begin{aligned} \max\ & \boldsymbol{\gamma} \\ \text{s.t.}\ & 0 \leqslant \boldsymbol{\gamma} \leqslant \prod_{k=1}^{p} w_k \\ & w_k = (d_k - c_k(x, y)) \quad \forall\, k = 1,...,p \\ & Ax + Gy \leqslant b \\ & x, y \geqslant 0,\ x \in \mathbf{R}^{n_1},\ y \in \mathbf{Z}^{n_2} \end{aligned} \tag{39}$$

It is clear that maximizing $\boldsymbol{\gamma}$ will push $\prod_{k=1}^{p} w_k$ to its maximum value due to the first constraint in the aforementioned formulation. An

optimization problem with the form of (39) can be written as a SOCP by introducing a set of non-negative variables and constraints. Let t be the smallest integer value such that $2^t \geqslant p$, then problem (39) can be changed to:

$$
\begin{aligned}
\max\ & \gamma \\
\text{s.t.}\ & 0 \leqslant \gamma \leqslant \Gamma \\
& 0 \leqslant \Gamma \leqslant \sqrt{\tau_1^{l-1}\tau_2^{l-1}} \\
& 0 \leqslant \tau_j^l \leqslant \sqrt{\tau_{2j-1}^{l-1}\tau_{2j}^{l-1}} \qquad \forall\, j = 1,...,2^{l-1} \text{ and } l = 1,...,t-1 \\
& 0 \leqslant \tau_j^0 = y_j \qquad \forall\, j = 1,...,p \\
& 0 \leqslant \tau_j^0 = \Gamma \qquad \forall\, j = p+1,...,2^t \\
& w_k = (d_k - c_k(x,y)) \qquad \forall\, k = 1,...,p \\
& Ax + Gy \leqslant b \\
& x, y \geqslant 0,\ x \in \mathbf{R}^{n_1},\ y \in \mathbf{Z}^{n_2}
\end{aligned}
\tag{40}
$$

The above formulation is a SOCP since any constraint of the form $\{u, v, w \geqslant 0: u \leqslant \sqrt{vw}\}$ is equivalent to $\left\{u, v, w \geqslant 0: \sqrt{u^2 + \left(\frac{v-w}{2}\right)^2}\right\} \leqslant \frac{v+w}{2}$ [26]. This last formulation is better than the original NBS formulation since we can use the SOCP solver of CPLEX or GUROBI to solve it efficiently.

Appendix B. Generator cost functions

See Table 1.

Table 1
Generator cost functions used in the case study; adopted from Das and Wollenberg [28].

Generator	Cost function
1a	$0.100P_g^2 + 12P_g + 100$
1b	$0.100P_g^2 + 20P_g + 30$
1c	$0.100P_g^2 + 08P_g + 40$
4a	$0.100P_g^2 + 10P_g + 50$
4b	$0.100P_g^2 + 25P_g + 150$
4c	$0.100P_g^2 + 19P_g + 70$
5a	$0.100P_g^2 + 17P_g + 60$
5b	$0.120P_g^2 + 18P_g + 50$
5c	$0.085P_g^2 + 20P_g + 80$

References

[1] Long Chao, Wu Jianzhong, Zhou Yue, Jenkins Nick. Aggregated battery control for peer-to-peer energy sharing in a community microgrid with pv battery systems. Energy Procedia 2018;145:522–7.
[2] Li Dan, Sun Hongjian, Chiu Wei-Yu, Poor HVincent. Multiobjective optimization for demand side management in smart grid. IEEE Trans Ind Inform 2017.
[3] Nguyen Hieu, Le Long. Bi-objective based cost allocation for cooperative demand-side resource aggregators. IEEE Trans Smart Grid 2017.
[4] Dehghanpour Kaveh, Nehrir Hashem. Real-time multiobjective microgrid power management using distributed optimization in an agent-based bargaining framework. IEEE Trans Smart Grid 2017.
[5] Lüth Alexandra, Zepter Jan Martin, Crespo del Granado Pedro, Egging Ruud. Local electricity market designs for peer-to-peer trading: The role of battery flexibility. Appl Energy 2018;229:1233–43.
[6] Zepter Jan Martin, Lüth Alexandra, Crespo del Granado Pedro, Egging Ruud. Prosumer integration in wholesale electricity markets: Synergies of peer-to-peer trade and residential storage. Energy Build 2018.
[7] Mohsenian-Rad Amir-Hamed, Wong Vincent WS, Jatskevich Juri, Schober Robert, Leon-Garcia Alberto. Autonomous demand-side management based on game-theoretic energy consumption scheduling for the future smart grid. IEEE Trans Smart Grid 2010;1(3):320–31.
[8] Mediwaththe Chathurika P, Stephens Edward R, Smith David B, Mahanti Anirban. Competitive energy trading framework for demand-side management in neighborhood area networks. IEEE Trans Smart Grid 2018;9(5):4313–22.
[9] Wang Shen, Taha Ahmad F., Wang Jianhui, Kvaternik Karla, Hahn Adam. Energy crowdsourcing and peer-to-peer energy trading in blockchain-enabled smart grids. arXiv preprint arXiv:1901.02390; 2019.
[10] Zhang Chenghua, Jianzhong Wu, Zhou Yue, Cheng Meng, Long Chao. Peer-to-peer energy trading in a microgrid. Appl Energy 2018;220:1–12.
[11] Long Chao, Jianzhong Wu, Zhou Yue, Jenkins Nick. Peer-to-peer energy sharing through a two-stage aggregated battery control in a community microgrid. Appl Energy 2018;226:261–76.
[12] Barabadi Behzad, Yaghmaee Mohammad Hossein. A new pricing mechanism for optimal load scheduling in smart grid. IEEE Syst J 2019.
[13] Abushnaf Jamal, Rassau Alexander. An efficient scheme for residential load scheduling integrated with demand side programs and small-scale distributed renewable energy generation and storage. Int Trans Elect Energy Syst 2019;29(2). e2720.
[14] Zhu Jiawei, Lin Yishuai, Lei Weidong, Liu Youquan, Tao Mengling. Optimal household appliances scheduling of multiple smart homes using an improved cooperative algorithm. Energy 2019;171:944–55.
[15] Elghitani Fadi, El-Saadany Ehab. Smoothing net load demand variations using residential demand management. IEEE Trans Industr Inf 2019;15(1):390–8.
[16] Gonçalves Ivo, Gomes Álvaro, Antunes Carlos Henggeler. Optimizing the management of smart home energy resources under different power cost scenarios. Appl Energy 2019;242:351–63.
[17] Elsayed Abdallah M, Hegab Mohamed M, Farrag Sobhy M. Smart residential load management technique for distribution systems' performance enhancement and consumers' satisfaction achievement. Int Trans Electr Energy Syst 2019:e2795.
[18] Nash Jr. John F. The bargaining problem. Econometrica: J Econ Soc 1950:155–62.
[19] Growe-Kuska Nicole, Heitsch Holger, Romisch Werner. Scenario reduction and scenario tree construction for power management problems. 2003 IEEE Bologna power tech conference proceedings, vol. 3. IEEE; 2003. p. 7.
[20] Subramanian Vignesh, Das Tapas K. A two-layer model for dynamic pricing of electricity and optimal charging of electric vehicles under price spikes. Energy 2019;167:1266–77.
[21] Boland Natashia, Charkhgard Hadi, Savelsbergh Martin. A criterion space search algorithm for biobjective mixed integer programming: The triangle splitting method. INFORMS J Comput 2015;27(4):597–618.
[22] Dai Rui, Charkhgard Hadi. Bi-objective mixed integer linear programming for managing building clusters with a shared electrical energy storage. Comput Oper Res 2018.
[23] Li Fangxing, Bo Rui. Small test systems for power system economic studies. IEEE

PES general meeting. IEEE; 2010. p. 1–4.
[24] Li Guoqing, Zhang Rufeng, Jiang Tao, Chen Houhe, Bai Linquan, Cui Hantao, et al. Optimal dispatch strategy for integrated energy systems with cchp and wind power. Appl Energy 2017;192:408–19.
[25] Data miner 2, pjm. https://dataminer2.pjm.com/feed/hrl_load_metered. Last accessed on March 26, 2019.
[26] Charkhgard Hadi, Savelsbergh Martin, Talebian Masoud. A linear programming based algorithm to solve a class of optimization problems with a multi-linear objective function and affine constraints. Comput Oper Res 2018;89:17–30.
[27] Ben-Tal Aharon, Nemirovski Arkadi. On polyhedral approximations of the second-order cone. Math Oper Res 2001;26(2):193–205.
[28] Das Dibyendu, Wollenberg Bruce F. Risk assessment of generators bidding in day-ahead market. IEEE Trans Power Syst 2005;20(1):416–24.

Appendix D: Article Submitted to the International Journal of Electrical Power & Energy Systems

A Nash-bargaining Model for Trading of Electricity Between Aggregations of Peers

Kevin A. Melendez, Tapas K. Das, and Changhyun Kwon

Department of Industrial and Management Systems Engineering, University of South Florida

***Abstract*—In the last several years, the growth in household solar generation and the lack of success of the feed-in-tariff programs have led to the rise of peer-to-peer (P2P) energy trading schemes among prosumers. However, a change that has started more recently is the growth of smart homes and businesses, of which loads are IoT controlled and are supported by advanced metering infrastructure (AMI). This has created a new opportunity for smart homes and businesses to form aggregations (coalitions) and participate in cooperative load management and energy trading. Unlike energy trading among individual prosumers in most P2P networks, a new trading opportunity that is emerging is between aggregations of peers of smart homes and businesses and electric vehicles (EVs). In this paper, we consider one such trading scenario between two aggregations, of which one has smart homes and businesses with load consuming entities (not prosumers), and the other has EVs only. The aggregation with smart homes and businesses derive cost reduction through optimal load scheduling based on load preferences, market-based pricing of electricity, and opportunity to trade (buy) energy from the aggregation with EVs. Whereas the aggregation of EVs optimally schedules charging to meet EV needs and uses stored energy to trade (sell). A generalized Nash bargaining model is developed for obtaining optimal trading strategies in the form of plain or swing option contracts. A sample numerical problem scenario is used to show that suitable contracts can be derived that allow aggregations of peers to mutually benefit from energy trading. Interactions among contract parameters (such as strike price, option value, and option quantity) and the relative market power of the aggregations are also examined.**

Keywords: Aggregation of peers, peer-to-peer energy trading, option contract, Nash bargaining solution

I. Introduction

Increasing adoption of internet-enabled load control and the move towards real-time pricing of electricity are creating opportunities for end-use consumers (peers) to form aggregations [11]. These aggregations are intended to reduce cost of the participating peers by optimally scheduling their loads and by trading energy. As these aggregations pay time varying market prices set by the system operator, strategies for load scheduling and energy trading depend on the hourly market price variations, consumption preferences of the participants, and any other prevailing network constraints. An aggregation can comprise a variety of participating peers including smart households and businesses, collection of electric vehicles, battery banks, wind mills, and solar farms. Depending on their composition, aggregations may have different characteristics, such as load consuming only, load consuming with storage, storage only, load consuming with storage and generation, among others. These characteristics in turn guide their cost minimization and trading approaches. For example, an aggregation of only load consuming entities (ALCEs) will optimally schedule its deferrable loads when the market prices are lower. Also, to reduce the risk from spikes in market prices, ALCEs may enter into contracts for electricity trading with aggregations having storage capacities. Such trading contracts can be drafted as option contracts. In this paper, we consider energy trading between two aggregations, one comprising smart load consuming entities only (ALCE) and the other is an aggregation of EVs (AEV). For the energy trading contract to be fair to both, we develop a Nash bargaining model using the operational strategies of the both ALCE and AEV. We limit our model to two aggregations in order to get better insight into their interactions.

We first develop cost minimizing operational models for ALCE and AEV. We consider that both aggregations buy needed electricity from the grid (paying the market price) and trade electricity using option contracts. The operational models are then used to develop a generalized Nash bargaining solution (GNBS) approach for designing option contracts. The approach also incorporates relative market powers of the aggregations. The ALCE is considered to have two types of loads, fixed and deferrable, of which only the deferrable load schedules are optimized. Deferrable loads in turn are considered to be of two types: shiftable and adjustable. Shiftable loads are scheduled at any time within their respective predefined time windows. Whereas for adjustable loads, both the time of operation and the level of power consumption can be altered while satisfying their total power requirement within a predefined time window. The EVs in the AEV are considered heterogeneous with different battery sizes, arrival and departure times, maximum and minimum allowable state of charge (SOC), and maximum rates of charge/discharge. The price of electricity is consider to be available to ALCE and AEV at the start of each time interval of a day (say, an hour). Price is assumed to vary with time based on demand, supply, and network conditions and is considered as an exogenous input to our model.

It is assumed that ALCE and AEV predict the time-varying electricity prices and optimize their daily operations. The ALCE's operational model is formulated as a mixed integer program that schedules all loads of the day to minimize cost. Electricity consumed by the ALCE loads is drawn from both the network (based on the price) as well as from the AEV (based on the contract). The AEV consumes electricity from the network to meet the SOC requirements of the EV owners

and also to store excess energy in the batteries to trade with ALCE. The operational model of AEV is formulated as a mixed integer program. It considers both cost and revenue. The cost is the amount paid to the grid for electricity, and the revenue comprises the payments it receives from the EV owners and the ALCE. The AEV is also considered to pay overcharge and undercharge penalties to the EV owners. These penalties are incurred if at the time of departure from the parking-lot, the SOC of an EV battery is either above or below the charge level desired by the EV owner. A schematic of the interactions between the ALCE, AEV, and the network is presented in Figure 1. We consider both plain and swing option contracts between ALCE and AEV. An option contract is defined by its time window, strike price, option quantity, and option value. The use of financial instruments like option contracts is common in trading electricity between market constituents (see for example [20, 23]). However, the design of such instruments in the context of various forms of energy trading among peers is still a growing research area.

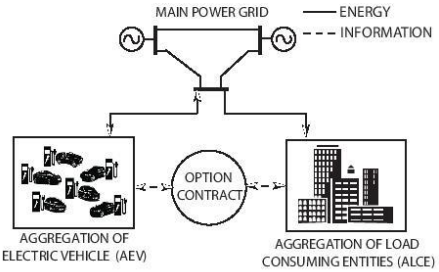

Fig. 1: Energy and information flow between ALCE and AEV

A. Contributions of this paper

Peer-to-peer trading in a power network is a well examined topic, where peers are commonly assumed to be prosumers (households with generation and storage capabilities). However, growth of IoT and advanced metering infrastructure has lead to the rise of a set of newly empowered peers, namely smart homes and businesses and EVs. In our previous work [11], we have shown how these peers are now able to form coalitions and reduce their operational cost by engaging in demand response, in markets with hourly price variations and price spikes. In this paper, we demonstrate that, in markets with price variations and spikes, aggregations formed by these peers can also effectively engage in energy trading and derive financial benefits that are fair to all. This is demonstrated by developing a generalized Nash bargaining solution (GNBS) model for obtaining trading contract between two aggregations and implementing it on a sample problem. The operational optimization models for the aggregations that we have formulated as input for the GNBS model are also novel in how they schedule load consumption and plan for energy sharing. Our contributions also include a computational strategy where instead of solving the GNBS model as one single nonlinear mixed integer program, we separately solve the operational models and use their results to solve GNBS model and obtain the contract parameters.

B. Related literature

Peer-to-peer trading in power markets is an ongoing area of research. Excellent reviews of the various aspects of prosumer-based peer-to-peer energy trading can be found in [23, 25]. However, effective mechanisms to schedule load and trade electricity in P2P networks are still in their early stages of development [10, 25]. The concept of nonprosumer peers forming coalitions to trade energy among themselves, as considered in this paper, is relatively new. One such mechanism has recently been modeled in [11], which demonstrates how an aggregation of peers comprising smart homes and businesses and EVs can generate cost savings and share it in a fair and equitable manner among the participating peers. The aforementioned paper considers a number of practical features of the power market, including modeling of price and demand data, network constraints, day ahead commitment, and real time price spikes. In what follows, we review some of the relevant literature in three categories: P2P trading mechanisms, use of options contract in power markets, and EV based P2P trading.

Bilateral contract networks as a new scalable market design for P2P energy trading is presented in [14]. It considers both real-time and forward markets for energy trading contracts between generators and consumers with fixed and deferrable loads and/or renewable sources. They show that utility-maximizing preferences for these contracts satisfy conditions essential for establishing the existence of a stable outcome from which agents do not wish to mutually deviate. Forward and real-time energy contracts were also considered in [27]. A coalition formation game framework is proposed in [24], to help prosumers decide whether or not it is profitable to bid its battery capacity in the P2P market for energy trading. The proposed mechanism allows prosumers to compare the benefit from participating in the P2P trading with and without using its battery, allowing the prosumer to form suitable social coalition groups. A discrete-time double-sided auction model to enable energy trading between prosumers in near real-time and forward markets was proposed in [5]. This device-oriented bidding strategy considers the physical characteristics and the technical limitations of each device type, such as EVs or heatpumps, and use them maximize the system reliability. It was shown that prosumers can reduce their cost on average by 23% using the proposed approach. The main challenges towards real world implementations of P2P mechanisms are to scalability and asynchronicity of the negotiation process. The work in [13] analyzed these challenges, by comparing distributed community-based market approaches to decentralized and distributed versions of P2P electricity markets. The computational properties of distributed and decentralized algorithms (ADMM and RCI) for market clearing were also assessed. It was shown that community-based distributed approaches are faster and more robust. Centralized and distributed P2P markets are also contrasted in [9]. The paper characterizes the solution of the P2P market as a variational equilibrium problem (without price arbitrage) and shows that the solution corresponds to that of social welfare optimization.

Choice of option contract for trading of electricity in the day-ahead market is studied in [21]. It is shown that the power producers participating in both day-ahead and option markets can get a higher share of the profit than those who only participate in the day-ahead market. A multi-stage stochastic model is proposed in [18] to determine optimal option and forward contracts for risk-averse producers. It is shown that option contracts can reduce price and availability risks in power markets. Real options approach is used in [6] to evaluate the economic value of demand response programs (DRPs). A probabilistic model for a real option contract between an aggregator and its customers can be found in [20]. The model determines the option value i.e., the incentive paid to the customers by the aggregator, for the right to engage in demand response by shifting loads. Other examples of option contract for electricity trading can be found in the literature, for example, between generators and SO [3], demand-side customers and SO [17], and among microgrids [16].

Although energy storage using stand-alone batteries is still quite expensive, impending growth of EVs may soon offer an alternative. It is estimated that the number of EVs in the U.S. will grow to 145 million by 2030 [26]. Considering an average battery capacity of 70 kWh, these vehicles have the potential to optimally store and share up to 1015 GWh per day. There is a significant body of literature on optimal operation of EVs i.e., optimal charging and discharging for trading (arbitrage). An auction-based game theoretic approach for optimal charging of a group of EVs over a finite horizon is examined in [29]. In [1], a stochastic programming methodology is developed to maximize aggregator's profit by optimally scheduling charging of EVs under varying market prices. Auction games for P2P energy trading using EVs in smartgrids is explored in [7]. A double-auction based noncooperative game approach in [19] examines how groups of PHEVs can benefit by selling a part of their stored energy back to the power market. The work in [2] examines P2P trading of electricity between two sets of EVs resulting in a significant reduction of the impact of charging process on the power network during business hours. It is shown that the trading also greatly reduces the energy cost paid by the EV owners.

The remainder of this paper is organized as follows. Section II presents mixed integer linear programs to obtain optimal operational strategies for ALCE and AEV for both plain and swing option contracts. In Section III, the GNBS model is presented and its solution approach is discussed. A case study in Section IV developed using price and demand data from PJM market (in the U.S.) demonstrates the efficacy of the GNBS model. Section V presents the concluding remarks.

II. Operational Models for ALCE and AEV with option contract

In this section, we develop separate operational models for ALCE and AEV considering two different types of call option contracts (plain and swing) for bilateral trading of electricity.

A. Operational Models with plain option

By participating in a plain call option, the ALCE holds the right, not the obligation, to acquire a fixed amount of electricity from AEV at a prespecified strike price during a time interval within a given time window. The ALCE pays a fee (option value) to the AEV for the right.

1) ALCE's model for plain option: We consider that the ALCE loads are of two types: fixed and deferrable loads. Schedules of fixed loads are not controlled. Deferrable loads are considered to have two subcategories, shiftable and adjustable loads. Operation of shiftable loads can be scheduled at any time within their respective time windows. Whereas, for adjustable loads, both time as well as level of power consumption can be altered, while satisfying their total power requirement during operational time windows.

Each load consuming entity (LCE) i within an ALCE (denoted by $\mathcal{C}$) has a set of shiftable loads denoted by $\mathcal{S}_i$. For an individual load $j \in \mathcal{S}_i$, the consumption level per unit time is s_{ij} and its length of operation is τ_{ij}. The start and finish time intervals within which shiftable load j can be scheduled are denoted by $\underline{T_j}, \overline{T_j} \in \mathcal{T}$, where $\mathcal{T}$ denotes the set of all time intervals of a day over which the loads are scheduled. Let x_{ijt} denote a binary variable indicating on/off status of the shiftable load j of i^{th} LCE during time interval $t \in \mathcal{T}$. Then, we can write:

$$\sum_{t=\underline{T_j}}^{\overline{T_j}} x_{ijt} = \tau_{ij}, \qquad \forall i \in \mathcal{C},\ \forall j \in \mathcal{S}_i. \tag{1}$$

We denote the set of adjustable loads within a LCE i as $\mathcal{A}_i$. The maximum (minimum) level of consumption per unit time of individual loads $j \in \mathcal{A}_i$ is denoted by $\overline{R_{ij}}$ ($\underline{R_{ij}}$) within the allowable time window $[\underline{R_j}, \overline{R_j}]$. Let y_{ijt} be a binary variable indicating on/off status of the adjustable load j of i^{th} LCE during time interval $t \in \mathcal{T}$, r_{ijt} be the energy consumption level, and σ_{ij} be the total required consumption. Then,

$$\underline{R_{ij}}\, y_{ijt} \le r_{ijt} \le \overline{R_{ij}} y_{ijt}, \quad \forall i \in \mathcal{C},\ \forall j \in \mathcal{A}_i,\ \forall t \in \mathcal{T}, \tag{2}$$

$$\sum_{t=\underline{R_j}}^{\overline{R_j}} r_{ijt} = \sigma_{ij}, \qquad \forall i \in \mathcal{C},\ \forall j \in \mathcal{A}_i. \tag{3}$$

Let $\mathcal{F}_i$ be the set of fixed loads and $f_{ijt} \in \mathcal{F}_i$ be the j^{th} fixed load of LCE i at time interval t. Then, the total energy that LCE i consumes at a given time interval t is:

$$d_{it} = \sum_{j \in \mathcal{F}_i} f_{ijt} + \sum_{j \in \mathcal{S}_i} s_{ij} x_{ijt} + \sum_{j \in \mathcal{A}_i} r_{ijt},\ \forall t \in \mathcal{T},\ i \in \mathcal{C}. \tag{4}$$

Thus, the energy that the ALCE must buy from the grid at a give time period is:

$$d_t = \begin{cases} \sum_{i \in \mathcal{C}} d_{it} - q_t, & t_s \le t \le t_e, \\ \sum_{i \in \mathcal{C}} d_{it}, & \text{Otherwise}, \end{cases} \tag{5}$$

where q_t is the energy bought form the AEV at time interval t within the option window defined by time intervals t_s and t_e. Recall that a plain call option can only be exercised once, and the ALCE has the right, but not the obligation, to exercise.

Hence, we need to add the following constraints. Let $z_t = 1$, if energy is purchased by the ALCE from the AEV during the time interval t and 0 otherwise, and Q is the option quantity. Then we can write that

$$\sum_{t=t_s}^{t_e} z_t \leq 1, \text{ and } q_t = Qz_t, \qquad \forall t_s \leq t \leq t_e. \tag{6}$$

Let Π_t, K and V be the market price of electricity, the option strike price, and the option value (paid once a day) respectively. The ALCE aims to minimize the total cost of its LCEs using the model below.

$$u^{\mathsf{ALCE}}(K, V, Q, \mathbf{\Pi}) =$$
$$\min \sum_{t\in\mathcal{T}} \Pi_t d_t + \sum_{t=t_s}^{t_e} Kq_t + V, \tag{7}$$
s.t., (1)–(6),
$$d_t, d_{it}, q_t, r_{ijt} \geq 0, \quad \forall t \in \mathcal{T},\ \forall i \in \mathcal{C}, \forall j \in \mathcal{A}_i, \tag{8}$$
$$x_{ijt} \in \{0,1\}, \quad \forall t \in \mathcal{T},\ \forall i \in \mathcal{C}, \forall j \in \mathcal{S}_i, \tag{9}$$
$$y_{ijt} \in \{0,1\}, \quad \forall t \in \mathcal{T},\ \forall i \in \mathcal{C}, \forall j \in \mathcal{A}_i, \tag{10}$$
$$z_t \in \{0,1\}, \quad \forall t \in \mathcal{T}. \tag{11}$$

2) AEV's model for plain option: Let $\mathcal{B}$ denote the set of EV batteries in the AEV. For a given time interval $t \in \mathcal{T}$, energy balance of the battery $b \in \mathcal{B}$ can be written as:

$$\phi_b s_{bt} = \phi_b s_{b,t-1} + p^+_{bt} - p^-_{bt}, \qquad \forall t \in \mathcal{T},\ \forall b \in \mathcal{B}, \tag{12}$$

where ϕ_b is the maximum capacity of the battery b, $s_{bt} \in (0,1)$ is the state of charge of battery b at the end of time interval t, p^+_{bt} is the amount of energy that the b^{th} battery draws from the grid at time interval t, and p^-_{bt} is the amount of energy that is extracted from battery. We assume that, the state of charge of EV batteries are not allowed to be 0 nor 1, and hence the following constraint is added to the model.

$$\underline{S_{bt}} \leq s_{bt} \leq \overline{S_{bt}}, \forall t \in \mathcal{T},\ \forall b \in \mathcal{B},\ 0 < \underline{S_{bt}} \leq \overline{S_{bt}} < 1. \tag{13}$$

Furthermore, the charging (discharging) rate of a battery have a technical upper bound, which in general is a convex and monotonically decreasing (increasing) function of the current state of charge. For simplicity, we assume the bounds to be constant. Hence, we can write that

$$0 \leq p^+_{bt} \leq P^+ w^+_{bt} \qquad \forall t \in \mathcal{T},\ \forall b \in \mathcal{B}, \text{ and} \tag{14}$$

$$0 \leq p^-_{bt} \leq P^- w^-_{bt}, \qquad \forall t \in \mathcal{T},\ \forall b \in \mathcal{B}, \tag{15}$$

where P^+ (P^-) is the charging (discharging) upper bound, and w^+_{bt} (w^-_{bt}) is 1 if battery b is charging (discharging) at time interval t, and 0 otherwise. The next constraint guarantees that the battery b is not in charging and discharging simultaneously during time interval t:

$$w^+_{bt} + w^-_{bt} \leq \omega_{bt}, \qquad \forall t \in \mathcal{T},\ \forall b \in \mathcal{B}, \tag{16}$$

where ω_{bt} is a binary parameter with the value of 1 if the b^{th} battery is connected, i.e., the EV is in the parking lot, and 0 otherwise.

We assume that the EV owners are assessed a flat price g ($¢/kWh$) for charging, even though the aggregation (AEV) pays to the system operator based on time varying prices. The flat price assumption is considered to relieve EV owners of price anxiety. Note that, the value of the flat price (g ($¢/kWh$)) can always be adjusted by the aggregation to meet its objective (profit or non profit). Hence, AEV receives a revenue from each EV equal to $g(s_{bT_b} - s_{b0})\phi_b$, where s_{b0} is the initial state of charge and $T_b \in \mathcal{T}$ is the departure time of the b^{th} EV. We denote the minimum required state of charge at the time of departure of the b^{th} EV as δ_{bT_b}. Similarly, we denote the desired state of charge at the time of departure as ρ_{bT_b}. If the state of charge at the time of departure is above ρ_{bT_b}, the revenue for the surplus energy is assessed by AEV at a lower rate of $g - \mu_1$, where μ_1 is the overcharge penalty. The AEV also pays the EV owner an undercharge penalty μ_2 ($¢/kWh$) for each unit of energy below ρ_{bT_b} at the time of departure. To calculate the total amount of undercharge and overcharge penalties, we introduce two continuous variables as follows:

$$s_{bT_b} - \rho_{bT_b} = s^1_b - s^2_b \qquad \forall b \in \mathcal{B}, \tag{17}$$

where $s^1_b, s^2_b \geq 0$. Then the total overcharge and undercharge penalty (revenue losses) are computed as $\mu_1 \sum_{b\in\mathcal{B}} \phi_b s^1_b$ and $\mu_2 \sum_{b\in\mathcal{B}} \phi_b s^2_b$, respectively. The option related constraints are discussed next.

The following constraint is introduced to account for the power that AEV commits to ALCE in the option window:

$$\sum_{b\in\mathcal{B}} p^-_{bt} = \tilde{q}_t(\mathbf{\Pi}, K), \qquad t_s \leq t \leq t_e. \tag{18}$$

The option quantity must be supplied using the stored power if the option is exercised. However, the AEV does not know the decision making process of the ALCE, therefore it must estimate q_t. We denote as estimate of the vector $\boldsymbol{q}$ given the random price of electricity $\mathbf{\Pi}$ as $\tilde{\boldsymbol{q}}(\mathbf{\Pi}, K)$, or in component-wise form, $\tilde{q}_t(\mathbf{\Pi}, K)$. Hence the AEV's model for the plain option is formulated as follows.

$$u^{\mathsf{AEV}}(K, V, Q, \mathbf{\Pi}) =$$
$$\min \sum_{t\in\mathcal{T}}\sum_{b\in\mathcal{B}} \Pi_t p^+_{bt} + \mu_1 \sum_{b\in\mathcal{B}} \phi_b s^1_b + \mu_2 \sum_{b\in\mathcal{B}} \phi_b s^2_b$$
$$- g(s_{bT_b} - s_{b0})\phi_b - K\sum_{t=t_s}^{t_e} \tilde{q}_t(\mathbf{\Pi}, K) - V, \tag{19}$$
s.t., (12)–(18),
$$p^+_{bt}, p^-_{bt}, s_{bt}, s^1_b, s^2_b \geq 0, \qquad \forall t \in \mathcal{T},\ \forall b \in \mathcal{B}, \tag{20}$$
$$w^+_{bt}, w^-_{bt} \in \{0,1\}, \qquad \forall t \in \mathcal{T},\ \forall b \in \mathcal{B}, \tag{21}$$

where

$$\tilde{q}_t(\mathbf{\Pi}, K) = Q\tilde{z}_t(\mathbf{\Pi}, K), \quad t_s \leq t \leq t_e, \tag{22}$$
$$\tilde{\boldsymbol{z}}(\mathbf{\Pi}, K) = \arg\max_{\tilde{\mathbf{z}}} \sum_{t=t_s}^{t_e} (\Pi_t - K)\tilde{z}_t, \tag{23}$$
$$\text{s.t.,} \sum_{t=t_s}^{t_e} \tilde{z}_t \leq 1, \tag{24}$$
$$\tilde{z}_t \in \{0,1\}, \quad t_s \leq t \leq t_e. \tag{25}$$

For simplicity of notation, we define $\boldsymbol{C} = (K, V, Q)$ for the plain option, and write the disutility functions as $u^{\mathsf{ALCE}}(\boldsymbol{C}, \boldsymbol{\Pi})$ and $u^{\mathsf{AEV}}(\boldsymbol{C}, \boldsymbol{\Pi})$. Note that these disutilities are random variables.

B. Operational Models with swing option

Swing call option for electricity, as considered here, differs from our plain call option in the following manner: purchase of contract quantity can be divided among one or more time intervals within the window; purchase quantities may have time dependent bounds; the strike price may either be fixed or vary for different time intervals; the ramp up/down rates of quantity purchased may also be bounded.

1) ALCE's model for swing option: In addition to constraints (1)–(5) and (8)–(11) in the ALCE's model for plain option, we need a few other constraints as described below. In a swing contract, if ALCE exercises the option, the energy bought at each interval as well as the total quantity bought over the contract window must satisfy

$$\underline{Q_t} z_t \le q_t \le \overline{Q_t} z_t, \quad t_s \le t \le t_e, \text{ and} \tag{26}$$

$$\underline{Q}\, z \le \sum_{t=t_s}^{t_e} q_t \le \overline{Q}\, z, \tag{27}$$

where $\underline{Q_t}(\overline{Q_t})$ and $\underline{Q}(\overline{Q})$ are the lower (upper) bounds for energy purchase during a time interval t and over the total contract window, respectively. Also, $z_t = 1$ if the option is exercised at time interval t and 0 otherwise, and $z = 1$ if the option is exercised at least once within the window. Therefore the relationship between z_t and z is given as

$$\sum_{t=t_s}^{t_e} z_t \le (t_e - t_s + 1) z. \tag{28}$$

Then the ALCE model for a swing call option can be given as

$$u^{\mathsf{ALCE}}(K, V, \underline{Q_t}, \overline{Q_t}, \underline{Q}, \overline{Q}, \boldsymbol{\Pi}) =$$

$$\min \sum_{t \in \mathcal{T}} \Pi_t d_t + \sum_{t=t_s}^{t_e} K q_t + V, \tag{29}$$

$$\text{s.t., } (1)-(5), (8)-(11), (26)-(28), z \in \{0,1\}. \tag{30}$$

2) AEV's model for swing option: Since the AEV is subjected to the value of q_t chosen by the ALCE, the same general model proposed for plain option in (19) applies for the second stage problem in a swing contract. However, the first stage must consider the additional contract parameters. Then we have that

$$u^{\mathsf{AEV}}(K, V, \underline{Q_t}, \overline{Q_t}, \underline{Q}, \overline{Q}, \boldsymbol{\Pi}) =$$

$$\min \sum_{t \in \mathcal{T}} \sum_{b \in \mathcal{B}} \Pi_t p_{bt}^{+} + \mu_1 \sum_{b \in \mathcal{B}} \phi_b s_b^1 + \mu_2 \sum_{b \in \mathcal{B}} \phi_b s_b^2$$
$$- g(s_{bT_b} - s_{b0})\phi_b - K \sum_{t=t_s}^{t_e} \tilde{q}_t(\boldsymbol{\Pi}, K) - V, \tag{31}$$

$$\text{s.t., } (12)\text{–}(18), (20), (21),$$

where

$$\tilde{\boldsymbol{q}}(\boldsymbol{\Pi}, K) =$$

$$\arg\max_{\tilde{q}} \sum_{t=t_s}^{t_e} (\Pi_t - K)\tilde{q}_t, \tag{32}$$

$$\text{s.t., } \underline{Q_t}\tilde{z}_t \le \tilde{q}_t \le \overline{Q_t}\tilde{z}_t, \quad t_s \le t \le t_e, \tag{33}$$

$$\underline{Q}\,\tilde{z} \le \sum_{t=t_s}^{t_e} \tilde{q}_t \le \overline{Q}\,\tilde{z}, \tag{34}$$

$$\sum_{t=t_s}^{t_e} \tilde{z}_t \le (t_e - t_s + 1)\tilde{z}, \tag{35}$$

$$\tilde{z}_t \in \{0,1\} \quad t_s \le t \le t_e, \tag{36}$$

$$\tilde{z} \in \{0,1\}. \tag{37}$$

For simplicity of notation, we define $\boldsymbol{C'} = (K, V, \underline{Q_t}, \overline{Q_t}, \underline{Q}, \overline{Q})$ for the swing option, and write the disutility functions as $u^{\mathsf{ALCE}}(\boldsymbol{C'}, \boldsymbol{\Pi})$ and $u^{\mathsf{AEV}}(\boldsymbol{C'}, \boldsymbol{\Pi})$. This two-stage formulation was adapted from [8].

III. Call option contract design

In this section, we present the model to obtain the optimal strike price and option value when all the other option parameters are given for the plain and swing option contracts. We use the Nash's approach to the bargaining problem to obtain a fair option contract for both ALCE and AEV while considering their relative market power.

The objectives of ALCE and AEV are to minimize their disutility by establishing an optimal option contract. However, since the objectives are in conflict, a contract that simultaneously minimizes their costs does not exist. In such a scenario, the aggregators may cooperatively bargain with each other to find the most appropriate contract. The bargaining problem can be formalized as follows [28]. Let $n = 1, 2, ..., N$ be the set of players, and S be a closed and convex subset of $\mathbb{R}^N$ that represents the set of feasible payoff (cost) allocations that the players can get if they cooperate. Let u_0^k denote the minimal (maximal) payoff (cost) that the k^{th} player would expect without cooperation. The vector (S,u_0^1, ..., u_0^N) is called a N-person bargaining problem. We chose the Nash bargaining solution (NBS) to address the two person (ALCE and AEV) bargaining problem. NBS is known to be invariant, Pareto optimal, independent of irrelevant alternatives, and symmetrical. In a bilateral negotiation, it is reasonable to expect that the player with higher market power will have a larger share of the benefits than the weaker player. To incorporate the market power, we use the generalized Nash bargaining solution (GNBS) approach [12]. The GNBS for the plain option contract can be formulated as:

$$\max \Big(\mathbb{E}[u^{\mathsf{ALCE}}(\boldsymbol{0}, \boldsymbol{\Pi})] - \mathbb{E}[u^{\mathsf{ALCE}}(\boldsymbol{C}, \boldsymbol{\Pi})]\Big)^{\alpha}$$
$$\Big(\mathbb{E}[u^{\mathsf{AEV}}(\boldsymbol{0}, \boldsymbol{\Pi})] - \mathbb{E}[u^{\mathsf{AEV}}(\boldsymbol{C}, \boldsymbol{\Pi})]\Big)^{1-\alpha} \tag{38}$$

$$\text{s.t., } (1)-(25),$$

where $\alpha \in (0,1)$ is an indicator of ALCE's relative market power, and $\mathbb{E}[u^{\mathsf{ALCE}}(\mathbf{0},\mathbf{\Pi})])$ is ALCE's expected payoff at the disagreement point; $\mathbb{E}[u^{\mathsf{AEV}}(\mathbf{0},\mathbf{\Pi})]$ denotes the same for AEV.

The GNBS formulation for the swing option is similar to that of plain option, the only difference being in the set of constraints that define the feasible set. It can be written as

$$\begin{aligned}\max\ &\Big(\mathbb{E}[u^{\mathsf{ALCE}}(\mathbf{0},\mathbf{\Pi})] - \mathbb{E}[u^{\mathsf{ALCE}}(\boldsymbol{C'},\mathbf{\Pi})]\Big)^{\alpha} \\ &\Big(\mathbb{E}[u^{\mathsf{AEV}}(\mathbf{0},\mathbf{\Pi})] - \mathbb{E}[u^{\mathsf{AEV}}(\boldsymbol{C'},\mathbf{\Pi})]\Big)^{1-\alpha} \qquad (39)\\ \text{s.t.,}\ &(1)-(5),(8)-(11),(12)\text{–}(18),(20),(21),\\ &(26)-(28),(30),(32)-(37).\end{aligned}$$

Note that, $u^{\mathsf{ALCE}}(\boldsymbol{C},\mathbf{\Pi})$ and $u^{\mathsf{AEV}}(\boldsymbol{C},\mathbf{\Pi})$ can be written as

$$u^{\mathsf{ALCE}}(\boldsymbol{C},\mathbf{\Pi}) = u^{\mathsf{ALCE}}(K,0,Q,\mathbf{\Pi}) + V, \qquad (40)$$

$$u^{\mathsf{AEV}}(\boldsymbol{C},\mathbf{\Pi}) = u^{\mathsf{AEV}}(K,0,Q,\mathbf{\Pi}) - V. \qquad (41)$$

Similar expressions can be written for the swing option.

In the rest of this section, we present an approach for obtaining the optimal values of the option parameters. An expression for the option value V can be found using the first and second order conditions for a given strike price K. Let, for the plain option, we denote the objective function of the NBS problem as $\overline{N}$, where

$$\begin{aligned}\overline{N} =&\Big(\mathbb{E}[u^{\mathsf{ALCE}}(\mathbf{0},\mathbf{\Pi})] - \mathbb{E}[u^{\mathsf{ALCE}}(\boldsymbol{C},\mathbf{\Pi})]\Big)^{\alpha} \\ &\Big(\mathbb{E}[u^{\mathsf{AEV}}(\mathbf{0},\mathbf{\Pi})] - \mathbb{E}[u^{\mathsf{AEV}}(\boldsymbol{C},\mathbf{\Pi})]\Big)^{1-\alpha}. \qquad (42)\end{aligned}$$

For swing option, the expression for $\overline{N}$ is same as above with $\boldsymbol{C}$ replaced by $\boldsymbol{C'}$.

Proposition 1. *For any given K and Q, the optimal option value V is given as*

$$\begin{aligned}V =&(1-\alpha)\Big(\mathbb{E}[u^{\mathsf{ALCE}}(\mathbf{0},\mathbf{\Pi})] - \mathbb{E}[u^{\mathsf{ALCE}}(\tilde{\boldsymbol{C}},\mathbf{\Pi})]\Big) \\ &- \alpha\Big(\mathbb{E}[u^{\mathsf{AEV}}(\mathbf{0},\mathbf{\Pi})] - \mathbb{E}[u^{\mathsf{AEV}}(\tilde{\boldsymbol{C}},\mathbf{\Pi})]\Big),\end{aligned} \qquad (43)$$

where $\tilde{\boldsymbol{C}} = [K,0,Q]$ for the plain option and $\tilde{\boldsymbol{C}} = [K,0,\underline{Q_t},\overline{Q_t},\underline{Q},\overline{Q}]$ for the swing option.

The value of V in (43) maximizes $\overline{N}$. Note that, since V does not appear in any of the constraints of the GNBS model (38) and (39), we can use the first and the second order conditions. Taking the logarithm of $\overline{N}$ and letting $\frac{\partial \log(\overline{N})}{\partial V} = 0$, we obtain the optimal V in (43). It can be checked that $\frac{\partial^2 \log(\overline{N})}{\partial V^2} < 0$ for all $\alpha \in (0,1)$. Note that the option value V can be obtained by independently solving the models of ALCE and AEV.

Note that, if both K and V are given, since there are no other common variables between the ALCE's and the AEV's models, the optimal solution of the GNBS formulation in (38) and (39) can be found by solving the models of the ALCE and AEV individually. However, if only V is given, the optimal solution of the problem can be found by effectively exploring the possible values of K. Also, to obtain optimal values for the option parameters (K and V) as well as the GNBS solution, we need to asses the value of $\mathbb{E}[u^{\mathsf{ALCE}}(\tilde{\boldsymbol{C}},\mathbf{\Pi})]$ and $\mathbb{E}[u^{\mathsf{AEV}}(\tilde{\boldsymbol{C}},\mathbf{\Pi})]$, for which we use the sequential Montecarlo simulation approach as implemented in [21] and [20].

IV. Numerical study

The numerical study objectives are: 1) to evaluate the cost and benefit of ALCE and AEV by entering into a bilateral trading contract, and 2) to examine the optimal choices of the contract parameter values. For this purpose we construct a sample numerical problem as follows. It is considered, for simplicity, that the ALCE and the AEV are connected to the same node of a network. The ALCE is comprised of five load consuming entities (LCEs), which are identical except that each has a separate time window (3–11, 5–14, 7–14, 12–21, and 10–17 hours) to operate its shiftable and adjustable loads. The total load of the ALCE is obtained by scaling down load data (by a factor of 240) from the DAY node of the PJM network in the U.S. The scaling factor was chosen to make the scope of ALCE's operation comparable to that of the AEV, described later. Of the total ALCE load, 40% is considered fixed and the remaining 60% is divided equally between shiftable and adjustable loads. The AEV is comprised of 200 EVs, each with battery capacity rating of 30 kWh. We assume that all EVs arrive at the parking facility at 8 AM and depart at 6 PM; random arrival and departure of EVs have been modeled in [22]. We also assume that EVs arrive to the parking facility with an average of 50% state of charge (SOC) and have an average desired SOC of 70% at the time of departure. The minimum and maximum SOC at the time of departure are 60% and 90%, respectively. It is considered that the EV owners pay a flat price to AEV for charging @ 8¢/kWh. The AEV incurs an undercharge/overcharge penalty (paid to the EV owners @ 5¢/kWh) if the SOC of an EV at the time of departure is below or above the desired SOC of 70%. The hourly locational marginal prices (LMPs) of electricity at the network node, where ALCE and AEV are connected, are obtained as follows. We consider the LMP data from DAY node of the PJM network during July 15, 2017 to July 30, 2017. From this LMP data, we calculate the mean and variance for each hour, and use those as parameters of the normal distributions that we assume to describe the hourly LMP variations. Random samples from these hourly distributions are drawn to generate a number of *daily price scenarios*, which are used in the Montecarlo simulation approach to solve the GNBS model.

Our GNBS model considers option quantity and market power as input. The decision variables are strike price and option value. However, since simultaneous optimization of both decision variables is computationally challenging, we optimize one parameter given the other. For the sample numerical problem, the time window for the option contract is considered to be from 3 PM to 6 PM. For the swing call option, the upper limit for quantity in any given time interval within the window is 250 kWh. Our model is implemented using Julia-0.6.2 and GUROBI 7.5.2. The results are summarized in Figures 2 through 4.

We first addressed our objective of assessing benefits of ALCE and AEV in entering into a bilateral contract. For this, we obtained the optimal values of their costs with and without

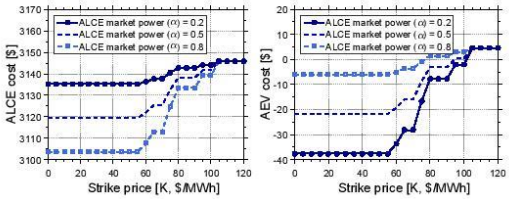

Fig. 2: ALCE and AEV cost for different optimal strike prices in plain call option

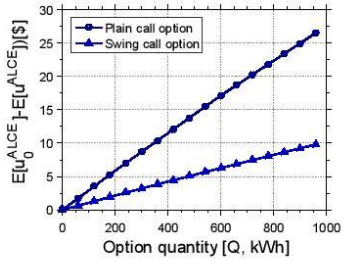

Fig. 3: ALCE cost saving comparison for different option quantites

contract, for various combinations of contract parameters K, V, and α, and a constant option quantity of 1000kWh. Figure 2 presents the results obtained from a plain option contract. For each value of the ALCE market power (α) and a wide range of strike prices (K), our solution approach obtained the corresponding optimal option values (V) as well as the expected costs for both ALCE and AEV (denoted as $\mathbb{E}[u^{\mathsf{ALCE}}]$ and $\mathbb{E}[u^{\mathsf{AEV}}]$). As observed from the figure, the cost reduces with increasing market power, for both parties. The cost curves have three distinct regions: for K values from \$0/MWh to \$55/MWh, \$55/MWh to \$105/MWh, and over \$105/MWh. The first region presents a number of alternative optimal solutions (i.e., various optimal combinations of K and V). In the second region, the cost increases with K for both ALCE and AEV. This is due to the fact that for $K >$\$55/MWh, the contract is often not exercised as some of the daily price scenarios do not exceed the strike price within the contract time window, thus reducing the benefits derived from the contract. In the third region, for $K >$\$105/MWh, none of the daily price scenarios generated for our sample numerical problem exceed the strike price. This yields an option value of zero, and the corresponding costs represent the case with no contract (disagreement point). The disagreement cost for ALEA and AEV are \$3145.8 and \$4, respectively. It is evident from the results that, for the chosen numerical problem and the price scenarios, the ALCE and AEV should select any strike price that is below the threshold of \$55/MWh to maximize their benefits from a bilateral contract. The maximum total benefit resulting from such a bilateral contract is \$52.65 per day, which is the sum of the differences between the disagreement cost and cost for K below \$55/MWh for ALCE and AEV. Their respective shares of the benefit are $\alpha \times \$52.65$ and $(1-\alpha) \times \$52.65$, respectively. Similar cost/benefit patterns have also been observed for swing option, and hence not presented here. We also examined benefits as a function of the option quantity (Q). Increasing trends for benefits vs. option quantity were observed for both option types, for the range Q between 0-1000 kWh. This is depicted in Figure 3 for ALCE. This increasing pattern should hold as long as ALCE has the capacity to fully consume the option quantity. If Q grows too large beyond ALCE's capacity, then the plain option benefit will sharply drop to zero. In our numerical problem, the AEV did not have the capacity to offer Q larger than what ALCE can accommodate. Hence, we could not generate a scenario where the plain option benefit would drop to zero.

Hereafter, per objective 2 of our numerical study, we explored the relationships between the optimal values of the contract parameters for plain option. Figure 4 (left) shows the optimal option values (V) corresponding to a range of strike prices (K), for various levels of ALCE market power (α). The optimal option values were obtained solving (43). It can be observed that V decreases monotonically (up to a certain point) with increases in K. Interestingly, the value of V drops below zero in some cases, which indicates that, beyond a certain value of K (e.g., approximately \$36/MWh for α=0.8), the GNBS makes the option value negative, where AEV pays the fee to ALCE. For lower values of ALCE's relative market power, V becomes negative at relatively higher strike prices. Beyond a certain strike price (\$70/MWh), the option value paid by AEV starts to decrease (move towards zero). This is due to the fact that, at such high values of K, an increasing number of the price scenarios remain below the strike price, thus not triggering the option purchase and reducing AEV's revenue. Further increases in the value of K gradually pushes the V to zero. It is observed that the turning point for V is independent of market power, as it depends only on the strike price and the considered set of price scenarios. A similar trend is observed (not presented here) for the swing call option, where the turning point for V is lower and approximately at $K =$ \$55/MWh. This reduction is as expected since AEV's revenue is higher in plain call option in this numerical example. Figure 4 (right) depicts the impact of option quantity Q on parameters V and K, for α=0.2. We observe the following. V increases with Q, albeit at a slower pace as K increases. Beyond a certain strike price (e.g., $K =$\$70/MWh), V decreases with increasing Q. Finally, if K is increased further (e.g., $K \geq$\$75/MWh), V remains constant at zero.

V. Concluding Remarks

Although energy trading in power markets is expanding among prosumers at the peer-to-peer level, trading among aggregations of end-use consumers has not yet been adequately explored. In this paper, our objective has been to promote local energy trading among aggregations of empowered end-use consumers. We have developed a bilateral option contract framework between two types of such aggregations , namely,

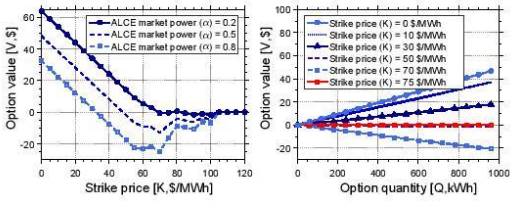

Fig. 4: Optimal option values for given strike prices and quantities (plain option)

aggregation of load consuming entities only (ALCE) and aggregation of electric vehicles (AEV). The framework uses a generalized Nash bargaining solution approach to find the optimal contract parameters. Using a sample numerical problem, we have examined the properties of two different kinds of option contracts (plain and swing) and assessed their benefits to the participating aggregations. We have demonstrated via numerical results that the aggregations of end-use consumers can benefit from bilateral contracts for trading electricity.

Our methodology has a few limitations that may be addressed in future work. First, we have assumed that both ALCE and AEV are loads on the same bus of the network. In practice, energy trading can occur between aggregations connected to different buses. In that case, congestion costs and differences in hourly LMPs must be considered for option contract design. This will require incorporation of an optimal power flow model in our methodology. Second, we have assumed in our model implementation that the EVs arrive to and depart from the parking facility at set times. A more generalized model implementation will consider the parking lots as smart hubs in which the EVs come and go throughout the day depending on their trip plans and charging needs. Finally, although we incorporate relative market power in bilateral contract design and examine its impact, it is not clear how to estimate its numerical value. The traditional approach to study market power in electricity markets uses concentration measures such as the Hirschman-Herfindahl Index (HHI) or the quantity modulated price index (QMPI) [15]. These measures are mostly used to estimate generators' market power and are used by FERC as fundamental screening tools for merger analysis in this sector. Research has shown that concentration based measures can be misleading indicators of the market power in electricity markets [4]. From a demand-side perspective, a body of research agrees that market power is a function of demand elasticity and the ability to respond to time-varying price signals. However, how to estimate the relative market power of peers engaged in energy trading remains an open research question.

References

[1] Alipour, M., B. Mohammadi-Ivatloo, M. Moradi-Dalvand, K. Zare. 2017. Stochastic scheduling of aggregators of plug-in electric vehicles for participation in energy and ancillary service markets. *Energy* **118** 1168–1179.

[2] Alvaro-Hermana, R., J. Fraile-Ardanuy, P. J. Zufiria, L. Knapen, D. Janssens. 2016. Peer to peer energy trading with electric vehicles. *IEEE Intelligent Transportation Systems Magazine* **8**(3) 33–44.

[3] Anderson, E. J., H. Xu. 2006. Optimal supply functions in electricity markets with option contracts and non-smooth costs. *Mathematical Methods of Operations Research* **63**(3) 387–411.

[4] Borenstein, S., J. Bushnell. 1999. An empirical analysis of the potential for market power in california's electricity industry. *The Journal of Industrial Economics* **47**(3) 285–323.

[5] El-Baz, W., P. Tzscheutschler, U. Wagner. 2019. Integration of energy markets in microgrids: A double-sided auction with device-oriented bidding strategies. *Applied energy* **241** 625–639.

[6] Fayaz-Heidari, A., M. Fotuhi-Firuzabad, R. Ghorani. 2019. Economic valuation of demand response programs using real option valuation method. *2019 27th Iranian Conference on Electrical Engineering (ICEE)*. IEEE, 685–691.

[7] Kang, J., R. Yu, X. Huang, S. Maharjan, Y. Zhang, E. Hossain. 2017. Enabling localized peer-to-peer electricity trading among plug-in hybrid electric vehicles using consortium blockchains. *IEEE Transactions on Industrial Informatics* **13**(6) 3154–3164.

[8] Kovacevic, R. M., G. C. Pflug. 2014. Electricity swing option pricing by stochastic bilevel optimization: a survey and new approaches. *European Journal of Operational Research* **237**(2) 389–403.

[9] Le Cadre, H., P. Jacquot, C. Wan, C. Alasseur. 2020. Peer-to-peer electricity market analysis: From variational to generalized nash equilibrium. *European Journal of Operational Research* **282**(2) 753–771.

[10] Lüth, A., J. M. Zepter, P. C. del Granado, R. Egging. 2018. Local electricity market designs for peer-to-peer trading: The role of battery flexibility. *Applied energy* **229** 1233–1243.

[11] Melendez, K. A., V. Subramanian, T. K. Das, C. Kwon. 2019. Empowering end-use consumers of electricity to aggregate for demand-side participation. *Applied Energy* **248** 372 – 382. doi: https://doi.org/10.1016/j.apenergy.2019.04.092. URL http://www.sciencedirect.com/science/article/pii/S0306261919307524.

[12] Moon, Y., C. Kwon. 2011. Online advertisement service pricing and an option contract. *Electronic Commerce Research and Applications* **10**(1) 38–48.

[13] Moret, F., T. Baroche, E. Sorin, P. Pinson. 2018. Negotiation algorithms for peer-to-peer electricity markets: Computational properties. *2018 Power Systems Computation Conference (PSCC)*. IEEE, 1–7.

[14] Morstyn, T., A. Teytelboym, M. D. McCulloch. 2019. Bilateral contract networks for peer-to-peer energy trading. *IEEE Transactions on Smart Grid* **10**(2) 2026–2035.

[15] Nanduri, V., T. K. Das. 2007. A reinforcement learning model to assess market power under auction-based energy pricing. *IEEE transactions on Power Systems* **22**(1) 85–

95.

[16] Nunna, H. K., S. Doolla. 2012. Demand response in smart distribution system with multiple microgrids. *IEEE transactions on smart grid* **3**(4) 1641–1649.

[17] Oren, S. S. 2001. Integrating real and financial options in demand-side electricity contracts. *Decision Support Systems* **30**(3) 279–288.

[18] Pineda, S., A. J. Conejo. 2013. Using electricity options to hedge against financial risks of power producers. *Journal of Modern Power Systems and Clean Energy* **1**(2) 101–109.

[19] Saad, W., Z. Han, H. V. Poor, T. Başar. 2011. A noncooperative game for double auction-based energy trading between phevs and distribution grids. *2011 IEEE international conference on smart grid communications (SmartGridComm)*. IEEE, 267–272.

[20] Schachter, J. A., P. Mancarella. 2015. Demand response contracts as real options: a probabilistic evaluation framework under short-term and long-term uncertainties. *IEEE Transactions on Smart Grid* **7**(2) 868–878.

[21] Sheybani, H. R., M. O. Buygi. 2017. Put option pricing and its effects on day-ahead electricity markets. *IEEE Systems Journal* (99) 1–11.

[22] Subramanian, V., T. K. Das. 2019. A two-layer model for dynamic pricing of electricity and optimal charging of electric vehicles under price spikes. *Energy* **167** 1266–1277.

[23] Tushar, W., T. K. Saha, C. Yuen, D. Smith, H. V. Poor. 2020. Peer-to-peer trading in electricity networks: An overview. *https://arxiv.org/abs/2001.06882 (last accessed on Jan 27, 2020)* .

[24] Tushar, W., T. K. Saha, C. Yuen, M. I. Azim, T. Morstyn, H. V. Poor, D. Niyato, R. Bean. 2020. A coalition formation game framework for peer-to-peer energy trading. *Applied Energy* **261** 114436.

[25] Tushar, W., C. Yuen, H. Mohsenian-Rad, T. Saha, H. V. Poor, K. L. Wood. 2018. Transforming energy networks via peer-to-peer energy trading: The potential of game-theoretic approaches. *IEEE Signal Processing Magazine* **35**(4) 90–111.

[26] Website. 2019. Global ev outlook 2019. https://www.iea.org/reports/global-ev-outlook-2019. Accessed: January 26, 2020.

[27] Zhang, B., C. Jiang, J.-L. Yu, Z. Han. 2018. A contract game for direct energy trading in smart grid. *IEEE Transactions on Smart Grid* **9**(4) 2873–2884.

[28] Zhang, Z., J. Shi, H.-H. Chen, M. Guizani, P. Qiu. 2008. A cooperation strategy based on nash bargaining solution in cooperative relay networks. *IEEE Transactions on Vehicular Technology* **57**(4) 2570–2577.

[29] Zou, S., Z. Ma, X. Liu, I. Hiskens. 2016. An efficient game for coordinating electric vehicle charging. *IEEE Transactions on Automatic Control* **62**(5) 2374–2389.

Appendix E: Article Submitted to Applied Energy

Optimal operation of a system of hubs and a fleet of shared autonomous electric vehicles in urban areas

Kevin A. Melendez*, Tapas K. Das, and Changhyun Kwon

Department of Industrial and Management Systems Engineering, University of South Florida

March 4, 2020

Abstract

Shared autonomous electric vehicles (SAEVs) are expected to replace a significant fraction of human driven ride sharing vehicles in cities and surrounding urban areas. This change will only be possible if proper cyber-physical system (CPS) infrastructure is made available to support their operations. We address this need by developing a methodology for planning as well as real-time decision making for operating a system of SAEVs and charging hubs located across the serving area. The charging hubs are considered to host limited capacity battery banks and photo voltaic (PV) generators. Our methodology considers a number of practical features of power and transportation systems, including consideration of day-ahead load commitment by solving an alternating current power flow model, real time price spikes of electricity, energy arbitrage, randomness in passenger demand, balking of passengers while waiting for a ride, and allowing charging for privately owned electric vehicles in the hubs. We demonstrated the utility of our methodology by implementing it on a sample CPS. It is shown through numerical results that the methodology is able to make planning decisions for day ahead commitment of power, as well as make real time operating decisions for the SAEVs and the hubs (including for its battery banks and PV generators). We also examine some of the system design issues such as hub capacity needed to support a fleet of given size, and impact of hub capacity and fleet size on system performance. We discuss the computational challenges of our methodology and propose a simplified myopic solution approach that is capable of dealing with much larger fleet sizes and a variety of hub capacities. Reduction in computation time and the optimality gap for the myopic approach are examined.

Keywords— Shared autonomous electric vehicles, day-ahead commitment, cyber-physical infrastructure

1 Introduction

Shared autonomous electric vehicles (SAEVs) are expected to replace a significant portion of the human driven automobiles on urban roads. The ride sharing companies serving cities and surrounding suburbs are

*Corresponding Author: kmelendez7@mail.usf.edu

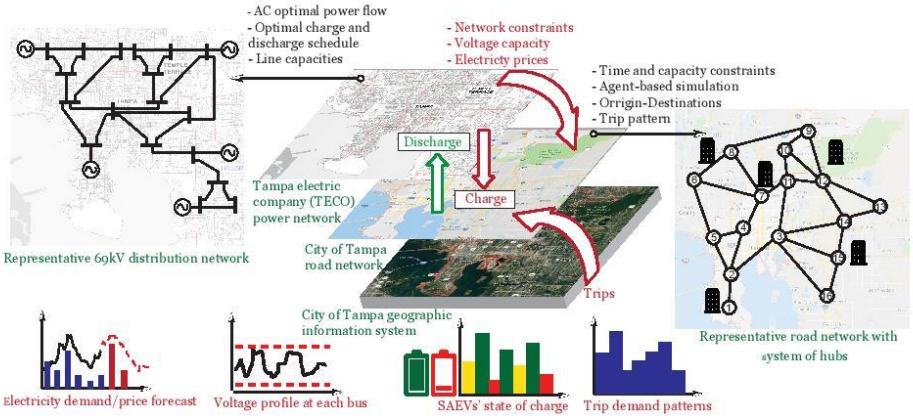

Figure 1: A three-tier diagram depicting interactions between population demographics, road network, and the power network in City of Tampa

soon likely to adopt a new business model, which will use SAEVs leased from large feet-owning companies instead of cars owned and driven by individual contractors. However, switching to a fleet of SAEVs for ride sharing will be feasible only if a proper cyber-physical system (CPS) is available for charging the batteries as well as coordinating among the vehicles and the transportation needs. The CPS will comprise physical hubs with charging stations, located across the service area, together with a supervisory communication and control system that will optimally manage the real-time (RT) operation of the SAEVs and the hubs. The hubs may have limited solar (PV) generation and stand alone battery banks. The hubs are capable of discharging both the SAEV batteries and the stand alone battery banks for selling power back to the grid, when appropriate (e.g., when the RT price of electricity is high). The hubs may allow private electric vehicle (EV) owners to charge for a fee when some charging stations are not occupied by fleet SAEVs. Hence, the control actions of the CPS will include the following: making day ahead (DA) power purchase commitment for each hub, and making real time operating decisions. The real time decisions will include 1) choosing the next action for each SAEV from among: serve a customer, charge or discharge at a hub, and idle at a parking lot, 2) for battery banks at each hub, either charge using grid/PV power or discharge to SAEVs and/or back to the grid, and 3) select the number of privately owned EVs to allow charging at each hub. Figure 1 presents a schematic of the interactions among the 3-tiers of infrastructure (geographic distribution of the population centers, the road network, and the power network) that is supported by the CPS.

In this paper, we develop a model-based methodology to obtain optimal operational strategies for a system of SAEVs and CPI serving an area. The objective of our methodology is to maximize the operational revenue of a given system for varying transportation demand and electricity prices. The system includes a fleet of heterogeneous SAEVs and a set of hubs characterized by their location, number and type of charging stations, PV generation capacity, and size of battery bank. It is assumed that there exists a varying level of demand for charging of privately owned EVs, which the system can serve, when deemed appropriate, to increase revenue. The operational revenue sources (for both income and expenses) are the following: passenger fare, selling power back to the grid, fees from the private EV owners, payment to the grid for electricity consumed, and parking fees for idling SAEVs. We consider that the operational decisions for the fleet and

the CPI are made by an operator as follows. S/he first commits a fraction of the estimated hourly charging load in the day ahead market, considering that any shortfall (excess) can be bought (sold) in the real time market. Thereafter, the fleet operator makes the real time operational decisions. The methodology is thus formulated as a sequential two-stage model. The first stage solves for the day ahead electricity purchase commitment decisions using a two-stage stochastic program, which considers the uncertainties in hourly load consumptions and real time prices. The second stage is formulated as a robust mixed integer linear program that decides the optimal actions in short time intervals for the SAEVs and the hubs.

The key contribution of this paper is a new methodology for operational decision making in an emerging cyber physical system (CPS) supporting both transportation and electric power networks. The application of the methodology on a sample problem yields insights for how to design such a CPS, for example determining the number of SAEVs, the number of the hubs with their locations and capacities, charging technology, and PV and battery bank sizes, together with whether to allow charging of privately owned EVs. Our methodology considers a number of practical features of power markets and the transportation sector including two-time scale (DA and RT) power market settlement, prices spikes in the RT market, power network constraints via AC optimal power flow (ACOPF) model, time varying travel demands, and balking of passengers. Our methodology addresses uncertainties in the RT electricity prices, PV generation, charging demands of privately owned EVs, and travel demand for the fleet vehicles. The novelty of our methodology also includes a reformulation of the model presented in Zhang et al. (2016) for SAEV scheduling and routing, which resulted in a reduction in the number of integer variables making the model easier to solve for a larger number of vehicles. The other novelty of our methodology is the integration within the transportation model a number of power network related constraints, which have been traditionally ignored; most of the openly available literature on electric vehicle integration focuses either mainly on the transportation aspects with simplifying assumptions about the electric power issues or vice versa.

Our methodology will create a number of other opportunities to benefit the electric power systems. As vehicle electrification soars, the percentage of electricity consumed for transportation will rise dramatically. A sizable part of this increase will be due to proliferation of SAEV-supported passenger ride sharing. Hence, a cyber-connected infrastructure for planned charging/discharging of large fleets of SAEVs will create an opportunity for network load balancing. Moreover, the temporal arbitrage potential of these fleets of vehicles would help power systems operators to reduce reserve generation requirement for maintaining system reliability. This will help to reduce operational cost of the power networks and consequently reduce cost to all consumers.

The rest of the paper is organized as follows. Section 2 presents a brief review of the recent literature on EV and SAEV operations. In Section 3 we give an overview of the step by step approach of our methodology. Section 4 contains the models used in each of the steps of the methodology, namely the ad hoc vehicle scheduling and charging model (Section4.1), load schedule and market clearing price estimation models (Section 4.2), two-stage stochastic model for day ahead commitment for the hubs (Section 4.3), and real time operational model (Section 4.4). The operational methodology is implemented on a case study built using demographic, transportation, and electric power information from the City of Tampa and its suburbs. Results from the case study are presented in Section 5. Due to the computational complexities of some of the steps of the operational methodology, an alternative myopic modeling approach and its comparative performance are presented in Section 6. Section 8 contains the concluding remarks.

2 Related literature

Though there is abundant literature on charging of privately owned EVs, work on SAEVs addressing issues like strategies for charge and discharge, locating charging stations, and algorithms for real-time control are still very limited (Iacobucci et al. 2019). Our study reveals that almost all of the relevant models for operation of EV or SAEV focus primarily on either the transportation or the electricity aspects of the problem. For example, charging-facility (hub) sizing and location models are typically approached from the transportation perspective. Whereas the models for optimal operation of the facilities deal mostly with power related considerations. Hub sizing and location models consider temporal-spatial distribution of the origin-destination of the trips, space availability across the road network, and charging strategies with implicit assumption that the power network related constraints are satisfied. On the other hand, the operational models are formed using electricity network characteristics, such as varying electricity prices, arbitrage contracts, active and reactive power, voltage capacities, and other network constraints, while considering the transportation related parameters as exogenous. In what follows, we examine the related literature on operation of EVs and SAEVs.

Optimal operation of EV fleets has received much attention in the recent literature. Operation of EV parking/charging lots at workplaces and commercial buildings by making power purchase commitments in the day ahead market is examined in Sedighizadeh et al. (2019). The paper considers uncertainties in the demand for charging, EV arrival and departure times, and electricity prices. However, some of the common features like providing services to the grid (e.g., load balancing) and charging of the EVs by renewable generation are not included. A real-time charging scheme for EV parking lots enabling them to participate in demand response programs is studied via a deterministic model in Yao et al. (2017). The model manages the impact of the parking lot on the power grid by setting a maximum limit for the power drawn at any point in time. It considers the charging priorities of all connected EVs to satisfy energy requirements while also guarantying fairness. The authors in Subramanian & Das (2019) present a model to study how increasing demand response capacity of a growing number of EV parking lots will promote dynamic pricing of electricity. The model considers day-ahead and real-time settlements, power network constraints (including congestion), real time prices uncertainties, and a granular parking lot operation with a large volume of EVs comprising different models, battery capacities, and charging needs; injecting power back to the grid or any other forms of temporal arbitrage are not considered. A model offered in Turan et al. (2019) minimizes power consumption and losses of an EV parking lot that is supplied by the grid as well as rooftop photo-voltaic panels. The model features include charging from non-dispatchable generation, dynamically varying electricity prices, reserve power for grid support, and meeting network capacity constraints.

Several papers on the operation of SAEV fleets and location of charging hubs have appeared in the open literature. A model proposed in Lam et al. (2018) studies how to coordinate a fleet of autonomous EVs to park at appropriate parking facilities to support vehicle-to-grid services. The authors also develop a distributed algorithm based on dual decomposition to solve the model efficiently. The model does not consider the electricity price and assumes that the availability of all vehicles is known in advance. A fleet of SAEV is simulated in Chen et al. (2016) via a discrete-time agent-based model to examine the capabilities of this vehicles to be shared, self-charged, and right sized considering passenger travels needs. The simulation model results are used to analyze the impacts of vehicle range and charging infrastructure on fleet size, charging station location, ability to meet trip demand, user wait times, and induced vehicle-miles traveled. The above agent-based simulation model was extended in Farhan & Chen (2018). The extended model determines the optimal routes to pick up and drop off multiple travelers within a given time interval using vehicles with fixed seating capacities. Thus the problem is formulated as a capacitated vehicle routing problem with time windows, which is then decomposed into a number of subproblems. The solution methodology first assigns

travel requests to vehicles, and then constructs an itinerary to pick up and drop off the travelers. According to the authors, Farhan & Chen (2018) is the first study that analyzes the dynamic ridesharing operations of SAEVs from the perspective of a fleet operator. A two-stage multi-objective optimization model for planning of an autonomous connected electric vehicle (ACEV)-based car-sharing system is given in Miao et al. (2019). Each stage is a multi-objective optimization model where both users and service providers objectives are considered. The authors also propose a hybrid parking mechanism to attain a compromise between user flexibility and system management efficiency. The work presented in Kang et al. (2017) offers a framework to optimally design a fleet of autonomous electric vehicles. The framework comprises four components, namely, fleet size and assignment schedule, sizing and location of charging stations, vehicle powertrain requirements, and service fees.

A methodology to simultaneously optimize SAEV charging, routing, and rebalancing can be found in Iacobucci et al. (2018*a*). It considers different time frames for the transport services and charging of the SAEVs by using a model-predictive control approach. The charging of the vehicles is optimized over longer time scales to minimize electricity costs. The results from the charging optimization problem are used as constraints for the vehicle routing and rebalancing problem, which is optimized at shorter time-scales to minimize waiting times for the passengers. The objective function for the above methodology is formulated as the weighted sum of the passenger waiting time, rebalancing time, and the cost of electricity, which is assumed to be known. The methodology in Iacobucci et al. (2018*a*) was extended in Iacobucci et al. (2019) to consider injecting power back to the grid (V2G). According to the authors, optimal rebalancing of SAEVs and their charging with time-varying electricity prices have not been presented to the literature earlier. A mixed-integer linear program to optimally schedule charge and discharge of an aggregation of SAEVs to minimize total operational costs of microgrids or virtual power plants can be found in Iacobucci et al. (2018*b*). Our methodology for optimal joint operation of a system of hubs and a large fleet of SAEVs differs from the literature discussed above in a number of significant ways. Instead of assuming time varying prices of electricity to be known, we incorporate power network operations in our methodology by embedding an ACOPF model. The ACOPF model yields the day ahead market clearing prices (MCPs) considering power consumption by the base load (of the community) as well as the loads generated by the SAEVs, which are determined by the vehicle scheduling and charging strategies. We model the time varying real time prices at the nodes by using the MCPs and estimates of frequency and amplitude of price spikes. We use the DA and RT prices to make the DA commitments for the hubs, which are then used to solve a real time model for making operational decisions for the SAEVs (i.e., to serve a demand, to charge, to discharge, or to park and idle). The hubs are assumed to have limited solar generation and battery storage capacities.

3 Overview of the Operational Methodology

In this section, we present a brief outline of the steps of our methodology. The complete details for each steps are presented the subsequent section. The methodology has the following steps: 1) for a large number of days, we use daily historical data on electricity prices, transportation demand, PV generation at the hubs, and EV charging demand to *develop ad-hoc load schedule scenarios* for the hubs, and then *select a smaller representative subset* using a scenario reduction technique, 2) for each selected load scenario, we *solve an ACOPF model to estimate the DA MCPs and the corresponding RT prices*, 3) we then use these MCPs and RT prices to *obtain the DA commitments for each hubs*, and 4) given the DA commitment, RT prices, and demands for transportation and EV charging, we solve a *RT operational model* to obtain optimal strategies for the CPS.

- **Step 1.** Develop ad hoc load schedule scenarios: For this step, we first gather a large number of daily time varying historical data sets on prices of electricity, transportation demand for SAEVs, amount of PV generation at the hubs, and charging demand for privately owned EVs. For each daily data scenario, we solve a planning model to obtain a system operational strategy that maximizes the gross profit. The gross profit includes: fare received from the passengers, receipts from selling power back to the grid, charging fees from the private EV owners, payment to the grid for electricity consumed, and parking fees paid for idling SAEVs. The planning model yields, for each daily data scenario, a time varying load consumption schedule for each hub. A scenario reduction technique, available in the literature, is then used to select a small subset of the load schedules at the hubs. As alluded earlier, the system operational strategy obtained by the planning model comprises decisions on 1) choosing the next action for each SAEV, namely, whether to serve a customer, charge or discharge at a hub, or idle at a parking lot, 2) operating the battery banks at each hub to either charge or discharge, and 3) selecting the number of privately owned EVs to allow charging at each hub.
- **Step 2.** Calculate DA MCPs and RT prices: For each of the selected load schedule scenarios from step 1, together with the existing base loads in the power network that supports the hubs, we solve an ACOPF model. The ACOPF yields the DA MCPs at each node. Using an existing approach from the literature, we use the DA MCPs to generate daily RT prices with spikes of chosen amplitudes and frequencies.
- **Step 3.** Obtain DA commitment for each hub: In this step, for each load schedule from Step 1 and corresponding DA MCP and RT prices from Step 2, we use a two stage stochastic model to determine DA commitment for each time interval for each hub. The two stage stochastic model minimizes cost of power purchase by optimally balancing purchase from the DA and the RT markets considering the variations in MCP and RT prices over the time intervals of a day.
- **Step 4.** Develop a real time operational strategy for the CPS: In this final step of our methodology, we use a robust version the planning model of Step 1 to accommodate the uncertainties associated with parameters such as transportation demand, RT prices, PV generation at the hubs, and EV charging demand. Instead of assuming the uncertain parameters to be known for all time intervals of the day, as in the planning model, the real time model is solved for each time period (say, an hour) while considering a range of possible values for the parameters, based on their confidence intervals, in the remaining time periods of the day.

4 Operational Methodology

In this section, we present the models for each of the four steps of our methodology. All notation used in these models is introduced as needed. However, a list of the complete notation is included in Appendix A for ease of reference.

4.1 Planning Model for Ad-Hoc Load Schedules

The planning model is formulated as a mixed integer program with the objective of maximizing the gross profit from the operation of the CPS. The operational elements considered in the model are: serving the transportation needs, charging and discharging of the SAEVs and the battery banks, utilization of the PV generation, and acceptance of EV charging requests. In what follows, we develop all the necessary constraints

associated with transportation (1)-(6), energy (7)-(19), and privately owned EVs (20)-(23). Thereafter, we present the objective function of the planning model.

The transportation problem formulation considered in our model is inspired by the vehicle scheduling and routing model for autonomous mobility-on-demand systems proposed in Zhang et al. (2016). This model was expanded to consider charging constraints in Iacobucci et al. (2018*a*) and V2G in Iacobucci et al. (2019). The model formulations in these papers keep track of the vehicles' position while traveling within an arc, which significantly increases the complexity of the models. We develop a simplified version of the original model presented in Zhang et al. (2016) and extend it to consider balking of the passengers and power-market-related constraints as follows.

Let $\overline{\mathcal{T}}$ be the set of all time periods, $\overline{\mathcal{N}}$ be the set of all nodes in the transportation network, and $\mathcal{A}$ be the set of all arcs in the network. We define γ_{ijt} and d_{ijt} as the number of passenger demand arrivals and the unserved demand, respectively, at node i with destination j $(i,j \in \mathcal{A})$ at time $t \in \overline{\mathcal{T}}$. Let $\mathcal{B}$ denote the set of all SAEVs. Let $\mathcal{B}$ is the set of all SAEVs. We define for $b \in \mathcal{B}$ $x^b_{ijt} = 1$ if vehicle b departs with a passenger from node $i \in \overline{\mathcal{N}}$ to node j at time period t, and 0 otherwise. The demand left unserved in any given node is equal to the number of customers already waiting, plus the new arrivals, minus the demand served at the current time period:

$$d_{ij,t+1} = (1-\beta)d_{ijt} + \gamma_{ijt} - \sum_{b\in\mathcal{B}} x^b_{ijt} - b_{ijt}, \qquad \forall (i,j) \in \mathcal{A}, t \in \overline{\mathcal{T}}, \tag{1}$$

where $\beta \in (0,1)$ denotes the fraction of the already waiting customers that balk and the dummy $0 \leq b_{ijt} \leq 1$ is introduced to cancel out the fractional part of $(1-\beta)d_{ijt}$ (avoiding infeasibilty for any β). Let $\mathcal{H}$ and $\mathcal{P}$ be the subsets of the nodes in the transportation network in which the smart hubs and parking facilities are located, respectively. We define $z^b_{it} = 1$ if vehicle b waited in node i from time $t-1$ to time t, and 0 otherwise. Then, the following constraint guarantees that SAEVs park only at nodes with parking lots or smart hubs.

$$z^b_{it} = 0, \qquad \forall t \in \overline{\mathcal{T}}, b \in \mathcal{B}, i \notin \mathcal{H} \cup \mathcal{P} \tag{2}$$

Let $y^b_{ijt} = 1$ if vehicle b is departing empty from node i to j at time period t, and 0 otherwise. Also let be $p^b_{it} = 1$ if at time period t, the vehicle b arrives at node i at time t. Then, the following constraints determine if vehicle b stays at, arrive to, or depart from node i at time t.

An SAEV arrives to node i at time t if it departed from node j exactly τ_{ji} time units before, where τ_{ji} is the travel time between nodes j and i. The following constraints considers the arrival to node i from all possible j.

$$p^b_{it} = \sum_{(j,i)\in\mathcal{A}:\tau_{ij}\leq t} (x^b_{ji,t-\tau_{ji}} + y^b_{ji,t-\tau_{ji}}), \qquad \forall i \in \overline{\mathcal{N}}, t \in \overline{\mathcal{T}}, b \in \mathcal{B}. \tag{3}$$

Constraint (4) ensures that the vehicle will either stay parked at a node or depart from it, both actions can not happen simultaneously.

$$\sum_{i\in\overline{\mathcal{N}}} (z^b_{i,t+1} + \sum_{(i,j)\in\mathcal{A}} x^b_{ijt} + \sum_{(i,j)\in\mathcal{A}} y^b_{ijt}) \leq 1, \qquad \forall t \in \mathcal{T}, b \in \mathcal{B}. \tag{4}$$

The next constraint considers that a vehicle is either arriving to a node, it was already parked there or neither.

Hence, we have that

$$z_{it}^b + p_{it}^b \leq 1, \qquad \forall i \in \overline{\mathcal{N}}, t \in \overline{\mathcal{T}}, b \in \mathcal{B}. \tag{5}$$

An SAEV stays at a node for the next time period if it was already idling at a node and did not depart in the current time period. This considered in the following constraint.

$$z_{i,t+1}^b = z_{it}^b + p_{it}^b - \sum_{(i,j)\in\mathcal{A}} (x_{ijt}^b + y_{ijt}^b), \qquad \forall i \in \overline{\mathcal{N}}, t \in \overline{\mathcal{T}}, b \in \mathcal{B}. \tag{6}$$

In the remaining part of this subsection, we model the vehicle charging aspect of the problem. We consider a system of smart hubs located at different nodes of a transportation network. The SAEV fleet operator coordinates the fleet of SAEVs to meet the transportation demand of the city while satisfying charging needs of the vehicles. Charging schedule depends on the varying electricity prices at the nodes and the transportation demand. In addition to the fleet of SAEVs, the smart hubs are considered to offer charging services to privately owned EVs. the fleet operator may charge SAEVs when the prices are low and sell the excess energy to the grid if the prices are high enough. The DA commitment of the system of hubs may also be sold back to the grid if the RT prices rise significantly. Finally, we consider that each hub also has a bank of stand-alone batteries and rooftop solar generation which give additional flexibility to the operator. The fleet of SAEVs is subject to routing constraints $(1) - (6)$ as well as some charging constraints as follows.

Let ϕ_b denote the battery capacity of SAEV b, ϵ^b be the energy consumed by SAEV b per unit time period on the road, p_{ht}^{b+} be the total charge added to SAEV b at hub h at time period t, and p_{ht}^{b-} be total energy discharged from SAEV b at hub h and time period t. The state of charge of SAEV b (s_t^b) changes over time depending on whether the vehicle is charging, discharging, idling or traveling. Then, we can write the energy conservation of SAEV b as

$$\phi_b s_{t+1}^b = \phi_b s_t^b + \sum_{h\in\mathcal{H}} p_{ht}^{b+} - \sum_{h\in\mathcal{H}} p_{ht}^{b-} - \epsilon^b (1 - \sum_{i\in\overline{\mathcal{N}}} z_{i,t+1}^b) \qquad \forall t \in \overline{\mathcal{T}}, b \in \mathcal{B}. \tag{7}$$

Note from (7) that if SAEV b has been parked at any node i (i.e., $z_{i,t+1}^b$), then the last term is equal to zero (no energy consumed). Total energy charged to an SAEV b might come from either the grid (g_{ht}^b), the rooftop solar system (f_{ht}^b), or the bank of stand-alone batteries (e_{ht}^b). Then, we can write the total amount charged as

$$p_{ht}^{b+} = e_{ht}^b + f_{ht}^b + g_{ht}^b, \qquad \forall t \in \overline{\mathcal{T}}, b \in \mathcal{B}, h \in \mathcal{H}, \tag{8}$$

where

$$f_{ht}^b \leq F_h^{\max} z_{h,t+1}^b \qquad \forall t \in \overline{\mathcal{T}}, b \in \mathcal{B}, h \in \mathcal{H}, \tag{9}$$

$$e_{ht}^b \leq E_h z_{h,t+1}^b \qquad \forall t \in \overline{\mathcal{T}}, b \in \mathcal{B}, h \in \mathcal{H}. \tag{10}$$

and $F_h^{\max}$ is the installed solar power and E_h is the aggregated battery capacity. Note that $F_h^{\max}$ and E_h are acting as big-Ms in these equations. We assume that both the charge and discharge rates are constant and denoted by $\overline{P}^+$ and $\overline{P}^-$, respectively. Hence, we can write that

$$p_{ht}^{b+} \leq \overline{P}^+ w_{ht}^{b+} \qquad \forall t \in \overline{\mathcal{T}}, b \in \mathcal{B}, h \in \mathcal{H}, \tag{11}$$

$$p_{ht}^{b-} \leq \overline{P}^- w_{ht}^{b-} \qquad \forall t \in \overline{\mathcal{T}}, b \in \mathcal{B}, h \in \mathcal{H}. \tag{12}$$

where w_{ht}^{b+} and w_{ht}^{b-} are binary variables equal to 1 if SAEV b is charging or discharging, respectively, at hub h at time period t, and 0 otherwise. The next constraint guarantees that 1) the SAEVs can charge or discharge only if they are parked at a hub and 2) they are not charging and discharging simultaneously during time period t:

$$w_{ht}^{b+} + w_{ht}^{b-} \leq z_{h,t+1}^{b} \qquad \forall t \in \overline{\mathcal{T}}, b \in \mathcal{B}, h \in \mathcal{H}. \tag{13}$$

In general, the state of charge of SAEV batteries is not allowed to be either 0 or 1. We define $\underline{S_b}$ and $\overline{S_b}$ as the minimum and maximum allowable state of charge for SAEV b at any time, respectively. Then SAEVs state of charge is bounded by

$$\underline{S^b} \leq s_t^b \leq \overline{S^b}, \qquad \forall t \in \overline{\mathcal{T}}, b \in \mathcal{B}. \tag{14}$$

Let P_h^+, and P_h^- be the charging and discharging rates, respectively, of the bank of stand alone battery at hub h. Let g_{ht} and f_{ht}^+ be the fraction of the energy charged to the bank of stand-alone batteries coming from the grid and the available solar power, respectively. Let p_{ht}^- denote the total energy discharged from the bank of stand-alone batteries at hub h and time period t and s_{ht} denote its state of charge. Then, power conservation of the bank of stand-alone batteries is given by:

$$\overline{E}_h s_{h,t+1} = \overline{E}_h s_{ht} + g_{ht} + f_{ht}^+ - p_{ht}^-, \qquad \forall t \in \overline{\mathcal{T}}, h \in \mathcal{H}. \tag{15}$$

where both the charging and discharging rates of the battery bank are bounded as:

$$g_{ht} + f_{ht}^+ \leq P_h^+, \qquad \forall t \in \overline{\mathcal{T}}, h \in \mathcal{H}, \tag{16}$$

$$p_{ht}^- \leq P_h^-, \qquad \forall t \in \overline{\mathcal{T}}, h \in \mathcal{H}. \tag{17}$$

Energy discharged from the bank of stand-alone batteries is used to 1) charge the SAEVs and the privately owned EVs at the hubs, and 2) to sell in the RT market (denoted by $\hat{p}_{ht}^-$). Hence, we can write that

$$p_{ht}^- = \sum_{b \in \mathcal{B}} e_{ht}^b + e_{ht}^{EV} + \hat{p}_{ht}^-, \qquad \forall t \in \overline{\mathcal{T}}, h \in \mathcal{H}, \tag{18}$$

where, e_{ht}^{EV} is the total energy added form the bank of Stand-alone batteries to the privately owned EVs at hub h at time period t. Similarly, the available solar power at the hubs (F_{ht}) is used to 1) charge the parked SAEVs, the bank of stand-alone batteries, and the privately owned EVs (f_{ht}^{EV}), and 2) to sell in the RT market (f_{ht}^-). Then we have that:

$$\sum_{b \in \mathcal{B}} f_{ht}^b + f_{ht}^{EV} + f_{ht}^+ + f_{ht}^- = F_{ht}, \qquad \forall t \in \overline{\mathcal{T}}, h \in \mathcal{H}. \tag{19}$$

If deemed appropriate, hubs' operator will disclose available charging stations to privately owned EVs. The EV owners will pay the RT price of electricity plus a fee ζ_h per time period they stay charging at the hubs. Without loss of generality, we consider that each EV will request v number of time periods to the hubs ($v = \{1, \cdots, V\}$, where V is the maximum number of time periods that a privately owned EV are allowed to stay (charging) in the smart hubs). Let W_{ht}^v be the number of EVs requesting v time periods at hub h at time period t, and w_{ht}^v is the number of requests that are accepted. The EV charging requests that are accepted in the current time period will occupy charging stations at the hubs at the beginning of the next

time period. Then, we have that:

$$w^v_{h,t+1} \leq W^v_{ht}, \qquad \forall h \in \mathcal{H}, t \in \overline{\mathcal{T}}. \tag{20}$$

The number of charging stations used by the privately owned EVs at any time period (c_{ht}) is equal to the number of accepted EVs in the current time period, plus, the number of EVs that were charging in the previous time period:

$$c_{ht} = \sum_{v=1}^{V} w^v_{ht} + \sum_{v=2}^{V} w^v_{h,t-(v-1)}, \qquad \forall h \in \mathcal{H}, t \in \overline{\mathcal{T}}. \tag{21}$$

As the total energy consumed by the privately owned EVs is supplied by the grid (g^{EV}_{ht}), the bank of stand-alone batteries (e^{EV}_{ht}), and solar power (f^{EV}_{ht}), we have that:

$$e^{EV}_{ht} + f^{EV}_{ht} + g^{EV}_{ht} = P^+ c_{ht}, \qquad \forall h \in \mathcal{H}, t \in \overline{\mathcal{T}}. \tag{22}$$

The number of available charging stations for SAEVs at any given time period is $C_h - c_{ht}$, hence we have that:

$$\sum_{b \in \mathcal{B}} (w^{b+}_{ht} + w^{b-}_{ht}) \leq C_h - c_{ht} \qquad \forall h \in \mathcal{H}, t \in \overline{\mathcal{T}} \tag{23}$$

We consider that the SAEVs can park at city parking lots, which has cost α_p for each time period it stays parked. The SAEVs also pay the cost of electricity consumed (π_{ht}) to the SO. The revenue for the fleet and the hub system comes from three sources, namely, energy sold to the grid (valuated at π_{ht}), payments from privately owned EVs, and payments received from the passengers (ψ_t per time period on the road). Then, the smart hubs operational model can be formulated as:

$$\begin{aligned}
\max \quad & \sum_{t \in \overline{\mathcal{T}}} \sum_{b \in \mathcal{B}} \sum_{(i,j) \in \mathcal{A}} \psi_t \tau_{ij} x^b_{ijt} - \sum_{p \in \mathcal{P}} \sum_{t \in \overline{\mathcal{T}}} \sum_{b \in \mathcal{B}} \alpha_p z^b_{pt} - \sum_{h \in \mathcal{H}} \sum_{t \in \overline{\mathcal{T}}} \pi_{ht} \Big(\sum_{b \in \mathcal{B}} \left(g^b_{ht} - p^{b-}_{ht} \right) \\
& + g_{ht} - \hat{p}^-_{ht} - f^-_{ht} + g^{EV}_{ht} \Big) + \sum_{h \in \mathcal{H}} \sum_{t \in \overline{\mathcal{T}}} \pi_{ht} P^+ c_{ht} + \sum_{h \in \mathcal{H}} \sum_{t \in \overline{\mathcal{T}}} \zeta_h c_{ht} \qquad (24) \\
\text{s.t.,} \quad & (1) - (23)
\end{aligned}$$

Each of the terms in the objective function correspond to the following:

- $\sum_{t \in \overline{\mathcal{T}}} \sum_{b \in \mathcal{B}} \sum_{(i,j) \in \mathcal{A}} \psi_t \tau_{ij} x^b_{ijt}$: fee paid by the passengers
- $\sum_{p \in \mathcal{P}} \sum_{t \in \overline{\mathcal{T}}} \sum_{b \in \mathcal{B}} \alpha_p z^b_{pt}$: parking cost
- $\sum_{h \in \mathcal{H}} \sum_{t \in \overline{\mathcal{T}}} \pi_{ht} \Big(\sum_{b \in \mathcal{B}} \left(g^b_{ht} - p^{b-}_{ht} \right) + g_{ht} - \hat{p}^-_{ht} - f^-_{ht} + g^{EV}_{ht} \Big)$: total electricity cost, including power bought and sold by the SAEVs and the stand-alone batteries, solar power injected to the grid, and power bought by the privately owned EVs
- $\sum_{h \in \mathcal{H}} \sum_{t \in \overline{\mathcal{T}}} \pi_{ht} P^+ c_{ht} + \sum_{h \in \mathcal{H}} \sum_{t \in \overline{\mathcal{T}}} \zeta_h c_{ht}$: fee paid by the privately owned EVs, including RT price of electricity and cost of using the smart hubs

We solve two modified versions at different stages of the methodology. First, we solve a deterministic version of the model in the "Ad hoc load schedule" step, and then we robustify the model in the "MPC-based RT operation" step. In what follows, we describe each of the steps of the methodology.

4.2 load Schedule and Market Clearing Price Estimation

In this step, we generate an ad hoc load schedule based on historical data. This schedule serves as an input for the day-ahead commitment model, which is described later. A few parameters of our model that are required for this step are: electricity price (π_{ht}, which is function of the DA and RT prices), charging demand of the privately owned EVs (captured by W^v_{ht}), available solar power (F_{ht}), and passenger arrivals (γ_{ijt}). All these parameters are stochastic. We construct distributions for these parameters based on prior information, and generate random samples of the vector $\mathcal{V} = \{\pi_{ht}, W^v_{ht}, F_{ht}, \gamma_{ijt}\}$, $\forall i, j, t, h$. Then, we can obtain the minimal-cost load schedule for each hub and for any given realization of $\mathcal{V}$ as $D_{ht} = \sum_{b\in\mathcal{B}} g^{b*}_{ht} + g^{*}_{ht} + g^{EV*}_{ht} \forall h \in \mathcal{H}, t \in \overline{\mathcal{T}}$, where the values of the variables are obtained from the optimal solution of (24), subjected to (1)-(23). Let $\mathcal{V}^j$ be a realization of the random vector $\mathcal{V}$. Then, we denote the set of minimal cost load schedule scenarios for each hub h as $\mathcal{D}_h = \{D_{ht}(\mathcal{V}^j) : \forall t, j = \{1, \cdots, N\}\}$, where N is the number of randomly selected samples of $\mathcal{V}$. We select a relatively large value for N so that the variations of the components of $\mathcal{V}$ are well represented in the samples.

To reduce computational burden in the DA commitment process, we select a representative subset of the load schedules, using a scenario reduction technique adopted form Growe-Kuska et al. (2003). This technique selects a subset of the load scenarios, denoted by Ω, and it assigns to each a probability of occurrence $\mu^\omega \; \forall \omega \in \Omega$. We use the load schedule D^ω_{ht} and the generators DA bids to solve the ACOPF model presented in Appendix B (Equations $(43) - (55)$). Solution of the ACOPF model yields an estimate of the day-ahead market clearing prices (MCP^ω_{nt}) at each bus $n \in \mathcal{N}$. The ACOPF model is solved in practice for each hour of the day, whereas our operational model has shorter time periods. Hence, to solve the ACOPF model for each hour, we sum the loads of all time periods within the hour. Note that, more than one hub may be directly connected by a single bus in the grid. The total real and reactive power load at each bus is equal to the sum of all the loads connected to the bus (houses, industries, the hubs, etc.). The real power load of each hub h, in a given scenario w, is equal to D^ω_{ht}, while the reactive power demand is a fraction of D^ω_{ht}.

4.3 Two-Stage Stochastic Model for Day Ahead Commitment

Using the method proposed in Das & Wollenberg (2005), we estimate the RT prices at bus n as $\pi^\omega_{nt} = \text{MCP}^\omega_{nt}[1+\epsilon]$, where $\epsilon = M_1\epsilon_1 + M_2\epsilon_2$. The values of the random variables ϵ_1 and ϵ_2 are drawn from normal and Cauchy distributions, respectively, and (M_1,M_2) is a bivariate random variable that takes values of $(0, 1)$ with probability p_s and (1,0) with probability $(1 - p_s)$, where p_s denotes the probability of occurrence of price spikes. The normal random variable ϵ_1 captures the usual variability in the real time prices, whereas the Cauchy random variable ϵ_2 generates the price spikes. Using the load schedules of each hub (D^w_{ht}), the estimated market clearing prices (MCP^w_{nt}), and the corresponding real time prices (π^ω_{nt}), we develop a two-stage stochastic model to optimally determine the DA commitment.

The two-stage model assumes that each hub can sell (buy) excess (shortfall) quantities in the RT market. We denote p^{DA}_{ht} as the quantity committed to in the DA market by hub h at time period t. Then, the hourly DA commitment is equal to the sum of the p^{DA}_{ht} for all time periods belonging to the hour. Let $p^{\omega,RT+}_{ht}$ and $p^{\omega,RT-}_{ht}$ be the quantities bought from and sold to the RT market, respectively, by hub h at time period t in scenario $\omega \in \Omega$. Then, the DA commitment for all the hubs is obtained by solving the following model.

$$\begin{aligned} \min \quad & \sum_{\omega\in\Omega} \mu^\omega \Big[\sum_{t\in\mathcal{T}} \sum_{n\in\mathcal{N}} \sum_{h\in\mathcal{H}_n} \Big(\text{MCP}^\omega_{nt} p^{\text{DA}}_{ht} + \pi^\omega_{nt} p^{\omega,RT+}_{ht} - (\pi^\omega_{nt} - \delta^{RT}) p^{\omega,RT-}_{ht} \Big) \Big] \\ \text{s.t.,} \quad & p^{\text{DA}}_{ht} + p^{\omega,RT+}_{ht} - p^{\omega,RT-}_{ht} = D^\omega_{ht}, \qquad \forall h \in \mathcal{H}, t \in \overline{\mathcal{T}}, \omega \in \Omega, \end{aligned} \tag{25}$$

where $\mathcal{H}_n$ is the set of hubs directly connected to bus n, and δ^{RT} is a penalty for not using the DA committed quantity. The objective of the above formulation is to minimize the expected electricity cost of the system of hubs.

4.4 Real Time operational model

Once the DA commitment for the hubs is made, the SO discloses the DA prices, π^{DA}_{ht}, and the fleet operator pays $\sum_{h\in\mathcal{H}}\sum_{t\in\overline{\mathcal{T}}}\pi^{DA}_{ht}P^{DA}_{ht}$. We divide the power bought form the grid, at any time period, using its DA and RT components as follows.

$$g^{b}_{ht} = g^{b,DA}_{ht} + g^{b,RT}_{ht}, \qquad \forall h\in\mathcal{H}, t\in\overline{\mathcal{T}}, b\in\mathcal{B}, \tag{26}$$

$$g_{ht} = g^{DA}_{ht} + g^{RT,}_{ht} \qquad \forall h\in\mathcal{H}, t\in\overline{\mathcal{T}}, \tag{27}$$

$$g^{EV}_{ht} = g^{EV,DA}_{ht} + g^{EV,RT}_{ht} \qquad ,\forall h\in\mathcal{H}, t\in\overline{\mathcal{T}}. \tag{28}$$

The DA commitment is used to 1) charge the batteries of the SAEVs, privately owned EVs, and the battery bank and 2) sell it in the RT market if profitable, i.e., if the RT prices are high, the hubs may use their DA commitment to arbitrage in the RT market. Then, we can write the following.

$$\sum_{b\in\mathcal{B}} g^{b,DA}_{ht} + g^{DA}_{ht} + g^{EV,DA}_{ht} + p^{RT-}_{ht} = p^{DA}_{ht}, \qquad \forall h\in\mathcal{H}, t\in\overline{\mathcal{T}}, \tag{29}$$

where p^{RT-}_{ht} is the actual quantities sold to the RT market by hub $h\in\mathcal{H}$ at time period $t\in\overline{\mathcal{T}}$. Selling back to the grid not only benefits the system of hubs (economically), but also helps the system operator to match demand and supply (RT prices are high when the current demand in the network is high in comparison to the supply).

To simplify the formulation of the RT operational model, we define the dummy variables a^{RT} and a^{RT}_{b} as:

$$a^{\mathrm{RT}} = \sum_{h\in\mathcal{H}}\sum_{t\in\overline{\mathcal{T}}} \pi^{RT}_{ht} l^{\mathrm{RT}}_{ht} \tag{30}$$

$$a^{\mathrm{RT}}_{b} = \sum_{h\in\mathcal{H}}\sum_{t\in\overline{\mathcal{T}}} \pi^{RT}_{ht} l^{b,\mathrm{RT}}_{ht} \qquad \forall b\in\mathcal{B} \tag{31}$$

where l^{RT}_{ht} and $l^{b,\mathrm{RT}}_{ht}$ are defined as:

$$l^{\mathrm{RT}}_{ht} = \overline{P}^{+}c_{ht} + \hat{p}^{-}_{ht} + f^{-}_{ht} - g^{RT}_{ht} - g^{EV,RT}_{ht}, \qquad \forall h\in\mathcal{H}, t\in\overline{\mathcal{T}}, \tag{32}$$

$$l^{b,\mathrm{RT}}_{ht} = p^{b-}_{ht} - g^{b,RT}_{ht}, \qquad \forall b\in\mathcal{B}, h\in\mathcal{H}, t\in\overline{\mathcal{T}}. \tag{33}$$

Note that when $l^{\mathrm{RT}}_{ht}\geq 0$, the hubs are getting revenue from RT transactions with the grid. Similarly, when $l^{b,\mathrm{RT}}_{ht}\geq 0$, SAEV b is injecting power to to the grid, else it is drawing power. Finally, to consider the fraction of the DA commitment that is sell back to the grid we include:

$$a^{DA} = \sum_{h\in\mathcal{H}}\sum_{t\in\overline{\mathcal{T}}} (\pi^{RT}_{ht} - \delta^{RT}) p^{RT-}_{ht} \tag{34}$$

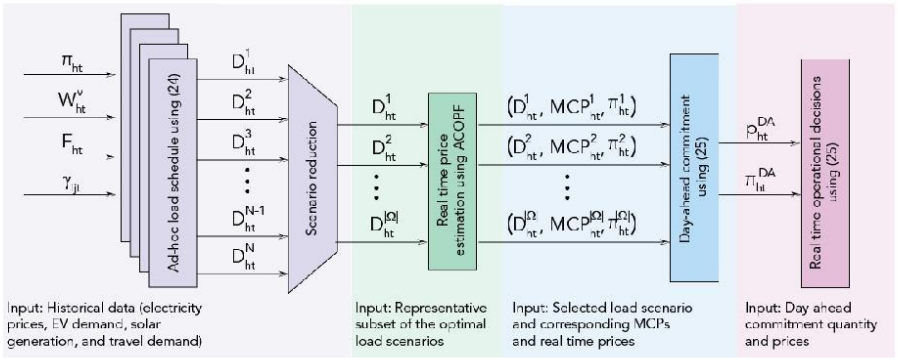

Figure 2: Summary of the operational methodology

Then, we can re-write the objective function 24 at any time period τ as:

$$\max \quad \sum_{t=\tau}^{|\overline{\mathcal{T}}|} \sum_{b\in\mathcal{B}} \sum_{(i,j)\in\mathcal{A}} \psi_t \tau_{ij} x_{ijt}^b + a^{RT} + \sum_{b\in\mathcal{B}} a_b^{RT} + a^{DA} + \sum_{h\in\mathcal{H}} \sum_{t\in\overline{\mathcal{T}}} \zeta_h c_{ht} - \sum_{t=\tau}^{|\overline{\mathcal{T}}|} \sum_{p\in\mathcal{P}} \sum_{b\in\mathcal{B}} \alpha_p z_{pt}^b. \tag{35}$$

The abode objective function is subjected to constraints $(2)-(18), (21)-(23), (26)-(29), (32)$ and (33), in which we must now replace $\forall t \in \overline{\mathcal{T}}$ by $\forall t \in \{\tau, \cdots, |\overline{\mathcal{T}}|\}$. Additionally, the model is also subjected to the robust versions of those constraints with uncertain parameters, namely, constraints (1), (19), (20), and (30). In Appendix D, we show the robust counterparts of such constraints. A schematic of our methodology is presented in Figure 2.

5 A Numerical Case Study

We demonstrate our methodology by implementing it on a sample problem where a CPS operates within a city's transportation and power networks; a schematic representation of the problem is given in Figure 3.

The CPS is considered to have the following features. It has fleet of 500 SAEVs, each with a battery size of 100 kWh and a range efficiency of 0.293 kWh per mile on city roads (similar to Tesla model S). The SAEVs are supported by a system of five hubs each with 50 super-chargers, each with a charge/discharge rate of 70kW. Each hub has a battery bank with a capacity of 600 kWh and a charge/discharge rate of 300 kW; these parameters are adopted from Kwon et al. (2015). Each hub is also considered to have solar generation facility with a peak capacity of 200 kW. Generation from these PV units across the day is modeled using the patterns obtained from Tampa Electric Company (TECO). It is considered that the above CPS supports passenger transportation in the City of Tampa, Florida, USA and its suburbs. For ease of computation, the origins and destinations (ODs) of transportation demand are clustered into twelve nodes as shown in Figure 4a. A similar clustering approach was used in Iacobucci et al. (2019). Five of those nodes are considered to be the locations of the hubs (nodes 1, 6, 8, 9 and 10). The average travel times from each hub to the rest of the service area are depicted in heat maps as shown in Figure 4b to Figure 4f; the travel time data is adopted from Uber (2020). Based on the travel time data, we assumed that all ODs are multiples of 15 minutes (one time period) apart and the maximum trip duration is 75 minutes (five time periods). The transportation

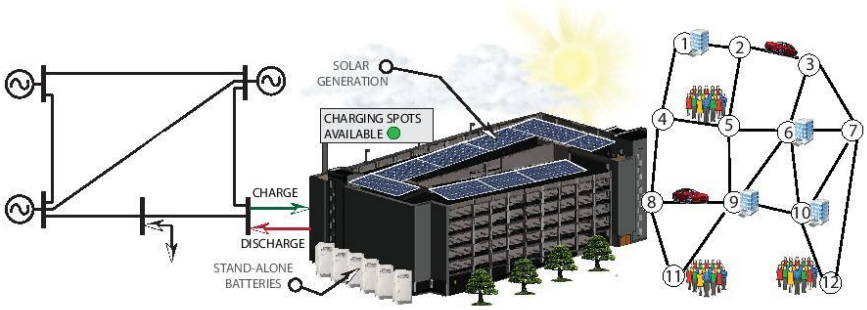

Figure 3: Schematic of a CPS interacting with power and transportation networks

Table 1: Generator cost functions used in the case study

Generator	Cost function	Generator	Cost function
1a	$0.100P_g^2 + 12P_g + 100$	4c	$0.100P_g^2 + 19P_g + 70$
1b	$0.100P_g^2 + 20P_g + 30$	5a	$0.100P_g^2 + 17P_g + 60$
1c	$0.100P_g^2 + 08P_g + 40$	5b	$0.120P_g^2 + 18P_g + 50$
4a	$0.100P_g^2 + 10P_g + 50$	5c	$0.085P_g^2 + 20P_g + 80$
4b	$0.100P_g^2 + 25P_g + 150$		

demands served by the SAEVs for each time period are generated using the actual daily travel requests in Tampa; we assume that 30% of these requests are for the SAEVs. The distribution of these demands over the time periods of a day are considered to be same as in Zhou et al. (2003). For charging demand of privately owned EVs, we use the arrival patterns and fleet composition as presented in (Subramanian & Das 2019). EVs request charging for up to four time periods, and once accepted they remain charging till the request is fulfilled. The cost and fees of the system are considered as follows. The SAEVs pay a parking fee of \$10/hour and receive \$45/hour for transporting passengers. The privately owned EVs pay a facility fee \$8/hour plus the prevailing real time price of electricity.

The power grid to which the CPS is connected is considered to be the modified PJM 5-bus network, as shown in Figure 3. The network has the two load nodes (2 and 3) and three generating nodes (1, 4, and 5) with three identical generators of 800 MW capacity in each. The characteristics of the six transmission lines, i.e., capacity, reactance, and susceptance, are adopted from Li & Bo (2010). The generator cost functions are assumed to be quadratic with parameters presented in Table 1, which are obtained from Das & Wollenberg (2005). The base load of the 5-bus network is considered to be same as the DAY zone of the PJM network (U.S.A.) between July 15, 2019 to July 30, 2019 (summer days only, to avoid seasonal variability). For each of the daily base load data, we solve an ACOPF model (43) (see appendix) to estimate the MCPs at the two load nodes.

For implementing our methodology, we need to develop historical data for transportation demand, electricity price, PV generation at the hubs, and EV charging demand. For this purpose, we use the available data, as described above, to estimate the parameters of the appropriate probability distributions for each time period of a day, namely normal distributions for the nodal electricity prices and PV generation, and

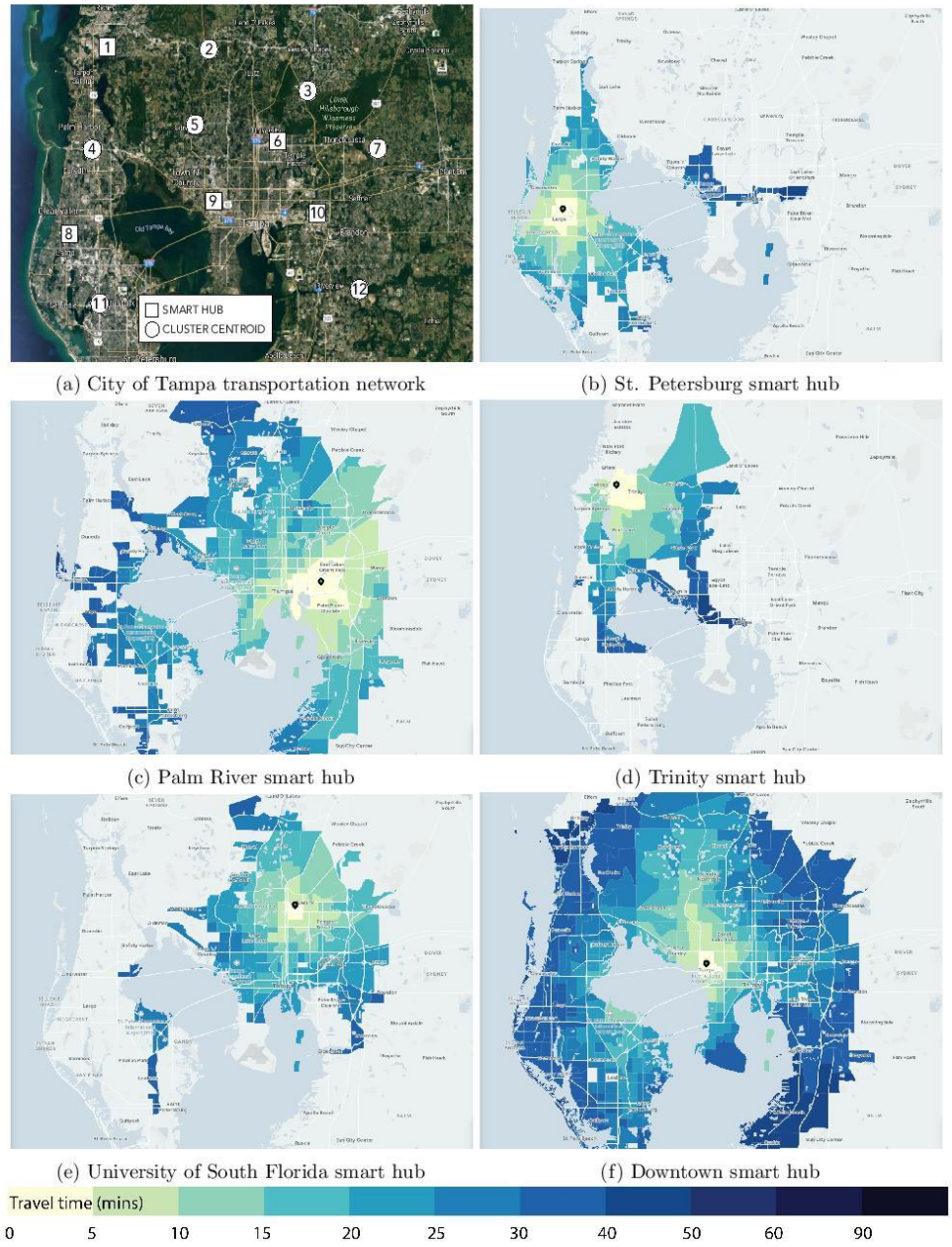

(a) City of Tampa transportation network

(b) St. Petersburg smart hub

(c) Palm River smart hub

(d) Trinity smart hub

(e) University of South Florida smart hub

(f) Downtown smart hub

Figure 4: Simplified City of Tampa transportation network and location of the smart hubs

Poisson distributions for the transportation and EV charging demands. We then draw one hundred samples for all time periods from each of these distributions and solve (24), as described in Section 4.2, to generate the ad-hoc load scenarios. The scenario reduction technique is then used to obtain ten representative load scenarios with respective probabilities. For each of these ten load scenarios along with the base load of the city, we solve the ACOPF model (43) to estimate the DA MCPs and then derive the RT prices at each load node. Hereafter, considering the selected load and price scenarios and their corresponding probabilities, we solve the two-stage model (25) to obtain the hourly DA commitments. Using the DA commitments, we solve the real time operational model in (35). We implemented our methodology on the sample problem using Julia 0.7.1 as programming language and GUROBI 9.0.0 as optimization solver. The results are organized to address three key goals of the numerical study: 1) to demonstrate that our methodology is capable of yielding real-time operational strategies for the CPS, 2) to demonstrate the influence of power network on CPS operation, and 3) to measure the added financial benefits of the CPS derived from power network considerations.

Our methodology was successful in obtaining real time action choices for the CPS elements (SAEVs, hubs, battery banks, and PV generators) for all 96 time periods of a day. Some of these action choices are depicted in the figures that are discussed next. Figure 5a illustrates the distribution of the SAEVs arriving at the nodes throughout the day (vehicles in between nodes are not included). Although, in our implementation, all the SAEVs were assigned to be at hub nodes (100 in each) at time period 1, it can be seen that the vehicles are well distributed across the city during the day. The maximum aggregated number of SAEVs arriving at the nodes at any time period is observed to be less than 40% of the fleet size, meaning 60% or more of the SAEVs are traveling between nodes. The SAEVs served a total of 10,288 trips during the day out of 53,441 trips generated. This indicates that the fleet size of 500 is inadequate for the demand considered here. Figure 5b shows the number of SAEVs charging at the hubs (at nodes 1, 6, 8, 9, and 10) throughout the day. Average occupancy of the hubs is observed to be around 35. Hence, a system of five hubs with 50 charging stations in each is generally underutilized for a fleet size of 500; only the hub at node 8 can be observed to be fully occupied for a few time periods of the day. This indicates that there is available capacity for the CPS to offer charging services to privately owned EVs. Figure 5c shows the number of privately owned EVs that were allowed to charge at the hubs, as determined by the optimal solution. Note that the pattern of EV charging demand, adopted from Subramanian & Das (2019), is mostly concentrated during the morning hours, which explains the result in Figure 5c. Figure 5d shows the number of SAEVs idling (neither serving trips, traveling empty, nor charging). SAEVs can be seen to idle only at the hub nodes and at those time periods when higher numbers of EVs are allowed at the hubs. The total idle time of the SAEVs is less than 1.6%, which aligns well with the fact that the demand for trips in the system is very high for the given fleet size. We noted that our methodology generated a total gross profit of $229,193 per day, which includes $3,494 from serving the privately owned EVs and $2498 from arbitrage using the battery banks. Hence, optimal operation of the CPS with 500 SAEVs and five hubs of 50 charging station could generate an estimated annual gross profit close to 84 million dollars. However, this estimate is high for the following reasons: 1) the trip demand for the sample problem is too high for a fleet size of 500 and hence there is little to no idle time for the vehicles, 2) no time lag is accounted for between drop off and pick up when a passenger is available at a node, 3) no connect/disconnect time loss at the hubs is considered, and 4) outages for vehicle break down and maintenance are not included.

Since our methodology does not address how to select the optimal number of hubs and their capacities needed for a system, we conducted a sensitivity analysis. For a number of different fleet sizes, between 100 and 500, we determined the approximate number of charging stations in each of the five hubs, beyond which

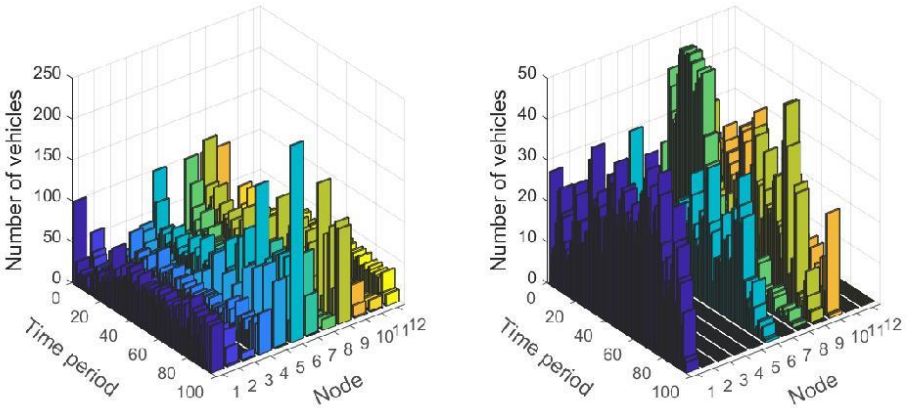

(a) Arrival of SAEVs

(b) Number of SAEVs charging

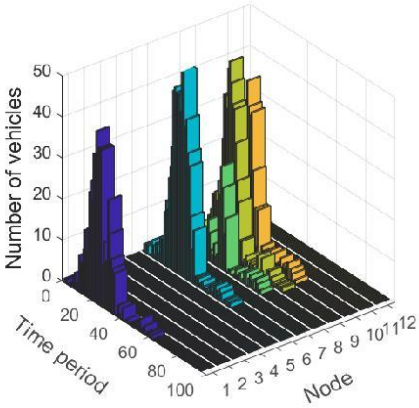

(c) Number of EVs charging

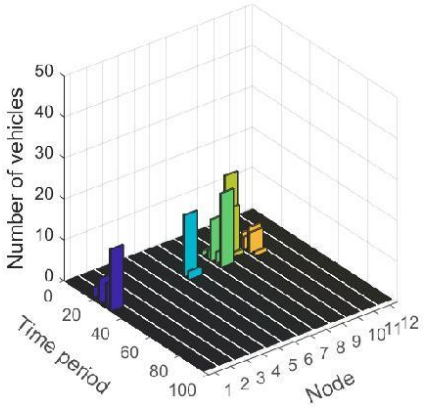

(d) Idle SAEVs

Figure 5: Distribution of SAEVs and charging patterns of SAEVs and EVs

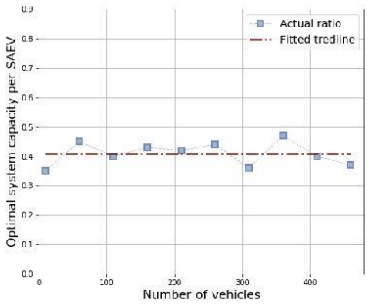

Figure 6: Optimal hub capacity - fleet size ratio

the gross profit of the CPS did not seem to increase significantly. We approximated these points using the fit3 technique presented in (**?**). We plotted the ratio of the total charging capacity (in all five hubs combined) to the number of SAEVs in the system. Figure 6 shows that the average value of the ratio is 0.41 (with a standard deviation of 0.038) for the fleet sizes considered.

To measure the influence of power network on CPS operation, the second goal of our case study, we plotted the actual grid consumption by the CPS in conjunction with the DA commitment and the RT prices, which together guide the charging strategy. The plots are shown in Figure 7 for only two hubs (1 and 10) that are connected to two different load buses in the sample power network. In these figures, the bars indicate DA commitment by the hubs, the red line represents the RT prices, and the bold line shows the energy consumed by the hubs from the grid. Figure 7a depicts the results for the case in which privately owned EVs are not allowed to charge at the hubs. We notice that the energy consumption from the grid is closely aligned with the DA commitment, which means that the CPS operator is able to hedge against the RT price risk through its two-stage stochastic DA commitment model. The consumption from the grid can be seen to be generally slightly higher that the DA commitment. However, at some of the time periods, say 24-36 (in hub 1) and 65-70 (in hub 10) when the RT prices are higher, the DA commitment is larger than actual consumption. This offers opportunities for arbitrage as the excess commitment is sold back to the RT market. We notice however that the energy arbitrage potential of the sample CPS, with only 500 vehicles serving a significantly high passenger demand, is very limited since the revenue from passenger fare is higher than that from energy arbitrage. Figure 7b presents results for the scenario when privately owned EVs are allowed to charge at the hubs. As we have seen in Figure 5c, the CPS allows more EVs to charge in the early morning hours (around time period 20). Hence for both hubs 1 and 10, the DA commitment as well as the grid consumption are much higher in the early hours (see Figure 7b), while for the remainder of the day they are similar to Figure 7a.

In order to fulfill the third goal of our numerical study, i.e., to assess the financial benefits derived from power network considerations, we measured the cost savings attained by the hubs by buying power through optimal DA commitments and reduce exposure to RT price variations. Recall that the DA commitment requires solution of the ACOPF model via steps 1-3 of our methodology. We obtained the operational strategies for the CPS using two approaches: 1) by using the complete methodology including optimal DA commitment and 2) by eliminating DA commitment and paying RT prices for the grid consumption at the

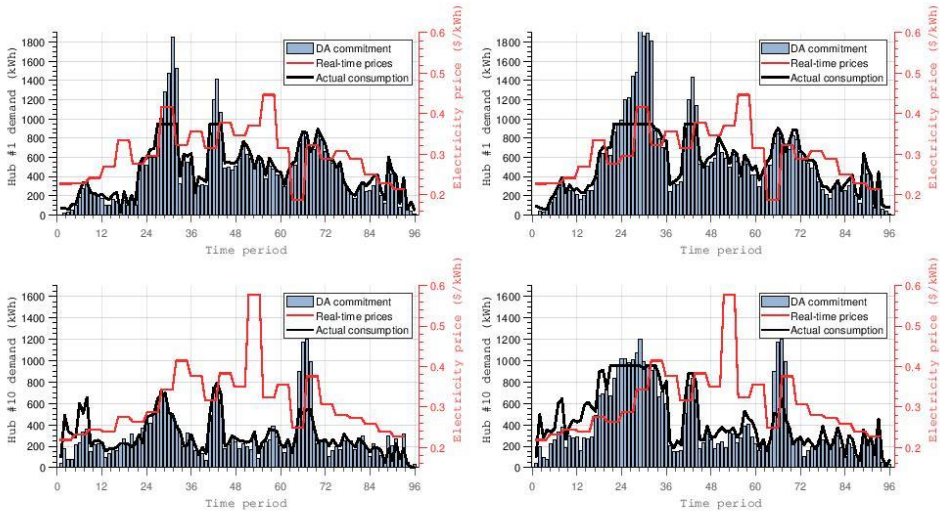

(a) Without privately owned EVs

(b) With privately owned EVs

Figure 7: Comparison of DA commitment with actual consumption for selected hubs

hubs. The increase in gross profit for using DA commitment was assessed for a number of scenarios with an increasing level of RT price spikes. This was accomplished by increasing the location parameter of the Cauchy distribution that was used to generate the price spikes. Note that the location parameter is the median/mode value of the price spike. As in Das & Wollenberg (2005), we kept the value of the scale parameter same as the location parameter. We plotted the increase in gross profit with increasing RT price spikes, see Figure 8. As expected, in the absence of price spikes (when location and scale parameters are set to zero), the increase in gross profit from using DA commitment is negligible. However, as the intensity of price spikes increases, DA commitment yields an increasing level of gross profit. For a typical range of median values of RT price spikes in the U.S. markets, for which the location parameter lies between \$0.2/kWh to \$0.4/kWh, the CPS achieved an increase in the gross profit between \$2000 to \$3000 per day.

5.1 Comments on computational challenges

Recall that, the part of our methodology that addresses the transportation needs uses a variant of an existing model (Zhang et al. 2016). However, we have reformulated the constraints in Zhang et al. (2016) and our version uses a significantly less number of binary variables. Though this reduction makes our methodology easier to solve, the computational times for both the planning and the real time operational models still increase exponentially with the fleet size. This is due to the fact that even when the number of integer variables in our methodology grows linearly with the fleet size, computation time for mixed integer programs (MIPs) increases exponentially with the number of integer variables. Furthermore, in our methodology we need to solve many iterations of the planning model, which is needed to capture the variability of the electricity price, transportation demand, solar generation, and charging demand of the privately owned EVs. This task is computationally burdensome, especially for large fleet sizes. We have also observed that with

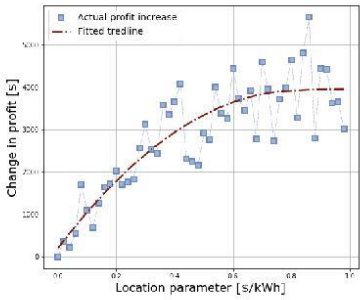

Figure 8: Financial impact of the DA commitment methodology on the profit

smaller hub capacities, finding acceptable solutions of the MIP models in our methodology becomes difficult using commercial optimization solvers (like GUROBI). We conjecture that this occurs because the number of feasible schedules for the SAEVs decreases with reduced hub capacities; this is analogous to the findings reported in studies that compared uncapacitated and capacitated facility location problems, e.g., Verter (2011). As we have discussed earlier, the fleet size of 500 is very small for the level of transportation demand in our CPS, and also five hubs of capacity fifty is perhaps more than what is optimal for a fleet of 500. Hence, we develop a simpler approach for the planning and operation models of our methodology that is expected to obtain near-optimal solutions efficiently for systems with larger fleet sizes and limited hub capacities.

6 A myopic approach for planning and operational decisions

The simplified methodology uses a myopic approach that applies to the tasks of obtaining ad hoc load schedules (in step 1) and real time operational strategies (in step 4). For step 1, the myopic approach works as follows. Instead of finding the operational strategies of SAEVs, battery banks, and EVs using a single optimization model, as in the optimal approach, we obtain the operational strategies sequentially as follows. First, we optimize the charge/discharge schedule of the battery banks at all hubs by considering the electricity prices only, i.e., based on temporal arbitrage alone. Then, we use this charge/discharge schedule of the battery banks, expected PV generation, and historical prices to solve a myopic model to determine the actions of the SAEVs that are not committed, for each time period of the day. This model is presented later in this section. Thereafter, we decide the number of privately-owned EVs that are allowed to enter the hubs at each time period of the day. The above sequential strategies determine the ad hoc load schedule (i.e., how much power to buy from the grid). Note that, the scheduled energy discharge from the battery banks and the generation by the PV are prioritized for use first by the SAEVs and then EVs; any unused quantity is injected back to the grid. For step 4 of our methodology, the myopic approach works in a similar manner as for step 1. The main difference being that instead of using historical prices, we use DA commitment and real time prices (along with discharge schedule of battery banks and PV generation) to obtain actions for SAEVs not committed to other tasks in each time period.

6.1 Myopic model for selecting actions for the SAEVs

We solve a sequence of (modified) linear assignment problems to decide the next action of SAEV b. Let $\hat{x}_{ij}^b$, $\hat{z}_i^b$, $\hat{w}_h^{b+}$, and $\hat{w}_h^{b-}$ be equal to 1 if SAEV b is assigned to 1) pick a customers from i to j, 2) park at node i, 3) charge at hub h, and 4) discharge and hub h, respectively, and 0 otherwise. Then, at each time period we can solve the following optimization model.

$$
\begin{aligned}
\max \quad & \sum_{(i,j)\in\mathcal{A}}\sum_{b\in\mathcal{B}} \psi_{ij}^b \hat{x}_{ij}^b - \sum_{i\in\overline{\mathcal{N}}}\sum_{b\in\mathcal{B}} \alpha_i^b \hat{z}_i^b - \sum_{h\in\mathcal{H}}\sum_{b\in\mathcal{B}} \pi_h^{b+}\hat{w}_h^{b+} + \sum_{h\in\mathcal{H}}\sum_{b\in\mathcal{B}} \pi_h^{b-}\hat{w}_h^{b-} \\
\text{s.t.,} \quad & \sum_{(i,j)\in\mathcal{A}} \hat{x}_{ij}^b + \sum_{i\in\overline{\mathcal{N}}} \hat{z}_i^b + \sum_{h\in\mathcal{H}} \left(\hat{w}_h^{b+} + \hat{w}_h^{b-}\right) = 1 \quad \forall b \in \mathcal{B} \\
& \sum_{b\in\mathcal{B}} \hat{x}_{ij}^b \le d_{ij} \quad \forall (i,j) \in \mathcal{A} \\
& \sum_{b\in\mathcal{B}} \left(\hat{w}_h^{b+} + \hat{w}_h^{b-}\right) \le \hat{C}_h \quad \forall h \in \mathcal{H} \\
& 0 \le \hat{x}_{ij}^b, \hat{z}_i^b, \hat{w}_h^{b+}, \hat{w}_h^{b-} \le 1
\end{aligned}
\tag{36}
$$

where, ψ_{ij}^b, α_i^b, π_h^{b+}, and π_h^{b-} is the revenues (cost) that vehicle b will receive for picking a customers from i to j, park at node i, charge at hub h, and discharge and hub h, respectively. These values depend on the arrival time θ at which each SAEV complete its trip. To compute each of these values, we define the minimum state of charge that an SAEV must have at arrival to node k as $s_k^{\min} = \underline{S}_b + \frac{1}{\phi_b}\tau_{jh}\epsilon_b$, for the closest hub h. Then, the revenue from picking a customer in i to j is defined as:

$$
\psi_{ij}^b = \begin{cases} \psi_{ij}\tau_{ij}, & \text{if } s_\theta^b \ge s_j^{\min} \\ -M, & \text{otherwise} \end{cases} \tag{37}
$$

where M is a big positive number. The cost from parking at node in i is defined as,

$$
\alpha_i^b = \begin{cases} \alpha_i + L, & \text{if } s_\theta^b \ge s_j^{\min} \\ M, & \text{otherwise} \end{cases} \tag{38}
$$

where L is a positive integer that is chosen such that the "apparent" cost of parking is higher that the average cost of electricity (such that an SAEV will choose to charge instead of park in most cases). When the electricity price spikes, it might be more convenient to park the vehicle until the price decreases; the value of L must be chosen to consider such situations. The discharging cost is defined as,

$$
\pi_h^{b-} = \begin{cases} \pi_{h\theta} \min\{P^-, \phi^b(s_\theta^b - \underline{S}^b)\}, & \text{if } s_\theta^b \ge s_j^{\min} \\ -M, & \text{otherwise} \end{cases} \tag{39}
$$

Finally, the charging cost is defined as,

$$
\pi_h^{b-} = \begin{cases} \overline{\pi}_{h\theta} \min\{P^+, \phi^b(\overline{S}^b - s_\theta^b)\}, & \text{if } s_\theta^b \ge s_j^{\min} \\ M, & \text{otherwise} \end{cases} \tag{40}
$$

Note that for the discharging cost is calculated using the electricity price at arrival, $\pi_{h\theta}$, whereas for the

charging cost we use $\overline{\pi}_{h\theta}$, which is defined as,

$$\overline{\pi}_{h\theta} = \max\Big\{\frac{C_h - N_{h\theta}}{C_h}, 0\Big\}\pi_{h\theta} \qquad \forall h \in \mathcal{H} \tag{41}$$

where,

$$N_{h\theta} = \left\lfloor \frac{F_{h\theta} + P^{-}_{h\theta} + P^{DA}_{h\theta}}{P^{+}} \right\rfloor \tag{42}$$

is the maximum number of vehicles that can be charged using either the expected available solar power, the discharged power from the bank of strand-alone batteries or the DA commitment. The logic behind Equation (41) is as follows. For simplicity, assume that $N_{h\theta} \leq C_h$ and that all charging (C_h) are assigned to be used at time θ. Then, the assigned SAEVs will pay $0 \times N_{h\theta} + \pi_{h\theta} \times (C_h - N_{h\theta})$. By multiplying and dividing the above equation by C_h, we have $\frac{C_h - N_{h\theta}}{C_h}\pi_{h\theta} \times C_h$. Hence, we have that $\frac{C_h - N_{h\theta}}{C_h}\pi_{h\theta}$ is the average price paid by the SAEVs if all charging stations are used. Considering that $N_{h\theta}$ might be greater that C_h leads to Equation (41). Hence, we are assigning SAEVs to charge assuming they will pay the average price.

7 Results from case study using the myopic approach

We first assess the performance of the myopic approach by comparing its computation time and gross profit with those obtained from the original version of our methodology. All computational experiments are carried out on a Dell Optiplex 9020 with Intel(R) Core(TM) i7-4790 CPU @ 3.60 GHz, 4-core processor, 16 GB RAM, and Microsoft Windows 10 Enterprise operating system. We first assessed the savings in computation time for a number of fleet sizes ranging from 50 to 500. Recall that the myopic approach is different from the original methodology only in steps 1 and 4. The savings in computational time from step 1 is much more significant than that obtained from step 4. In step 1 of the original methodology, we sequentially solve for 100 iterations of the planning model using a single thread, for which the total solution time is approximately 10 days. Whereas, the myopic approach completes step 1 in a little over 4 hours. As regards step 4, the savings are more modest, though significant. For each of the fleet sizes, we compute 20 iterations of the step 4, 10 using the myopic approach and 10 using the original methodology. The box plots in Figure 9a show the reductions in computation time. It can be seen that for 500 SAEVs, the myopic approach obtains the solution in about 2 minutes, whereas the original methodology takes about 120 minutes. Hereafter, we assessed the quality of the solution obtained by the myopic approach as shown in Figure 9b. We notice that the myopic approach yields on average an optimality gap of 21.5%, and it does not appear to be influenced by the fleet size.

Using the myopic approach, we examined the impact of the hub capacity on gross profit, SAEV idle time, and unsatisfied demands in the CPS for a 24 hour period. Hub capacities between 50 and 250 for each hub were considered for fleet sizes of 500, 1000, 2000, and 5000. The results are shown in Figure 10. Regarding gross profit, we notice that for fleet size of 500, the gross profit is almost constant. The hub capacity of 50 for a fleet of 500 is already too high and by increasing it further it has little to no impact on gross profit. The fleet of 1000 vehicles benefits from an increase in hub capacity beyond 50, but its gross profit does not grow much after a hub capacity of 100. For fleet sizes of 2000 and 5000, the gross profit continues to rise as the hub capacity increases. An interesting observation is that for the fleet of 5000, the gross profits are lower than those for the fleet of 2000. This is due to the fact that the fleet size of 5000 is too high for the range of hub capacities (50-250), and hence many of the SAEVs have to park and idle at the hubs and wait for

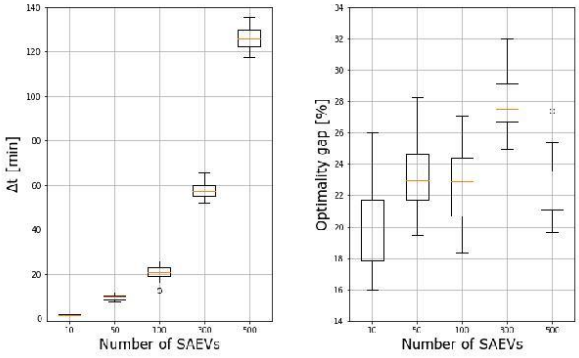

Figure 9: Myopic vs. Optimal solution: time and optimality gap comparison

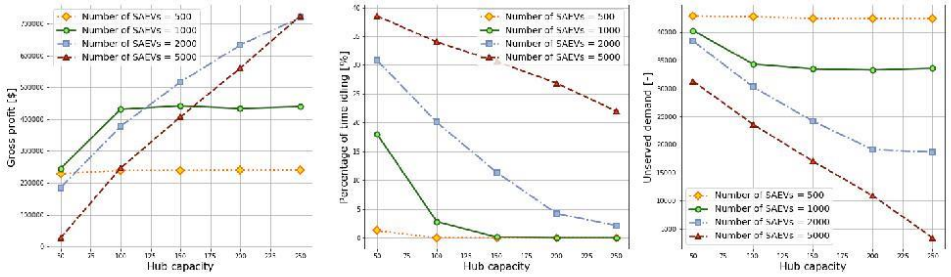

Figure 10: Impact of hub capacity on system performance

charging facility to become available. While parked, SAEVs pay a parking fee, thus lowering the gross profit. The gross profit from the fleet of 5000 is higher than the fleet of 2000 for hub capacities beyond 250. As regards idle time of the SAEVs, it approaches zero as the hub capacity increases, for all fleet sizes. Note that in the myopic approach, SAEVs idle only when there is either no demand for transportation and/or there is no available charging/discharging facility. Since 50 charging stations per hub is large enough, the fleet of 500 has little to no idle time. For a fleet size of 1000, the idle time reaches zero at hub capacity of 150. Fleets of 2000 and 5000 can benefit from hub capacities higher than 250, as the idle time continues to decrease and gross profit continues to increase. Finally, as expected, the unserved passenger demand also decreases as the hub capacity increases. Note that the unserved demand can be reduced only to a point, which depends on the fleet size, by increasing hub capacity. Since the fleet size of 5000 is very large for the given demand, it appears that by increasing hub capacity beyond 250 the unserved demand may be driven to zero.

8 Conclusions

Various alliances of technology and manufacturing companies are earnestly developing and testing autonomous electric vehicles capable of navigating busy streets in major cities. These developments are likely to bring a major transformation in which shared autonomous electric vehicles (SAEVs) will replace a significant number of the human driven automobiles used by the ride sharing companies. However, effective switching to fleets of SAEVs will be possible if supporting cyber-physical system (CPS) infrastructures are available in cities and suburbs. These systems will provide the physical facilities (hubs) for the vehicles to charge and discharge as well as make the real time decisions for the vehicles and the hubs. This paper presents a methodology that yields optimal operational strategies for a fleet of SAEVs and its supporting CPS aimed at maximizing gross profit. Recognizing the computational challenges of our methodology, we have also developed a heuristic (myopic) version of the methodology, which is capable of obtaining near optimal operating strategies for ride sharing services with large fleets of SAEVs.

Our methodology is novel as it incorporates power network considerations in SAEV fleet operation planning. Existing papers addressing transportation with autonomous electric vehicles focus mostly on the transportation aspects while making simplifying assumptions for power related issues. Use of an alternating current optimal power flow (ACOPF) model to engage the service providers to commit for power purchase in the day ahead market, considering real time price spikes, arbitrage with battery banks, and solar generation, has not been presented to the literature. Numerical study shows that ACOPF guided consideration of power networks in SAEV fleet planning can yield between \$2000-\$3000 in savings per day (near a million dollars per year) for a service provider with a relatively small fleet size of 500 SAEVs under the given conditions of our study. Our numerical study also unravels interesting insight about limited potential for energy arbitrage via vehicle-to-grid (V2G) using SAEV batteries; as in the presence of sufficient transportation demand and a moderate level of real time price spikes, SAEVs can earn more revenue serving passengers compared to sitting idle and engaging in V2G.

Not considered in our methodology are the issues of selecting the optimal number of hubs needed for a system as well as locating the hubs appropriately within the transportation service network. We also did not consider the costs of the vehicles, the hubs (land, building, and charging technology), repair and maintenance, and other statutory needs. Adequate consideration of all of these in addition to the aspects considered already can yield a comprehensive methodology for both design and operation of a system of SAEVs and supporting CPS. However, computational complexities associated with obtaining the optimal solution of such a methodology might make its implementation difficult. It remains a topic of our future research.

References

Alonso-Mora, J., Wallar, A. & Rus, D. (2017), Predictive routing for autonomous mobility-on-demand systems with ride-sharing, *in* '2017 IEEE/RSJ International Conference on Intelligent Robots and Systems (IROS)', IEEE, pp. 3583–3590.

Bell, M. G. (1991), 'The estimation of origin-destination matrices by constrained generalised least squares', *Transportation Research Part B: Methodological* **25**(1), 13–22.

Bertsimas, D. & Sim, M. (2004), 'The price of robustness', *Operations research* **52**(1), 35–53.

Chen, T. D., Kockelman, K. M. & Hanna, J. P. (2016), 'Operations of a shared, autonomous, electric vehicle

fleet: Implications of vehicle & charging infrastructure decisions', *Transportation Research Part A: Policy and Practice* **94**, 243–254.

Das, D. & Wollenberg, B. F. (2005), 'Risk assessment of generators bidding in day-ahead market', *IEEE Transactions on power systems* **20**(1), 416–424.

Farhan, J. & Chen, T. D. (2018), 'Impact of ridesharing on operational efficiency of shared autonomous electric vehicle fleet', *Transportation Research Part C: Emerging Technologies* **93**, 310–321.

Growe-Kuska, N., Heitsch, H. & Romisch, W. (2003), Scenario reduction and scenario tree construction for power management problems, *in* 'Power tech conference proceedings, 2003 IEEE Bologna', Vol. 3, IEEE, pp. 7–pp.

Iacobucci, R., McLellan, B. & Tezuka, T. (2018*a*), Model predictive control of a shared autonomous electric vehicles system with charge scheduling and electricity price response, *in* '2018 3rd IEEE International Conference on Intelligent Transportation Engineering (ICITE)', IEEE, pp. 110–114.

Iacobucci, R., McLellan, B. & Tezuka, T. (2018*b*), 'The synergies of shared autonomous electric vehicles with renewable energy in a virtual power plant and microgrid', *Energies* **11**(8), 2016.

Iacobucci, R., McLellan, B. & Tezuka, T. (2019), 'Optimization of shared autonomous electric vehicles operations with charge scheduling and vehicle-to-grid', *Transportation Research Part C: Emerging Technologies* **100**, 34–52.

Inman, R. H., Pedro, H. T. & Coimbra, C. F. (2013), 'Solar forecasting methods for renewable energy integration', *Progress in energy and combustion science* **39**(6), 535–576.

Jabr, R. A. (2006), 'Radial distribution load flow using conic programming', *IEEE transactions on power systems* **21**(3), 1458–1459.

Jabr, R. A. (2008), 'Optimal power flow using an extended conic quadratic formulation', *IEEE transactions on power systems* **23**(3), 1000–1008.

Kang, N., Feinberg, F. M. & Papalambros, P. Y. (2017), 'Autonomous electric vehicle sharing system design', *Journal of Mechanical Design* **139**(1), 011402.

Kwon, S., Xu, Y. & Gautam, N. (2015), 'Meeting inelastic demand in systems with storage and renewable sources', *IEEE Transactions on Smart Grid* **8**(4), 1619–1629.

Lam, A. Y., James, J., Hou, Y. & Li, V. O. (2018), 'Coordinated autonomous vehicle parking for vehicle-to-grid services: Formulation and distributed algorithm', *IEEE Transactions on Smart Grid* **9**(5), 4356–4366.

Li, F. & Bo, R. (2010), Small test systems for power system economic studies, *in* 'IEEE PES general meeting', IEEE, pp. 1–4.

Miao, H., Jia, H., Li, J. & Qiu, T. Z. (2019), 'Autonomous connected electric vehicle (acev)-based car-sharing system modeling and optimal planning: A unified two-stage multi-objective optimization methodology', *Energy* **169**, 797–818.

Sedighizadeh, M., Mohammadpour, A. & Alavi, S. M. M. (2019), 'A daytime optimal stochastic energy management for ev commercial parking lots by using approximate dynamic programming and hybrid big bang big crunch algorithm', *Sustainable cities and society* **45**, 486–498.

Subramanian, V. & Das, T. K. (2019), 'A two-layer model for dynamic pricing of electricity and optimal charging of electric vehicles under price spikes', *Energy* **167**, 1266–1277.

Turan, M. T., Ates, Y., Erdinc, O., Gokalp, E. & Catalão, J. P. (2019), 'Effect of electric vehicle parking lots equipped with roof mounted photovoltaic panels on the distribution network', *International Journal of Electrical Power & Energy Systems* **109**, 283–289.

Uber (2020), 'Uber movement', `https://movement.uber.com/?lang=en-US`. accessed: February 23, 2020.

Verter, V. (2011), Uncapacitated and capacitated facility location problems, *in* 'Foundations of location analysis', Springer, pp. 25–37.

Yao, L., Lim, W. H. & Tsai, T. S. (2017), 'A real-time charging scheme for demand response in electric vehicle parking station', *IEEE Transactions on Smart Grid* **8**(1), 52–62.

Zhang, R., Rossi, F. & Pavone, M. (2016), Model predictive control of autonomous mobility-on-demand systems, *in* '2016 IEEE International Conference on Robotics and Automation (ICRA)', IEEE, pp. 1382–1389.

Zhou, X., Qin, X. & Mahmassani, H. S. (2003), 'Dynamic origin-destination demand estimation with multiday link traffic counts for planning applications', *Transportation Research Record* **1831**(1), 30–38.

Appendix A Summary of important notation

Sets

- $\overline{\mathcal{N}}$: Set of all nodes on the transportation network
- $\mathcal{B}$: Set of all SAEVs
- $\overline{\mathcal{T}}$: Set of all time periods; note that in general $\overline{\mathcal{T}} \neq \mathcal{T}$ as the transportation and power network operations might have different time frames
- $\mathcal{A}$: Set of all arcs in the transportation network
- $\mathcal{H}$: Subset of the nodes in the transportation network in which the smart charge/discharge hubs are located
- $\mathcal{P}$: Subset of the nodes in the transportation network in which there are parking/idling facilities
- $\mathcal{D}_h$: Set of minimum cost load schedules at hub h for given historical information (price, demand, etc.)
- Ω: Subset of selected scenarios through a scenario reduction technique

Parameters

- γ_{ijt}: Number of passenger arrivals at node i with destination j $(i, j \in \mathcal{A})$ at time $t \in \overline{\mathcal{T}}$
- τ_{ij}: Travel time between nodes i and j $(i, j \in \mathcal{A})$
- β: Balking rate $(0 \leq \beta \leq 1)$
- α_p: Parking fee per time period at parking lot $p \in \mathcal{P}$
- ψ_t: Price paid by the customer per unit time period for a trip originating at time $t \in \overline{\mathcal{T}}$
- ζ_h: Facility fee paid by privately owned EVs per unit time period when charging at hub $h \in \mathcal{H}$
- π_{ht}: Historical price of electricity at the node supporting hub $h \in \mathcal{H}$ at time $t \in \overline{\mathcal{T}}$
- π_{ht}^{DA}: Actual DA price at node $h \in \mathcal{H}$ at time $t \in \overline{\mathcal{T}}$
- π_{ht}^{RT}: Actual RT price at node $h \in \mathcal{H}$ at time $t \in \overline{\mathcal{T}}$
- π_{ht}^{ω}: Estimated RT price in scenario $\omega \in \Omega$ at hub $h \in \mathcal{H}$ at time period $t \in \overline{\mathcal{T}}$
- ϕ_b: Battery capacity of SAEV $b \in \mathcal{B}$
- ϵ_b: Energy consumption of SAEV $b \in \mathcal{B}$ per unit time period on the road
- $\underline{S_b}, \overline{S_b}$: Lower and upper bounds to SAEV $b \in \mathcal{B}$ state of charge
- $\overline{P}^{+}$: Maximum energy that can be added to a vehicle per unit time period, same for all hubs
- $\overline{P}^{-}$: Maximum energy that can be discharged from a vehicle per unit time period, same for all hubs
- $F_{ht}, F_h^{\max}$: Solar generation at hub $h \in \mathcal{H}$ at time $t \in \overline{\mathcal{T}}$ and installed solar capacity, respectively
- $E_h, \overline{P}_h, \underline{P}_h$: Capacity, charging rate, and discharging rate, respectively, of the bank of stand alone battery at hub $h \in \mathcal{H}$
- V: Maximum number of time periods that a privately owned EV can charge in a hub
- W_{ht}^{v}: Number of privately owned EVs requesting charging services for $v \leq V$ time periods at hub $h \in \mathcal{H}$ at time $t \in \overline{\mathcal{T}}$
- C_h: Total number of charging stations installed at hub $h \in \mathcal{H}$
- D_{ht}: Minimal cost load schedule for each time period $t \in \overline{\mathcal{T}}$ at hub $h \in \mathcal{H}$
- D_{ht}^{ω}: Selected load schedule for each time period $t \in \overline{\mathcal{T}}$ at hub $h \in \mathcal{H}$ from scenario $\omega \in \Omega$
- μ_{ω}: Probability of scenario $w \in \Omega$
- P_{ht}^{DA}: DA commitment of hub $h \in \mathcal{H}$ at time period $t \in \overline{\mathcal{T}}$

Decision variables

- x_{ijt}^b: 1 if vehicle $b \in \mathcal{B}$ is departing with passengers from node i to node j $(i, j \in \overline{\mathcal{N}})$ at time $t \in \overline{\mathcal{T}}$, and 0 otherwise
- y_{ijt}^b: 1 if vehicle $b \in \mathcal{B}$ is departing empty from node i to node j $(i, j \in \overline{\mathcal{N}})$ at time $t \in \overline{\mathcal{T}}$, and 0 otherwise
- p_{ht}^{b+}: Total charge added to SAEV $b \in \mathcal{B}$ at hub $h \in \mathcal{H}$ at time period $t \in \overline{\mathcal{T}}$
- p_{ht}^{b-},p_{ht}^{-}: Total energy discharged from SAEV $b \in \mathcal{B}$ and from the bank of stand-alone batteries, respectively, at hub $h \in \mathcal{H}$ and time period $t \in \overline{\mathcal{T}}$
- $\hat{p}_{ht}^{-}$: Fraction of the total discharged energy sold to the main grid by the bank of stand-alone battery at hub $h \in \mathcal{H}$ and time period $t \in \overline{\mathcal{T}}$
- e_{ht}^b,e_{ht}^{EV}: Energy added form the bank of Stand-alone battery to SAEV $b \in \mathcal{B}$ and privately owned EVs, respectively, at hub $h \in \mathcal{H}$ at time period $t \in \overline{\mathcal{T}}$
- f_{ht}^b,f_{ht}^{+},f_{ht}^{EV}: Solar energy added to SAEV $b \in \mathcal{B}$, bank of stand-alone batteries, and privately owned EVs, respectively, at hub $h \in \mathcal{H}$ and time period $t \in \overline{\mathcal{T}}$
- f_{ht}^{-}: Solar energy sold directly to the main grid
- g_{ht}^b,g_{ht},g_{ht}^{EV}: Total energy bought from the grid to charge SAEV $b \in \mathcal{B}$, the bank of stand alone batteries, and the privately owned EVs, respectively, at hub $h \in \mathcal{H}$ and time period $t \in \overline{\mathcal{T}}$
- w_{ht}^{b+}: 1 if SAEV $b \in \mathcal{B}$ is charging at hub $h \in \mathcal{H}$ and time period $t \in \overline{\mathcal{T}}$, 0 otherwise
- w_{ht}^{b-}: 1 if SAEV $b \in \mathcal{B}$ is discharging at hub $h \in \mathcal{H}$ and time period $t \in \overline{\mathcal{T}}$, 0 otherwise
- p_{ht}^{RT-}: Fraction of the DA commitment sold to the RT market by hub $h \in \mathcal{H}$ at time period $t \in \overline{\mathcal{T}}$
- w_{ht}^{v}: Number of charging stations assigned to privately owned EVs at hub $h \in \mathcal{H}$ at time period $t \in \overline{\mathcal{T}}$; the vehicles stay v time period units at the smart hubs

Other variables

- z_{it}^b: 1 if vehicle $b \in \mathcal{B}$ waited in node $i \in \overline{\mathcal{N}}$ from time $t-1$ to time t $(t \in \overline{\mathcal{T}})$, and 0 otherwise
- p_{it}^b: 1 if at time period $t \in \overline{\mathcal{T}}$, the vehicle $b \in \mathcal{B}$ will arrived at node $i \in \overline{\mathcal{N}}$
- d_{ijt}: Number of passengers left unserved at node i with destination j $(i, j \in \overline{\mathcal{N}})$ at time period $t \in \overline{\mathcal{T}}$
- b_{ijt}: Dummy variable to avoid infeasibility $(0 \leq b_{ijt} \leq 1)$
- s_t^b,s_{ht}: State of charge of SAEV $b \in \mathcal{B}$ and the bank of stand-alone batteries in hub $h \in \mathcal{H}$, respectively, at time period $t \in \overline{\mathcal{T}}$; $0 < s_t^b, s_{ht} < 1$, $\forall b, v, h, t$
- a^{RT}: RT electricity profit, i.e., revenue from selling to the grid in the RT market minus cost of buying in the RT market
- c_{ht}: Number of charging stations occupied by privately owned EVs at hub $h \in \mathcal{H}$ at time period $t \in \overline{\mathcal{T}}$

Appendix B Alternative current optimal power flow (ACOPF)

It has been shown that the conventional non-linear load flow equations for both radial (Jabr 2006) and meshed networks (Jabr 2008) can be transformed into a second order cone program (SOCP). In this subsection, we present a modified version of such formulations.

B.0.1 ACOPF model notations

Sets

- $\mathcal{G}$: Set of all generators in the network
- $\mathcal{N}$: Set of all buses in the network
- $\mathcal{G}_i$: Subset of generators that are connected to bus $i \in \mathcal{N}$
- $\mathcal{N}_i$: Subset of buses that are directly linked to bus $i \in \mathcal{N}$
- $\mathcal{T}$: Set of all time periods
- $\mathcal{L}$: Set of all lines in the network

Parameters

- P_{it}^L: Active power load at bus $i \in \mathcal{N}$ at time $t \in \mathcal{T}$
- Q_{it}^L: Reactive power load at bus $i \in \mathcal{N}$ at time $t \in \mathcal{T}$
- G_{ij}: Conductance of line $ij \in \mathcal{L}$
- B_{ij}: Susceptance of line $ij \in \mathcal{L}$
- F_{ij}^+, F_{ij}^-: Real and reactive power capacity of line $ij \in \mathcal{L}$, respectively
- $\underline{P_g}$, $\overline{P_g}$: Lower and upper bound, respectively, of real power supply by generator $g \in \mathcal{G}$
- $\underline{Q_g}$, $\overline{Q_g}$: Lower and upper bound, respectively, of reactive power supply by generator $g \in \mathcal{G}$
- $\underline{V_i}$, $\overline{V_i}$: Voltage lower and upper bound, respectively, at node $i \in \mathcal{N}$

Decision variables

- p_{gt}: Real power dispatch from generator $g \in \mathcal{G}$ at time $t \in \mathcal{T}$
- q_{gt}: Reactive power dispatch form generator $g \in \mathcal{G}$ at time $t \in \mathcal{T}$

Other variables

- p_{ijt}: Real power flow from bus $i \in \mathcal{N}$ to node $j \in \mathcal{N}$ at time $t \in \mathcal{T}$
- q_{ijt}: Reactive power flow from bus $i \in \mathcal{N}$ to node $j \in \mathcal{N}$ at time $t \in \mathcal{T}$
- u_{it}: Transformed voltage at bus $i \in \mathcal{N}$ and time $t \in \mathcal{T}$; $u_{it} = \frac{V_{it}^2}{\sqrt{2}}$, where V_{it} is the actual voltage at node $i \in \mathcal{N}$ and time $t \in \mathcal{T}$ and it can be calculated after the optimization model is solved
- r_{ijt}: Intermediate variable; $r_{ijt} = V_{it}V_{jt}\cos(\theta_i - \theta_j)$, where θ_i and θ_j are the voltage angles at buses $i \in \mathcal{N}$ and $j \in \mathcal{N}$, respectively
- $\bar{r}_{ijt}$: Intermediate variable; $\bar{r}_{ijt} = V_{it}V_{jt}\sin(\theta_i - \theta_j)$

Appendix C ACOPF model formulation

The SOCP formulation of the traditional non-linear ACOPF problem is presented below.

$$\min \quad \sum_{t\in\mathcal{T}}\sum_{g\in\mathcal{G}} C_g(p_{gt}) \tag{43}$$

$$\text{s.t.,} \quad \sum_{g\in\mathcal{G}_i} p_{gt} - \sum_{j\in\mathcal{N}_i} p_{ijt} = P^L_{it} \qquad \forall i\in\mathcal{N}, t\in\mathcal{T} \tag{44}$$

$$\sum_{g\in\mathcal{G}_i} q_{gt} - \sum_{i\in\mathcal{N}_i} q_{ijt} = Q^L_{it} \qquad \forall i\in\mathcal{N}, t\in\mathcal{T} \tag{45}$$

$$p_{ijt} = \sqrt{2}G_{ij}u_{it} - G_{ij}r_{ijt} + B_{ij}\bar{r}_{ijt} \qquad \forall ij\in\mathcal{L}, t\in\mathcal{T} \tag{46}$$

$$q_{ijt} = \sqrt{2}B_{ij}u_{it} - B_{ij}r_{ijt} - G_{ij}\bar{r}_{ijt} \qquad \forall ij\in\mathcal{L}, t\in\mathcal{T} \tag{47}$$

$$-F^+_{ij} \le p_{ijt} \le F^+_{ij} \qquad \forall ij\in\mathcal{L}, t\in\mathcal{T} \tag{48}$$

$$-F^-_{ij} \le q_{ijt} \le F^-_{ij} \qquad \forall ij\in\mathcal{L}, t\in\mathcal{T} \tag{49}$$

$$\underline{P_g} \le p_{gt} \le \overline{P_g} \qquad \forall g\in\mathcal{G}, t\in\mathcal{T} \tag{50}$$

$$\underline{Q_g} \le q_{gt} \le \overline{Q_g} \qquad \forall g\in\mathcal{G}, t\in\mathcal{T} \tag{51}$$

$$\frac{1}{\sqrt{2}}\underline{V_i}^2 \le u_{it} \le \frac{1}{\sqrt{2}}\overline{V_i}^2 \qquad \forall i\in\mathcal{N}, t\in\mathcal{T} \tag{52}$$

$$r^2_{ijt} + \bar{r}^2_{ijt} \le 2u_{it}u_{jt} \qquad \forall ij\in\mathcal{L}, t\in\mathcal{T} \tag{53}$$

$$r_{ijt} = r_{jit} \qquad \forall ij\in\mathcal{L} \tag{54}$$

$$\bar{r}_{ijt} = -\bar{r}_{jit} \qquad \forall ij\in\mathcal{L} \tag{55}$$

In the objective function (43), $C_g(\cdot)$ denotes the cost function of generator g. Hence, the above formulation minimizes the total electricity cost of the network over all time periods. Real and reactive power balance at node i and time period t are considered by equations (44) and (45), respectively. Equations (46) and (47) are the real and reactive power flows, respectively, from node i to node j at time period t. Real and reactive line flow capacities of arc ij are given by equations (48) and (49). Equation (50) and (51) bound the generators real and reactive power outputs, respectively. Equation (52) bounds the voltage of each node of the network. Equation (53) is a conic constraint to account for the relation between power flow components and the voltage at each node. Finally, Equations (54) and (55) consider the relation between the power flowing from node i to j and the power flowing from j to i. Also, the voltage at node 1 (substation node) is considered to be known. Hence, we can write that $u_{1t} = \frac{V_1^2}{\sqrt{2}}\ \forall t\in\mathcal{T}$. The above formulation is a SOCP since any constraint of the form $\{u,v,w\ge 0 : u \le \sqrt{vw}\}$ is equivalent to $\{u,v,w\ge 0 : \sqrt{u^2+(\frac{v-w}{2})^2}\} \le \frac{v+w}{2}\}$.

Appendix D Robustification of the operational model

D.1 Robust optimization

Robust optimization studies how to solve linear optimization problems with uncertain data. Under this approach, we are willing to settle for suboptimal solutions for the mean values of the data in order to ensure that the solution remains feasible and near optimal when the data changes. To formulate a robust linear

program, consider the following linear optimization problem:

$$\begin{aligned} \max \quad & c^{\intercal}x \\ \text{s.t.,} \quad & Ax \leq b \\ & x \in \mathcal{X} \end{aligned} \tag{56}$$

where A is an $m \times n$ matrix, x is an $n \times 1$ vector (decision variables), $c^{\intercal}$ is a $1 \times n$ vector, and b is a $m \times 1$ vector. Without loss of generality, it is considered that data uncertainty only affects the elements in matrix A. This is the case since we can re-write the problem as:

$$\begin{aligned} \max \quad & z \\ \text{s.t.,} \quad & z - c^{\intercal}x \leq 0 \\ & Ax - bY \leq 0 \\ & x \in \mathcal{X} \\ & Y = 1 \end{aligned} \tag{57}$$

if there are uncertainties in c or b. Consider a particular row i of the matrix A and let $\mathcal{J}_i$ represent the set of coefficients in row i that are subject to uncertainty. Also, it is considered that the probability distribution of each component $a_{ij}, j \in \mathcal{J}_i$ is unknown, but the values in which a_{ij} ranges are known and defined by $[\bar{a}_{ij} - \hat{a}_{ij}, \bar{a}_{ij} + \hat{a}_{ij}]$, where $\bar{a}_{ij}$ is the best estimate of a_{ij}, and $\hat{a}_{ij}$ is maximum feasible deviation from $\bar{a}_{ij}$. Bertsimas & Sim (2004) proved that the robust counterpart of a linear problem with the form of (56) can be also formulated by introducing a set of non-negative variables (y_j, p_{ij}, and z_i) and a parameter Γ_i that takes values in the interval $[0, |\mathcal{J}_i|]$. The role of Γ_i is to adjust the robustness of the proposed method against the level of conservatism of the solution (Bertsimas & Sim 2004). Then, the robust reformulation is given by:

$$\begin{aligned} \max \quad & c^{\intercal}x \\ \text{s.t.,} \quad & \sum_j \bar{a}_{ij}x_j + z_i\Gamma_i + \sum_{j \in \mathcal{J}_i} p_{ij} \leq b_i \qquad \forall i \\ & z_i + p_{ij} \geq \hat{a}_{ij}y_j \qquad \forall i, j \in \mathcal{J}_i \\ & -y_j \leq x_j \leq y_j \qquad \forall j \\ & x_j \in \mathcal{X} \qquad \forall j \\ & p_{ij} \geq 0 \qquad \forall i, j \in \mathcal{J}_i \\ & y_j \geq 0 \qquad \forall j \\ & z_i \geq 0 \qquad \forall i \end{aligned} \tag{58}$$

By solving (58), we are robust against expected disturbances in the parameters of our model.

D.2 Robust counter part of the operational model

In this subsection we present the robust versions of the constraints with uncertain parameters, namely, constraints (1), (19), (20), and (30). Recall that the state of the system is completely known at the current time period τ, and hence, the robust constraints are only included for time periods $\tau + 1$ and onward. Then, we have that:

- Robust counterpart of constraint (1):

$$d_{ij,\tau+1} = \beta d_{ij\tau} + \gamma_{ij\tau} - \sum_{b\in\mathcal{B}} x^b_{ij\tau} - b_{ijt} \qquad \forall (i,j) \in \overline{\mathcal{N}} \tag{59}$$

$$d_{ij,t+1} = \beta d_{ijt} + \overline{\gamma}_{ijt} Y^{\gamma}_{ijt} - \sum_{b\in\mathcal{B}} x^b_{ijt} - b_{ijt} - z^{\gamma}_{ijt}\Gamma^{\gamma}_{ijt} - q^{\gamma}_{ijt}\ \forall (i,j) \in \overline{\mathcal{N}}, t \in \{\tau+1,\cdots,|\overline{\mathcal{T}}|\} \tag{60}$$

$$z^{\gamma}_{ijt} + q^{\gamma}_{ijt} \geq \hat{\gamma}_{ijt} y^{\gamma}_{ijt}\ \forall (i,j) \in \overline{\mathcal{N}}, t \in \{\tau+1,\cdots,|\overline{\mathcal{T}}|\} \tag{61}$$

$$-y^{\gamma}_{ijt} \leq Y^{\gamma}_{ijt} \leq y^{\gamma}_{ijt} \qquad \forall (i,j) \in \overline{\mathcal{N}}, t \in \{\tau+1,\cdots,|\overline{\mathcal{T}}|\} \tag{62}$$

$$Y^{\gamma}_{ijt} = 1 \qquad \forall (i,j) \in \overline{\mathcal{N}}, t \in \{\tau+1,\cdots,|\overline{\mathcal{T}}|\} \tag{63}$$

- Robust counterpart of constraint (19):

$$\sum_{b\in\mathcal{B}} f^b_{h\tau} + f^+_{h\tau} + f^-_{h\tau} = F_{ht} \qquad \forall h \in \mathcal{H} \tag{64}$$

$$\sum_{b\in\mathcal{B}} f^b_{ht} + f^+_{ht} + f^-_{ht} = \overline{F}_{ht} Y^F_{ht} - z^{\mathrm{F}}_{ht}\Gamma^F_{ht} - q^F_{ht} \qquad \forall h \in \mathcal{H}, t \in \{\tau+1,\cdots,|\overline{\mathcal{T}}|\} \tag{65}$$

$$z^F_{ht} + q^F_{ht} \geq \hat{F}_{ht} y^F_{ht} \qquad \forall h \in \mathcal{H}, t \in \{\tau+1,\cdots,|\overline{\mathcal{T}}|\} \tag{66}$$

$$-y^F_{ht} \leq Y^F_{ht} \leq y^F_{ht} \forall h \in \mathcal{H}, t \in \{\tau+1,\cdots,|\overline{\mathcal{T}}|\} \tag{67}$$

$$Y^F_{ht} = 1, \qquad \forall h \in \mathcal{H}, t \in \{\tau+1,\cdots,|\overline{\mathcal{T}}|\} \tag{68}$$

- Robust counterpart of constraint (20):

$$w^v_{h,\tau+1} \leq W^v_{h\tau} \qquad \forall h \in \mathcal{H}, v \in \{1,\cdots,V\} \tag{69}$$

$$w^v_{h,t+1} \leq \overline{W}^v_{ht} Y^{v,\mathrm{EV}}_{ht} - z^{v,\mathrm{EV}}_{ht}\Gamma^{v,\mathrm{EV}}_{ht} - q^{v,\mathrm{EV}}_{ht}\ \forall h \in \mathcal{H}, t \in \{\tau+1,\cdots,|\overline{\mathcal{T}}|\}, v \in \{1,\cdots,V\} \tag{70}$$

$$z^{v,\mathrm{EV}}_{ht} + q^{v,\mathrm{EV}}_{ht} \geq \hat{W}^v_{ht} y^{v,\mathrm{EV}}_{ht}\ \forall h \in \mathcal{H}, t \in \{\tau+1,\cdots,|\overline{\mathcal{T}}|\}, v \in \{1,\cdots,V\} \tag{71}$$

$$-y^{v,\mathrm{EV}}_{ht} \leq Y^{v,\mathrm{EV}}_{ht} \leq y^{v,\mathrm{EV}}_{ht}\ \forall h \in \mathcal{H}, t \in \{\tau+1,\cdots,|\overline{\mathcal{T}}|\}, v \in \{1,\cdots,V\} \tag{72}$$

$$Y^{v,\mathrm{EV}}_{ht} = 1\ \forall h \in \mathcal{H}, t \in \{\tau+1,\cdots,|\overline{\mathcal{T}}|\}, v \in \{1,\cdots,V\} \tag{73}$$

- Robust counterpart of constraint (30):

$$a^{\mathrm{RT}} = \sum_{h\in\mathcal{H}} \pi^{\mathrm{RT}}_{h\tau} l^{\mathrm{RT}}_{h\tau} + \sum_{h\in\mathcal{H}} \sum_{t=\tau+1}^{|\overline{\mathcal{T}}|} \overline{\pi}^{\mathrm{RT}}_{ht} l^{\mathrm{RT}}_{ht} - z_{\mathrm{RT}}\Gamma_{\mathrm{RT}} - \sum_{h\in\mathcal{H}} \sum_{t=\tau+1}^{|\overline{\mathcal{T}}|} q^{\mathrm{RT}}_{ht} \tag{74}$$

$$z_{\mathrm{RT}} + q^{\mathrm{RT}}_{ht} \geq \hat{\pi}^{\mathrm{RT}}_{ht} y^{\mathrm{RT}}_{ht} \qquad \forall h \in \mathcal{H}, t \in \{\tau+1,\cdots,|\overline{\mathcal{T}}|\} \tag{75}$$

$$-y^{\mathrm{RT}}_{ht} \leq l^{\mathrm{RT}}_{ht} \leq y^{\mathrm{RT}}_{ht} \qquad \forall h \in \mathcal{H}, t \in \{\tau+1,\cdots,|\overline{\mathcal{T}}|\} \tag{76}$$

- Robust counterpart of constraint (31):

$$a^{\mathrm{RT}}_b = \sum_{h\in\mathcal{H}} \pi^{\mathrm{RT}}_{h\tau} l^{b,\mathrm{RT}}_{h\tau} + \sum_{h\in\mathcal{H}} \sum_{t=\tau+1}^{|\overline{\mathcal{T}}|} \overline{\pi}^{\mathrm{RT}}_{ht} l^{b,\mathrm{RT}}_{ht} - z_{b,\mathrm{RT}}\Gamma_{b,\mathrm{RT}} - \sum_{h\in\mathcal{H}} \sum_{t=\tau+1}^{|\overline{\mathcal{T}}|} q^{b,\mathrm{RT}}_{ht}\ \forall b \in \mathcal{B} \tag{77}$$

$$z_{b,\mathrm{RT}} + q^{b,\mathrm{RT}}_{ht} \geq \hat{\pi}^{\mathrm{RT}}_{ht} y^{b,\mathrm{RT}}_{ht} \qquad \forall b \in \mathcal{B}, h \in \mathcal{H}, t \in \{\tau+1,\cdots,|\overline{\mathcal{T}}|\} \tag{78}$$

$$-y^{b,\mathrm{RT}}_{ht} \leq l^{b,\mathrm{RT}}_{ht} \leq y^{b,\mathrm{RT}}_{ht} \qquad \forall b \in \mathcal{B}, h \in \mathcal{H}, t \in \{\tau+1,\cdots,|\overline{\mathcal{T}}|\} \tag{79}$$

- Robust counterpart of constraint (34):

$$a^{\mathrm{RT}} = \sum_{h\in\mathcal{H}} (\pi_{ht}^{RT} - \delta^{RT}) p_{ht}^{RT-} + \sum_{h\in\mathcal{H}} \sum_{t=\tau+1}^{|\overline{\mathcal{T}}|} (\hat{\pi}_{ht}^{RT} - \delta^{RT}) p_{ht}^{RT-} - z_{\mathrm{DA}}\Gamma_{\mathrm{DA}} - \sum_{h\in\mathcal{H}} \sum_{t=\tau+1}^{|\overline{\mathcal{T}}|} q_{ht}^{\mathrm{DA}} \tag{80}$$

$$z_{\mathrm{DA}} + q_{ht}^{\mathrm{DA}} \geq \hat{\pi}_{ht}^{\mathrm{RT}} y_{ht}^{\mathrm{DA}} \qquad \forall h \in \mathcal{H}, t \in \{\tau+1, \cdots, |\overline{\mathcal{T}}|\} \tag{81}$$

$$-y_{ht}^{\mathrm{DA}} \leq p_{ht}^{\mathrm{RT}-} \leq y_{ht}^{\mathrm{DA}} \qquad \forall h \in \mathcal{H}, t \in \{\tau+1, \cdots, |\overline{\mathcal{T}}|\} \tag{82}$$

All the new variables introduced in this model satisfy the conditions established in subsection D.1. Also note that, $\pi_{h\tau}^{RT}$, $F_{h\tau}$, W_{ht}^{v}, and $\gamma_{ij\tau}$ are known, while $\overline{\pi}_{ht}^{RT}$, $\overline{F}_{ht}$, $\overline{W}_{ht}^{v}$, and $\overline{\gamma}_{ijt}$ $\forall t \in \{\tau+1, \cdots, |\overline{\mathcal{T}}|\}$ are the best estimates of such parameters in the upcoming time periods. We estimate the RT prices (with spikes) as $\overline{\pi}_{ht}^{RT} = \pi_{ht}^{DA}(1+\epsilon)$. There are many techniques available to estimate the available solar power $\overline{F}_{ht}$. In Inman et al. (2013), the authors review the theory behind these forecasting methodologies, and present a number of successful applications of solar forecasting methods for both the solar resource and the power output of solar plants. Estimating origin-destination (O-D) matrices is also a widely studied area. A mayor reference in this area is Bell (1991). More recently, an O-D prediction algorithm for autonomous mobility-on-demand systems with ride-sharing was proposed in Alonso-Mora et al. (2017). Based on historical data, the authors compute a probability distribution over future demand and then, samples from the learned probability distribution are incorporated into a decoupled vehicle routing and passenger assignment method to take into account the predicted future demand. The values of $\overline{W}_{ht}^{v}$ and $\overline{\gamma}_{ijt}$ are chosen equal to the mean value of the fitted probability distributions. Finally, the values of $\hat{\pi}_{ht}^{RT}$, $\hat{F}_{ht}$, $\hat{W}_{ht}^{v}$, $\hat{\nu}_{ht}$, and $\hat{\gamma}_{ijt}$ $\forall t \in \{\tau+1, \cdots, |\overline{\mathcal{T}}|\}$ can be chosen such that the maximum deviation from the best estimate matches the confidence interval of the selected forecast method.